Bayfordbury Single-object Integral Field Spectrograph (BASIS)

Samuel Richards

School of Physics, Astronomy and Mathematics, University of Hertfordshire, Hatfield, AL10 9AB, UK

SN: 08169597, AST4, BSc (Hons) Astrophysics with a Research Year

29th March 2012

ACKNOWLEDGMENTS

I would like to extend my deepest gratitude to Prof. William Martin and Prof. Hugh Jones for their continuous guidance and help throughout this project. It has been an honour to have them as joint supervisors and I will cherish the wisdom given in this time. In addition, I would like to also thank Prof. Joss Bland-Hawthorn (USyd), Dr. Julia Bryant (USyd), Dr. Sergio Leon-Saval (USyd), Dr. Lisa Fogarty (USyd), Dr. Jon Lawrence (AAO) and Dr. Michael Goodwin (AAO) for their help in the start-up of this project whilst I was in Sydney working as part of the SAMI Group. For their comments and guidance, I would like to thank Prof. Elias Brinks, Dr. Mark Sarzi, Dr Daniel Smith, Dr. Mark Gallaway and Mr. David Campbell. I take this opportunity to highlight the assistance of Mr. David Campbell in the commissioning phase of the project; a true asset of Bayfordbury Observatory. I would also like to thank the Science and Technology Research Institute and the Centre for Atmospheric & Instrumentation Research at the University of Hertfordshire for the use of their Optics Laboratory and 3D Printer respectively. Funding for this project came from the University of Hertfordshire's School of Physics, Astronomy & Mathematics Final Year Student Projects budget.

I appreciate all the support from my family and friends throughout the duration of this project, in particular, Caroline Richards and Nick Buttenshaw for their time in proofing this report.

ABSTRACT

The art of integral field spectroscopy is one that has come on in leaps and bounds over the last decade, and is really pushing our understanding of galaxy formation and evolution. Of the 30 such instruments around the world, all but one are on 2+meter class telescopes. It is now possible to exploit recent advancements in small aperture telescopes (<0.5m) to enable an integral field spectrograph with a performance that allows taxonomy via optical emission line analysis (Hβ to SII). Here is presented a cheap and easily replicable integral field spectrograph for such use on small aperture telescopes, in this case a Meade LX200 16-inch Schmidt-Cassegrain (LX200), a telescope that many institutions around the world have as part of their respective observatories. The spectrograph used for this instrument is a Santa-Barbara Instrument Group Self-Guiding Spectrograph (SBIG SGS), which is again an instrument that many institutions around the world already use. The integral field unit (IFU) is positioned at the Cassegrain focus of the telescope, and consists of a 19 optical fibre bundle, with each fibre having a 50µm diameter core and a pitch of 250µm. Coupled with the f/10 beam from the telescope, its overall field-of-view is 1 arc minute, 2.6 arc seconds per core. There are four sky fibres displaced from the fibre bundle providing night sky spectra for data reduction and calibration purposes. The fibre run has an overall length of 5m, which is terminated at the other end with a 1-D fibre array positioned at the slit of the spectrograph. The SBIG SGS permits a wavelength range of 4710-6830Å and a resolution of 7Å. Working with an overall instrument efficiency of 5% means that it is possible to achieve a signal-to-noise ratio of 10 for a 20min exposure of a 13mag/arcsec^2 source. BASIS's performance not only allows for teaching the principles of experimental and observational integral field spectroscopy but also can bridge the divide between amateur astronomy and research science providing a first-pass survey of $10^2 – 10^3$ nearby galaxies in 100 nights. Future observations and analysis of 50 galaxies will act as a proof of concept for the survey mode.

Table of Contents

Bayfordbury Single-object Integral Field Spectrograph (BASIS) 1

ACKNOWLEDGMENTS 2

ABSTRACT 3

1 Initial Plan 5

1.1 A brief overview of the project 5

1.2 Project Time-Line 7

1.3 Initial Plan comments 7

2 Introduction 8

2.1 The case for integral field spectroscopy and its teaching 8

2.2 Scientific rationale 9

3 Bayfordbury Single-object Integral Field Spectrograph (BASIS) 14

3.1 Choosing the site 14

3.2 Existing equipment 15

3.3 Meade LX200 16-inch 15

3.4 Santa Barbara Instrument Group Self Guiding Spectrograph (SBIG SGS) 16

3.5 SBIG ST-7E CCD 17

3.6 Optical fibre cable 18

3.7 Integral Field Unit (IFU) 19

3.8 1-D fibre array 25

3.9 Manufacturing of integration parts & wavelength calibration check 26

3.10 Control units and software (acquisition and guiding) 29

3.11 BASIS instrument summary 30

4 Data Reduction 34

4.1 First order data reduction 34

4.2 Data reduction software 34

4.3 Pipeline 36

5 Commissioning 37

5.1 Focus 37

5.2 Wavelength solution 38

5.3 Alignment (position/rotation) 38

5.4 Throughput 38

5.5 Initial observations 39

6 Proposed Instrument Upgrades 42

7 Observations 43

7.1 Standard stars 43

7.2 Target galaxies 43

7.3 Target galaxy imaging 44

7.4 (super)nova watch 46

8 Future Work 48

9 Conclusions 49

10 References 50

11 Appendix A – BASIS SNR Calculator 52

12 Appendix B – BASIS Time-line Chart 53

13 Appendix C – BASIS Purchased Products List 54

14 Appendix D – Commission Reports 55

15 Appendix E – Original Initial Plan 65

1 INITIAL PLAN

1.1 A brief overview of the project

The Bayfordbury Observatory, University of Hertfordshire, UK, is acclaimed to be the best teaching observatory in the UK with six optical telescopes, four 16-inch and two 14-inch, a 4.5m radio dish, and a 115m-baseline radio interferometer. Due to the number of telescopes available, it has been possible for the optical telescopes to each host a different instrument. Current instruments available are high spec CCDs, a fast frame rate camera for planetary or lunar imaging, a slit spectrograph (SBIG SGS), an Hα filter for solar observations, and more. Recent developments have now enabled a robotic drive for one of the 16-inch telescopes, once again pushing Bayfordbury Observatory further into the lead as the UK's best teaching observatory. To keep in line with Bayfordbury Observatory's status, I will build and commission an Integral Field Unit (IFU) for one of the 16-inch telescopes. It appears that not only will this be the UK's first teaching IFU, but also the first IFU hosted by such a class of telescope (<0.5m).

The benefit of using an IFU is that it enables the observer to obtain spatially resolved spectra of a certain target in a single observation. In the field of Astronomy, IFUs are primarily used to observe galaxies, nebulae and Hα features, and can come in a variety of array sizes depending on the specifications of the host telescope and science goals. Current world-leading IFUs include FLAMES (Pasquini et al., 2002) based at VLT, GMOS (Hook et al., 2004) at Gemini North-South, SAURON (Bacon et al., 2001) at WHT, and SPIRAL (Sharp & SPIRAL Team, 2006) at AAT. All of these are monolithic lenslet arrays that chase similar science goals – galactic kinematics, stellar mass and population, host halo mass, and merger history. As BASIS uses an IFU, it would pursue similar science goals, though sights will first be set on finding the instrument's limits to see which science goals are possible. BASIS's IFU is a 19-fibre bundle, out of which coupled optical fibres feed an SBIG SGS. Originally, the IFU was to be a 1x19 Hexabundle (Bland-Hawthorn et al., 2011), but it was not possible to source one in time, so the closest match is built.

The SBIG SGS (Figure 1.1.1) has a slit length of ~6mm, which is long for such a compact spectrograph. This length is what constricts how many fibres can be used in this system, as the fibres are positioned along the slit in a 1-D array, and therefore constricts how many elements can be used in the IFU. The fibre to be used is OM2 communication fibre (50µm core, 125µm cladding, and 250µm buffer), which gives rise to a 2.875mm long 1-D array comprising of the 19-fibre IFU and 4 sky fibres displaced from the main bundle to minimise contamination (see Figure 1.1.2). The fibre feed will be ~5m long and protected in a flexible and lightweight rubber conduit. Mounts for both the IFU onto the telescope and the 1D-array onto the SBIG SGS will be made using a 3D printer (Object3D®, FullCure™ - VeroBlack). The plate scale of the LX200 is 51.6"/mm meaning that each IFU element (of 50µm core diameter) has an aperture of 2.6". Therefore, the 19-fibre bundle will have a field of view of ~1'.

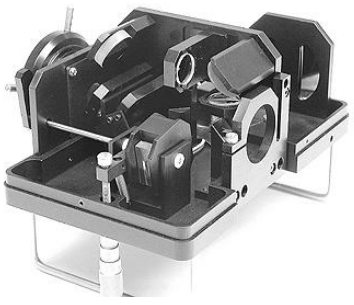

Figure 1.1.1 – (Holmes & SBIG, 2001) – SBIG SGS

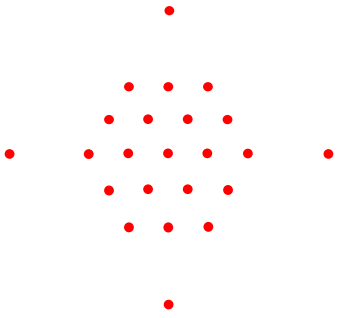

Figure 1.1.2 – Schematic of the fibre bundle configuration with sky fibres (four fibres displaced from main bundle – actually ~5x the distance shown). The red dots are representative of the 50µm fibre cores. Note that the hexagonal shape is ideal though most likely not possible for BASIS.

The SBIG SGS's camera is an ST-7E, which uses a Kodak KAF-0402ME chip with 9µm pixels in a 764x510 array (Holmes & SBIG, 2001). Using the 150 lines/mm grating, and with the 1-D fibre array giving a 50µm slit, it is possible to obtain a resolution of R≈750 at 500nm (~7Å). This means that with taking into account the specifications of the SBIG SGS, and applying an overall instrument efficiency/Total Throughput of 0.05, a 20min exposure of a 13mag/arcsec^2 source gives a possible SNR of 10 (see Appendix A). If multiple exposures were stacked to produce a 2hr exposure it would be possible to get a Signal-to-Noise Ratio (SNR) of 12 for ~13mag/arcsec^2 source.

The overall instrument efficiency/Total Throughput of 5% is a harsh estimation. The reason for setting it at this level is that instruments always perform worse than originally predicted. The SBIG SGS has five optical surfaces between the slit and the CCD. Most of the components of the SBIG SGS have good coatings and come from Melles Griot (Holmes, 2011) giving a 0.90 efficiency per surface. The ST-7E uses a Kodak KAF-0402ME CCD chip that has an average optical quantum efficiency (QE) of ~0.65, resulting in the efficiency of the SBIG SGS equating to 0.38. The overall size of the telescope/spectrograph/dome permits the use of a short length of fibre; in this case 5m. This means the optical performance of the communication fibre used in BASIS is at worst 15% loss in the blue, and at best 7% loss in the red. Communication grade fibre was chosen to keep cost to a minimum. Therefore, working with the following efficiencies: LX200 (0.90), IFU (0.90), Fibre (0.70 including Transmission and Fresnel reflection losses and Focal Ratio Degradation), SBIG SGS (0.38), the expected efficiency of BASIS is ~0.22.

There is uncertainty in the efficiencies set for the IFU and slit interfaces, which have the possibility of swinging either way. The main constraint on these interfaces would be the selected tolerances. This will depend on a number of factors; 3D printer tolerances including cost factors, the alignment of the fibres at the slit with respect to the optical axis of the spectrograph optics, the thermal expansion and the variable expansions between different materials, the quality of end face polishing, and the induced stress on the fibres when housed/glued in the interfaces.

The components needed to build this instrument are listed in §1.2 under the header *Sourcing* and those to be purchased are listed in Appendix C. A stand-alone camera will be mounted to the guide scope of the LX200, which will do the acquisition and guiding. This is necessary as the SBIG SGS self-guiding feature only works when using the slit at the focal plane of the LX200, not when using a pseudo slit comprising of fibre optics.

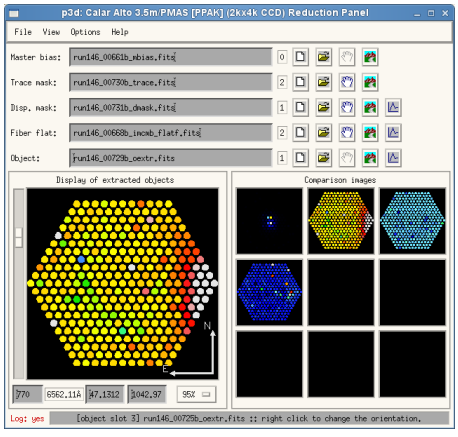

Figure 1.1.3 – (p3d, 2011) – A screenshot of the p3d software using the Potsdam Multi-Aperture Spectrophotometer (PMAS) instrument as an example.

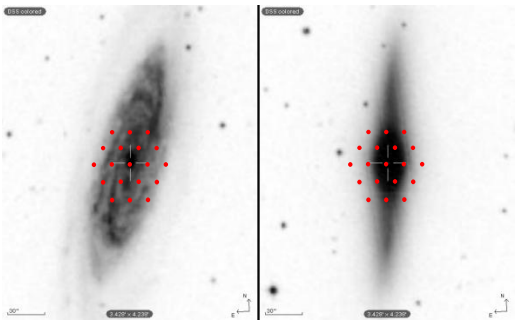

Figure 1.1.4 – Example of a suitable target selected from the RC3 catalogue with the BASIS IFU overlaid to scale.

To reduce the data given by the ST-7E I intend to use pre-written software called "p3d" (Sandin et al., 2010) (see Figure 1.1.3). p3d, is a general data-reduction tool for fibre-fed Integral Field Spectrographs (IFSs). It has a user-friendly interface, and includes a vast range of options for case specific data-reduction. Initial data reduction will be done manually by visually inspecting the spectra.

There will be an inevitable uncertainty on the expected performance of this instrument, so decisions on exact science goals and the use of the instrument will be left for a future project. My aim will be to carry out various observations to discover the limits of the instrument so viable science goals can be drawn. To do this I will reduce various catalogues; RC3 (de Vaucouleurs et al., 1991), NGC (Dreyer & Sinnott, 1988), HyperLEDA (Paturel et al., 2003) and NED (Schmitz et al., 2011) to find suitable targets (see Figure 1.1.4).

1.2 Project Time-Line

For this project, there will be four main stages: Sourcing, Assembly, Commissioning, and Science Limits. Due to the nature of instrument building, the dates assigned to the following tasks are deadlines, meaning that as long as they are completed before this date the project is on track, though I will endeavour to complete the tasks ahead of these dates to allow for inevitable delays. The dates shown are in Week Number (w#), where Week Number 1 (w1) is the week starting 03/10/2011. A visual spreadsheet representation is provided in Appendix B though this is the original Gantt chart (Time-Line Chart). It holds then that all parts below need to be in before wk9 noted by the suffix (l) for latest.

Sourcing: (see Appendix C)

w09(l)	Optical Fibre (24 core)
w09(l)	Polishing paper
w09(l)	Glue
w09(l)	Fibre cleaver
w09(l)	3D printing of IFU, IFU Mount, Focus Mount, 1-D array housing, SBIG SGS Mount
w09	p3d software

Assembly:

w10	IFU
w11	Fibre-feed
w12	Slit to SBIG SGS interface

Commissioning:

w15	Installation onto LX200
w15	Auto-guiding
w18	Commissioning

Science Limits:

w22	Instrument efficiency
w22	True SNR against mag/arcsec^2

Report Deadlines:

27/10/2011(w04)	Initial Plan
08/12/2011(w10)	Poster Presentation
09/02/2012(w19)	Sample Chapter & Contents Page
29/03/2012(w26)	Project Report & Viva (in May)

SPIE Important Dates:

19/13/2011(w12)	Abstract Submission
24/02/2012(w21)	Author Acceptance Notification
04/06/2012(w36)	Manuscripts Due
01-06/07/2012(w40)	Conference (Amsterdam, NLD)

1.3 Initial Plan comments

The above initial plan is somewhat different to the original one drafted at the start of this project (given in Appendix E). The reason for the change is one that is inherent to all instrumentation projects; the unpredictability of difficulties and problems that arise as the project develops. This meant the instrument itself has changed and so the plan had to change. The main differences were the decision to no longer use a fibre-fed micro-lens array as the IFU, to keep the buffer on the fibres such that the IFU doubles in diameter but fill factor is lost, and to only use 19 fibres in the bundle instead of the proposed 37 fibres. Full details of these changes will be discussed within their respective sections, mainly §3.3. The dates for the Report deadlines were met, so too were the SPIE Important Dates, which resulted in a future paper of this project being accepted for publication in July 2012 at the SPIE Astronomical Telescopes and Instrumentation conference.

2 INTRODUCTION

In attempting to answer the question, "Why do galaxies look and behave the way they do?" one must perform complex analysis of multi-wavelength data from many sources. It is because of this complexity that integral field spectroscopy, the ability to simultaneously obtain a 2-D image of a source and the spectra from each spatial pixel, was born and now flourishes.

2.1 The case for integral field spectroscopy and its teaching

The art of integral field spectroscopy is one that has come on in leaps and bounds over the last decade and is really pushing our understanding of galaxy formation and evolution. It also overcomes the single aperture biases found in some of the world-leading instruments that have contributed so much to this field already e.g. 2dfGRS and SDSS (Lahav & Suto, 2004) & (Bland-Hawthorn et al., 2011). These biases arise because when a single fibre is placed over a target, galaxy or other, then the spectrum that is observed is the convolution of the light from the entire galaxy. This is bad because the emission observed from a certain part of a galaxy is different to that from another. If one area, e.g. the core of the galaxy, is much brighter than another area, e.g. extended regions, then the information about the emission from the extended region is hidden behind the bright spectrum of the core. There is another problem when using single fibre spectroscopy, which is the exact placement of the fibre on sky, and which part of the galaxy or extended region it is observing if the galaxy is larger than the aperture of the fibre. This results in spectra being assigned to the galaxy that is not a full representation of the galaxy it is observing. Both of these biases, in addition to some others, are greatly reduced or even removed when observing a source with an integral field spectrograph.

An integral field spectrograph (IFS) that has really shown the true abilities of integral field spectroscopy is SAURON (Bacon et al., 2001) on the 4.2m William Herschel Telescope (WHT), and in particular the recent project ATLAS 3D (Cappellari et al., 2011) carried out using SAURON collecting data on 260 early-type galaxies. Integral field spectroscopy will only become more important in the years to come and with this, the next generation of astronomers will be the ones to analyse the vast swathes of data that will be produced by large-scale surveys. These large-scale surveys (tens of thousands of galaxies) are only possible by taking advantage of recent advancements in astrophotonics and their implementation on world-class 4+ meter telescopes, such as SAMI (Croom et al., 2011). There is one area that has not yet been exploited, which is the main premise for this project; the continued advancements in commercially available small aperture telescopes and their respective instruments that have the potential to achieve initial integral field spectrographic observations of hundreds or even thousands of galaxies. This opens the door for the science provided by integral field spectroscopy to be more attainable by institutions around the world. In this attainability, it is possible for the next generation of astronomers to get hands on experience of the instrumentation and science of IFSs.

There are currently in the order of thirty IFSs around the world ranging from lenslet arrays to fibre-feeds (with or without lenslets) to image-slicers (Westmoquette et al., 2009) (see Figure 2.1.1), though all but one are on 2+m telescopes making hands-on astronomy teaching a difficult task due to time constraints and practicality. It is because of this that most institutions around the world have an on campus or near campus observatory for teaching, whether it be a single small aperture telescope on the department's rooftop or multiple small aperture telescopes at a nearby isolated site. Therefore, creating an IFS that is well within an institution's budget (<$500) and utilises existing equipment is an attractive solution to the gap of integral field spectroscopy teaching found in observational astronomy practicals. With a practical on integral field spectroscopy students can learn not only the fundamentals of astrophotonic instrumentation, including the spectrograph, but also, and maybe more importantly, the physics of galaxies or other extended sources e.g. planetary nebula (discussed in §3.11).

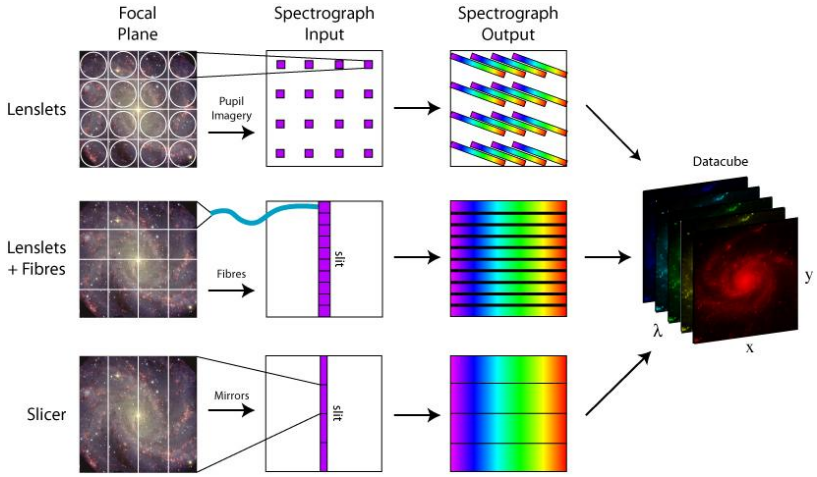

Figure 2.1.1 – (Westmoquette et al., 2009) & (Allington-Smith, 2006) – Schematic of different types of IFSs, all resulting in a data cube for a particular source. There are benefits and drawbacks for each style, so all types can be found in operation today.

There is another attractive outcome of creating an IFS for a small aperture telescope, which is the possibility of doing a first-glance survey of hundreds or even thousands of galaxies. This of course all depends on the performance of the instrument, and the requirements are outlined in §2.2. The type of galaxies that can be observed with a small aperture telescope are near-by (redshift $z \sim 10^{-3}$) and bright (apparent surface brightness $\lesssim 14$). Most of this class of galaxies have not been observed with an IFS yet, so any data that can be obtained would contribute to our understanding of galaxy composition and evolution. All the current IFSs around the world have a purpose, and most of them are probing into a set of parameter space that is specific to that instrument. Combined, they are unravelling some of the greatest mysteries about galaxy composition and evolution, so for a new parameter space to be added to this knowledge is only beneficial.

2.2 Scientific rationale

The spectral energy distribution of a star tends to peak in the optical, and as the luminosity of a galaxy primarily comes from the stars it contains; the host galaxy normally has strong spectral features in the optical. Analysis of these spectral features gives insight into galaxies' stellar and gas kinematics, star forming regions and rates, what the primary ionisation source is via placement onto a BPT diagram (see §2.2.2), and much more. Spectral line analysis is a widely used tool, and there are many ways in which you can extract information to find answers to the above properties. Figure 2.2.0 shows a template optical emission spectrum from an Sc type galaxy, with the average telluric spectrum overlaid. By looking at such a spectrum, the variations in emission line strengths and widths are easily visible, which is why they are used to probe the properties of the source of emission. The labels for each line are also given, and knowing which lines are which, is key to the analysis.

Fundamental physics dictates the positions of these lines, most of which are due to the ionisation of that particular atom. Roman numerals are given after the atomic symbol to denote the level of ionisation, where "I" is the neutral atom (no ionisation), "II" is the first level of ionisation (one electron removed), "III" is the second level of ionisation (two electrons removed), and so on. The Greek letters "α, β, γ, etc..." denote the level of transition in the Balmer Series of atomic Hydrogen, from principal quantum number n=3 to n=2 (3-2), 4-2, 5-2, etc… respectively. The line widths and strengths are a product of the environment and makeup of the location of ionisation. Therefore, by knowing the observed features we can know something about the ionisation source and its environment. Spectral classification of galaxies depends greatly on these data, so when spectral data is obtained with spatial information, via an IFS, much more can be known about the galaxy than by just using a single aperture instrument.

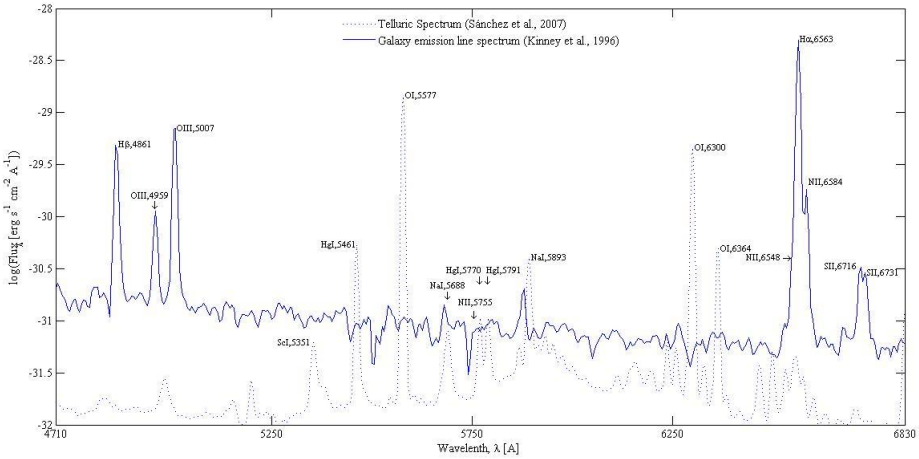

Figure 2.2.0 – Template Sc galaxy and telluric spectra. Data for templates was taken from (Kinney et al., 1996) & (Sanchez et al., 2007) respectively. Emission line labels are given to denote the atom and ionisation state that creates them.

2.2.1 Velocity Fields

The easiest property of a galaxy obtained via spectral analysis would be the galaxy's kinematics in the form of velocity fields using the Hα line relative to its control position (rest frame wavelength = 6563Å). As stars and gas move within, but primarily rotate with the galaxy, they cause a Doppler shift on the spectra observed. If you can obtain spectra from different parts of the galaxy, i.e. from an IFS, then you can get Doppler shifts for the spectra from each sample point. Knowing the position of the rest frame wavelength after fitting a Gaussian profile to the line, the simple subtraction of the observed line position (λ_{obs}) away from the control line position (λ_{ctrl}) and then dividing by the control line position yields the Doppler shift (see [Eq.2.2.1]). Care must be taken to make sure the overall Redshift (z) of the galaxy has been accounted for. This is done by looking at the integrated spectrum of the entire galaxy, finding where the position of the emission line is, and correcting for a factor of (1+z). If the redshift is unknown then this is how it is obtained. Multiplying the observed Doppler shift by the speed of light (c) gives a measure of the line of sight velocity (v) of the stars or gas within the galaxy (see [Eq.2.2.2]).

$$Doppler\ shift = \frac{\lambda_{obs} - \lambda_{ctrl}}{\lambda_{ctrl}} = \frac{v}{c} \qquad \text{[Eq.2.2.1]}$$

$$v = c\left(\frac{\lambda_{obs} - \lambda_{ctrl}}{\lambda_{ctrl}}\right) \qquad \text{[Eq.2.2.2]}$$

If the velocity is negative then it is said to be "blue shifted" and if it is positive then it is said to be "red shifted", normally shown by their respective colours on a velocity field. An example of such a velocity field showing the galaxy kinematics derived from the Hα line position is given in Figure 2.2.1, which has been taken from (Croom et al., 2011).

In the same way that single fibre spectroscopy is the integration of all the spectra from the individual sample points (known as spatial pixels, or spaxels) in an IFS, each spaxel is still the integration of the all the spectra from the emission sources within its aperture. The line width of a particular spectral line contains information of the velocities of the emission sources within the observation aperture, meaning that the smaller the spaxel, the narrower the line will become. Even though it is impossible to deconvolve spectra, the line widths do give information about the peculiar motions of the gas/stars within the aperture. The wider the line, the greater spread of velocities.

Hexabundle #009's Velocity Field

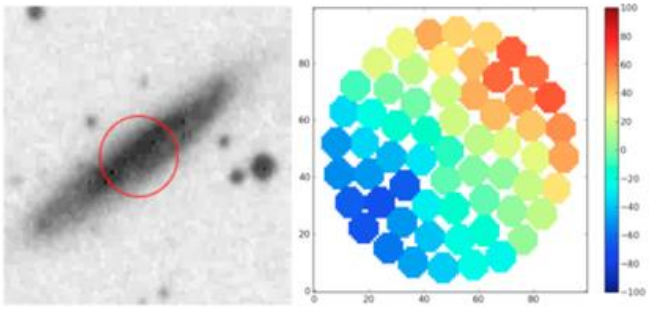

Figure 2.2.1 – (Croom et al., 2011) – Hα velocity field of spiral galaxy 6dFGS gJ195722.2-55081. The red circle overlaid on the image on the left shows the outer circumference of the IFU (Hexabundle) shown on the right. Each spaxel shown on the right is an individual fibre and has its own corresponding velocity shown by the scale on the far right in units of kms^{-1}.

2.2.2 BPT diagrams

On top of dealing with line positions and line widths, the next piece of information that can be extracted from spectral line data is the strengths of lines. It follows that the greater the line strength (or line height), the more of that ionisation is present. Fundamental physics allows the understanding of comparing different line strengths to each other. This has long been done, and is still one of the greatest ways to truly probe the environment and composition of the emission source. Baldwin, Phillips & Terlevich (1981) pioneered the way in a simple graphical classification system, the product of which are BPT diagrams. They compare different line strength ratios to find out which category an emission spectrum would fall into. This is because there are a variety of different ionisation sources. The main ones known to date are:

Active Galactic Nuclei (AGN) – Essentially these are as the name suggests; the nuclei of galaxies that are incredibly active, extremely energetic phenomena that closely match the luminosity of their host galaxy. They are the result of gas accreting onto a Super Massive Black Hole (SMBH). As the gas accretes onto the SMBH it heats up due to the conversion of kinetic and potential energies, i.e. angular momentum, gravitational, etc… (Rees, 1984). The heating up disassociates electrons from atoms, ionising them, producing a peak in the ultraviolet / optical wavebands (Osterbrock, 1991). There are quite a few sub-classes of AGN, and further more sub-classes of those sub-classes. The first biggest category classification is between types: Quasars and Seyfert. The separation is due to the luminosity of the AGN and host galaxy, and boarders at an absolute M_B = -23 (Schmidt & Green, 1983). If the galaxy and AGN are brighter than M_B = -23 it is classified as a Quasar (or QSO), and if fainter a Seyfert. Seyfert galaxies make up most of the known AGN. They can be divided into two sub-classes called Seyfert I and Seyfert II. The divide this time comes from the emission line width. If the Full-Width Half-Maximum shows peculiar velocities of ~3000kms^{-1} then it is a Seyfert I galaxy, if ~350kms^{-1} then it is a Seyfert II galaxy (Dahari & De Robertis, 1988).

Low-Ionisation Nuclear Emission-line Regions (LINERs) – When spectra only really show emission lines up to the first ionisation level of any atom, and are relatively strong, it is safe to assume that the environment is in a state of low-ionisation. When centred around the nucleus, these regions are known as LINERs. They may resemble Seyfert II galaxies, but are lower in luminosity and have a distinguishable stronger OI optical line strength (Kewley et al., 2006).

Low-Ionisation Emission-line Regions (LIERs) – These are distinguishable from LINERs by their high dependence on the Hydrogen Balmer Line series, and a stronger Helium line at 3970Å (rest frame). It is suggested that this is because LIERs are more associated with star forming regions than AGN (Buttenshaw, 2011).

HII Regions – These are regions of the galaxy in which Star Formation (SF) is active. Massive young stars are born, which peak their emission in the ultraviolet resulting in the ionisation of the surrounding Hydrogen cloud (hence HII). The greater the star formation rate (SFR), the stronger the Hydrogen Balmer Line series. If SF is strong, then when other emission line strengths are compared to the Balmer Series their respective ratios are lower. The age of the galaxy does play a part in this relationship, as the older the galaxy the lower the SFR, and more generations of stars (meaning metal-rich stars, which have a lower effective temperature and therefore lower ionisation ability) (Dunlop, 2011).

Wolf-Rayet (WR) Stars – Stars of mass >20-30$M_{\odot}$ go through intense mass loss on the main-sequence and by the time they have reached the Red Giant Branch (RGB) have shed their Hydrogen envelope exposing a Helium rich core. There are two main types of WR stars, categorised by the composition of their core, either WN (Nitrogen rich cores) or WC (Carbon and Oxygen rich cores). If emission spectra has a strong, broad Helium emission line, as well as respective strong, broad emission lines of Nitrogen for WN and Carbon and Oxygen for WC, then it is safe to assume that the ionisation source is from WR stars.

All of the above ionisation sources exhibit different spectral features so spectral line analysis can differentiate between them. Spatially resolved spectral data from an IFS can lead to analysis of the different regions of the galaxy, instead of assuming the whole galaxy is ionised by one source. This is why integral field spectroscopy can remove the biases found in single aperture spectroscopy. Figure 2.2.2 shows BPT diagrams comparing different line strength ratios and the classification regions for each ionisation source. First order interpretation of the three main regions of the BPT diagrams is as follows:

Star Formation – Produces strong Hydrogen Balmer Series giving rise to low ratios in comparison to any other line strengths. Bottom left on BPT diagram.

AGN – Strong high ionisation of all atoms leading to a high ratio of OIII/Hβ, near equal ratios of NII/Hα and SII/Hα, and a fair ratio of OI/Hα. Top on BPT diagram.

LINERs – Low ionisation meaning a low or near equal ratio of OIII/Hβ, and closer to equal ratios of NII/ Hα, SII/ Hα and OI/ Hα. Right on BPT diagram.

Each of these category definitions need to pass certain mathematical criteria to be classified, and such formulae and definitions can be found in Table 2.2.2, which also show an example spectrum of each classification. The flux value is obtained after fitting a Gaussian profile to each emission line. It is accepted that meeting two of the criteria is enough to be classified (Baldwin et al., 1981). Which criteria are used is normally confined by the wavelength parameters of the observation, i.e. the bandwidth of the spectrograph. It holds though that the more criteria that are met, the greater the accuracy of the classification. The empirical cut-offs shown in Figure 2.2.2 are a good way to get a first order classification.

The line ratios OIII/Hβ and NII/Hα are the most commonly used ratios for classification as they are normally the brightest lines, and fall within an optical bandwidth obtainable by most spectrographs. To be able to observe these lines (rest frame wavelengths: Hβλ4861 – OIIIλ4959, 5007 – NIIλ6548, 6584 – Hαλ6563) a resolution of ≲1nm is needed along with the ability to either obtain all of them in one observation (bandwidth of ~210nm) or by patching together two observations (bandwidth ~40nm) centred around OIIIλ4959 and Hαλ6563 respectively. A signal-to-noise ratio of ~few at minimum is required to be able to get flux values. The greater the number of spaxels the better, with a realistic minimum being ~19 (hexagon with two rings), and the greater the fill factor (the ratio of spaxel on-sky area to surface area of observed source) the better, but at minimum a few percent. These lines are the ones that can be observed using a small aperture telescope, and are therefore the lines that can be used for not only teaching the physics of galaxies, but also contributing to current knowledge of galaxy composition and evolution.

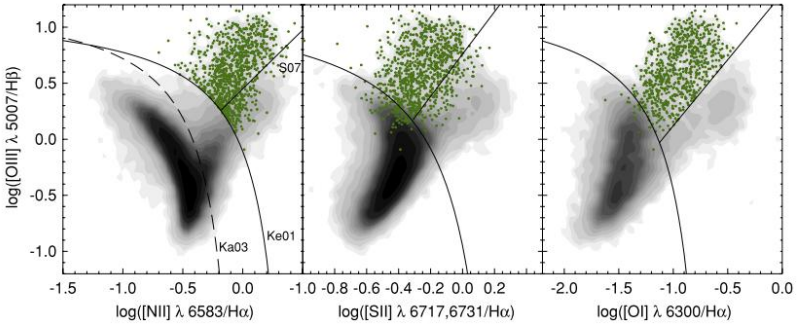

Figure 2.2.2 – (Schawinski et al., 2010) – BPT diagrams comparing different line strength (flux) ratios. The dotted curve (Kauffmann et al., 2003) [Ka03] represents the theoretical maximum cut-off for ionisation due to star formation. The solid curve (Kewley et al., 2001) [Ke01] represents the empirical cut-off for ionisation due to star formation. The solid line (Schawinski et al., 2007) [S07] represents the empirical separation between ionisation from AGN (above the line) and ionisation from LINERs (below the line).

Primary source of ionisation	Standard line ratio formula for classification (Kewley et al., 2006)	Example spectra for each classification (Ho et al., 1993)
Star Formation	$\log\left(\frac{[OIII]}{H\beta}\right) < \frac{0.61}{\left(\log\left(\frac{[NII]}{H\alpha}\right) - 0.05\right)} + 1.30$	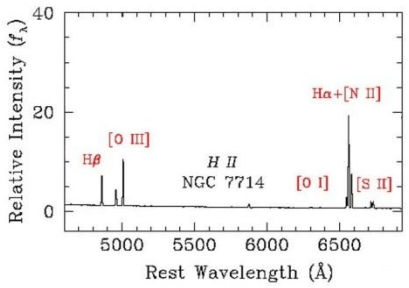
	$\log\left(\frac{[OIII]}{H\beta}\right) < \frac{0.72}{\left(\log\left(\frac{[SII]}{H\alpha}\right) - 0.32\right)} + 1.30$	
	$\log\left(\frac{[OIII]}{H\beta}\right) < \frac{0.73}{\left(\log\left(\frac{[OI]}{H\alpha}\right) + 0.59\right)} + 1.33$	
AGN	$\log\left(\frac{[OIII]}{H\beta}\right) > \frac{0.61}{\left(\log\left(\frac{[NII]}{H\alpha}\right) - 0.47\right)} + 1.19$	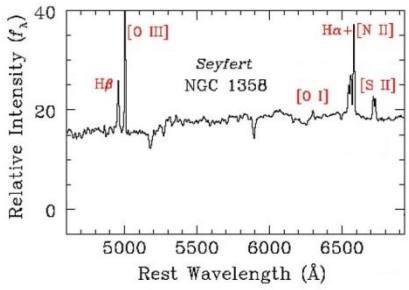
	$\log\left(\frac{[OIII]}{H\beta}\right) > \frac{0.72}{\left(\log\left(\frac{[SII]}{H\alpha}\right) - 0.32\right)} + 1.30$	
	$\log\left(\frac{[OIII]}{H\beta}\right) > \frac{0.73}{\left(\log\left(\frac{[OI]}{H\alpha}\right) + 0.59\right)} + 1.33$	
LINERs	$\log\left(\frac{[OIII]}{H\beta}\right) > \frac{0.61}{\left(\log\left(\frac{[NII]}{H\alpha}\right) - 0.47\right)} + 1.19$	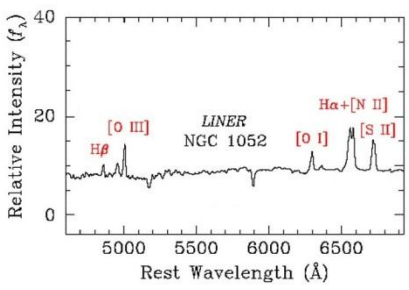
	$\log\left(\frac{[OIII]}{H\beta}\right) > \frac{0.72}{\left(\log\left(\frac{[SII]}{H\alpha}\right) - 0.32\right)} + 1.30$	
	$\log\left(\frac{[OIII]}{H\beta}\right) < \frac{0.73}{\left(\log\left(\frac{[OI]}{H\alpha}\right) + 0.59\right)} + 1.33$	

Table 2.2.2 – Standard emission line flux ratios for the classification of the source of ionisation in an emission line spectrum extracted from (Kewley et al., 2006). An example spectrum for each classification is given for visual interpretation of the spectral analysis. The spectra shown here have been extracted and modified for comparison from (Ho et al., 1993).

3 BAYFORDBURY SINGLE-OBJECT INTEGRAL FIELD SPECTROGRAPH (BASIS)

The main drive for building BASIS was the attempt to create an IFS that could be used by institutions and amateur astronomers around the world. To do this, a number of constraints had to be put on the instrument. These included: to use as much Commercial-Of-The-Shelf (COTS) products as possible, to be installed at an average site (i.e. not at the top of a mountain), to use existing components where possible, to be within a reasonable budget (<$500) (see Appendix C), and to be as easily replicated as possible with construction methods available to the average user. The following sections cover these constraints and describe the development and method of construction for each part.

3.1 Choosing the site

When it came to choosing the site to install BASIS there was not much of a choice, though this was not by any means a disadvantage. Due to BASIS being built within the University of Hertfordshire, the Bayfordbury Observatory, which is a part of the university, was the default choice. If there were a number of sites to choose from, Bayfordbury would still have been chosen. This is because Bayfordbury is acclaimed to be the best teaching observatory in the UK, with four 16-inch and two 14-inch optical telescopes, a 4.5m radio dish, and a 115m-baseline radio interferometer. With this amount of telescopes at hand it is possible to assign each telescope with a specific instrument / purpose. Bayfordbury continues to push its capabilities and lead at the forefront of using small aperture telescope technology, with recent the commissioning of the UK's first fully remote telescope, the UK's best Lucky Camera (sensitive high frame rate camera that can obtain high-resolution imaging), and the UK's longest baseline radio interferometer within a university's observatory. It is only right then that this project follows in these footsteps and so implementing the World's first IFS on a small aperture telescope at Bayfordbury seems fitting.

As with all astronomical observatories in the UK, Bayfordbury suffers from the unpredictable weather patterns, and so only gets ~26% clear time (see Table 3.1). Its location, just outside of Greater London in the countryside, means that light pollution is a factor, but not as much as most UK observatories that are inside cities. Table 3.1 gives descriptive figures of Bayfordbury. With all factors considering, including existing equipment, Bayfordbury is a great site to host BASIS and to test its capabilities.

Bayfordbury Observatory

Location	Hertfordshire, UK
Longitude	-0.094399
Latitude	+51.774891
Altitude	65m
Percentage of clear time	26.2%
Average seeing	~3"

Table 3.1 – Bayfordbury Observatory site data taken from the Ordnance Survey, UK, and (Bayfordbury, 2012).

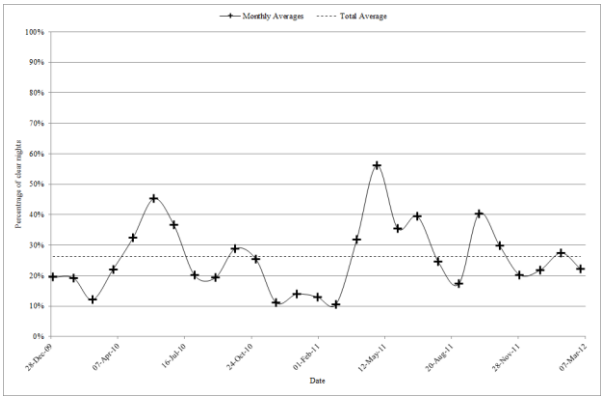

Figure 3.1 – Bayfordbury Observatory monthly average percentages for clear nights.

3.2 Existing equipment

A big part of keeping the cost down is the use of existing equipment. The main components of BASIS are the telescope it is mounted on, the IFU and the spectrograph. Two of those are pre-existing at Bayfordbury, the telescope, Meade LX200 16-inch, and the spectrograph, Santa Barbara Instrument Group Self Guiding Spectrograph (SBIG SGS) (see §3.4 for a full detail of the SBIG SGS). For the IFU, the method of construction was chosen be done on an Object3D® printer, using the FullCure™ – VeroBlack material. The 3D printer was already in house at the University of Hertfordshire, and has the great benefit of being able to do one-offs, essential for product development. It takes a while to print some parts, dependant on the height of the part (~half an hour per millimetre of height / depth). This time is offset against the labour hours that would go into building it by hand, so in the end it is much more efficient to print parts. This ability to print one-offs meant that changes could be made very easily, but also meant that changes happened frequently. From the initial design of some parts to what the final print looked like is quite different. The process of development of individual parts is detailed in the following respective sections.

3.3 Meade LX200 16-inch

The telescope chosen to host BASIS was the Meade LX200 16-inch Schmidt Cassegrain optical telescope (see Figure 3.3.1), one of the most sold high-end small aperture telescopes around the world. This means that not only does it fit BASIS as being a telescope that can achieve deep-sky research, but also that it makes BASIS that little bit more replicable for other institutions and amateur astronomers. It has a 3-inch opening for mounts at the focal plane, though most instruments have 2-inch or even 1¼-inch mounts that fit into either an adapter or usually a focuser that acts as the adapter. This is because the focal plane is not a perfect plane and is curved, meaning the further away from the optical axis the more unfocused it will be. To this end, most instruments are designed to a working focal plane of ~40mm (1¾-inch). BASIS is well within this tolerance with the largest separation of fibres (sky fibre to sky fibre) being 10mm (¼-inch). It can be assumed then that the focal plane is uniform in focus across the entire IFU. There is a screw lock on the back of the primary mirror that enables the user to adjust coarse focus, and which can be tightened to minimise mirror lag.

Figure 3.3.1 – (Galactica, 2012) – Meade LX200 16-inch Schmidt Cassegrain optical telescope with an equatorial mount.

3.4 Santa Barbara Instrument Group Self Guiding Spectrograph (SBIG SGS)

The spectrograph chosen to be used for BASIS is the Santa Barbara Instrument Group Self Guiding Spectrograph (SBIG SGS) (see Figure 3.4.1). Again, this is a widely used spectrograph, one that most institutions around the world have, with over 500 sold globally (Holmes, 2012). The capability of being able to adjust the central wavelength on the CCD by using a micrometer to change the grating angle is one of the main reasons for choosing the SBIG SGS. Not only can the user change the grating angles, but also change the grating all together from low resolution (150 lines per millimetre) to a high resolution (600 lines per millimetre = 600 l/mm). SBIG have recently released an even higher grating that has 1800 l/mm, though only the 150 l/mm and 600 l/mm are available on the SGS used for BASIS. There is a trade-off with using higher resolution gratings, and that is the bandwidth due to the higher dispersion from a greater line density.

The decision to use the 150 l/mm grating over the 600 l/mm was made due to the science goals. As mentioned in §2.2, more science can be achieved with a bandwidth that spans from the Hβλ4861 to SIIλ6731 emission lines. This ~2000Å bandwidth is only achievable when using the 150 l/mm. The trade-off is lower resolution, but with a 50µm slit this is ~7Å, which is valid for the proposed science goals in §2.2. It would be possible to switch to the 600 l/mm grating to achieve a higher resolution (~2Å), but it would mean having to take two exposures, adjusting the central wavelength in between due to the shorter bandwidth (~400Å). If the user only wanted to obtain one line or one set of lines, i.e. Hαλ6563, then switching to the 600 l/mm is valid, but because the dispersion is greater (less light per unit area), the exposure would need to be longer to achieve the same signal-to-noise ratio. A representation of the 150 l/mm grating is given in Figure 3.4.3, which also contains expected performance that includes the expected performance of the SBIG SGS (without the CCD ≈ 59% [five optical surfaces each with 90% efficiency]). In Figure 3.4.3 the vertical red lines show the bandwidth (~2120Å), which contains all desired emission lines for the science goals with some leeway either side in case of misjudgement with the central wavelength / dispersion. The solid blue line is a template emission line spectrum (Kewley et al., 2001) that has a resolution of 15Å. It shows then, that even if the theorised 7Å is an overestimation, the spectral lines needed for the science goals can still be resolved, though realistically a 15Å resolution is the limit before some lines become too convolved to be resolved.

Small modifications had to be made to the SBIG SGS for use in BASIS, mainly the removal of the slit mask, the calibration LED, the entrance aperture glass mask and other unneeded components to the self-guiding system that were obstructing instalment. How the fibre slit is attached to the SBIG SGS will be covered in §3.8.

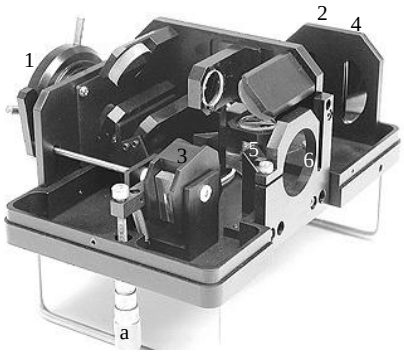

Figure 3.4.1 – (Holmes & SBIG, 2001) – SBIG SGS. The numbers are respective to those in Figure 3.4.2, though in this case there is a mirror similar to stage 5 that is in between stages 1 and stage 2. Here the letter "a" indicates the micrometer that adjusts the grating angle, and therefore the central wavelength on the CCD.

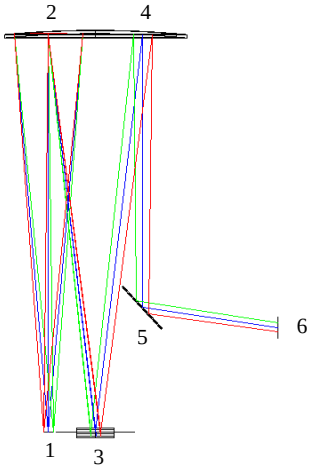

Figure 3.4.2 – (Holmes, 2011) – SBIG SGS Zemax Optical Ray trace design, without the first mirror. Light path starts: 1. Entrance slit (1-D array of fibres = 50µm slit), 2. Collimator, 3. Adjustable grating, 4. Focuser, 5. Mirror, 6. CCD.

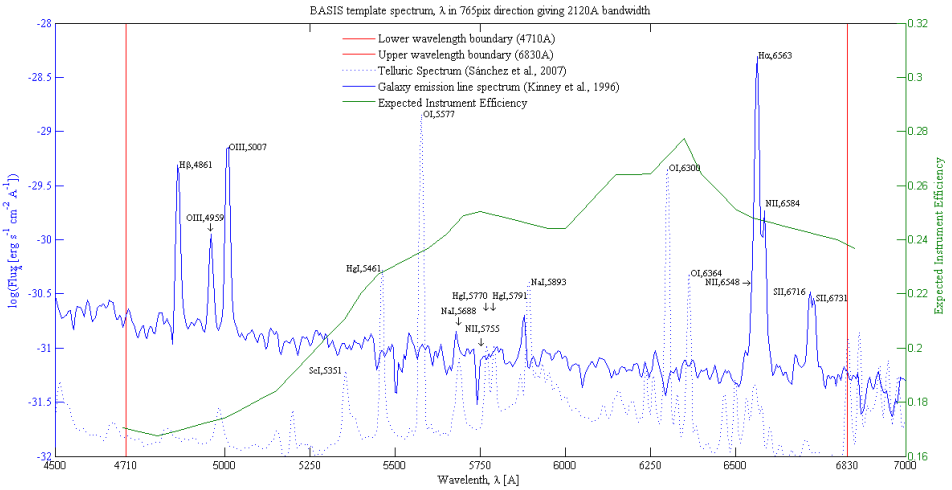

Figure 3.4.3 – Representation of the spectra able to be obtained using the 150 l/mm grating. The vertical red lines show the bandwidth (~2120Å). The template galaxy spectrum (solid blue line) has a resolution of 15Å. The expected efficiency (solid green line) is a convolution of all efficiencies and will be discussed in §3.11. The dotted blue line is the telluric spectrum at similar resolution.

3.5 SBIG ST-7E CCD

The SBIG SGS's camera is an ST-7E, which uses a Kodak KAF-0402E CCD. The main factor that affects the performance of BASIS when it comes to using the ST-7E is the Quantum Efficiency (QE) of the chip itself. QE is defined as the ratio of outgoing electrons against incoming photons where 100% would be for every photon the pixel collects, one electron is displaced (i.e. one count). The specifications of the CCD are given in Table 3.5, the QE of the KAF-0402E is shown in Figure 3.5.1, and an image of the ST-7E connected to the SBIG SGS is shown in Figure 3.5.2. The QE is included in the convolved efficiency shown in Figure 3.4.3.

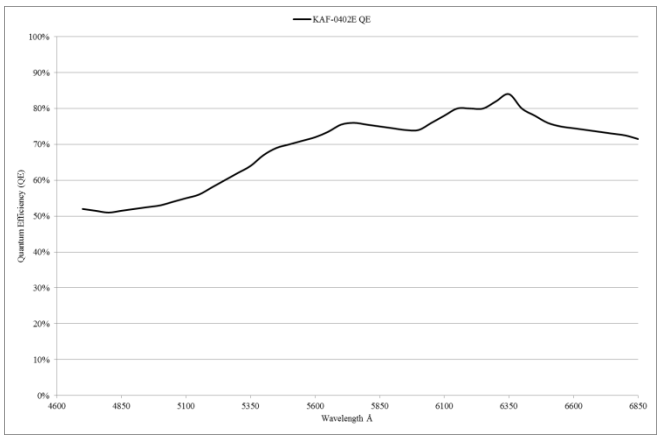

Figure 3.5.1 – KAF-0402E Quantum Efficiency. Average efficiency ≈ 65%.

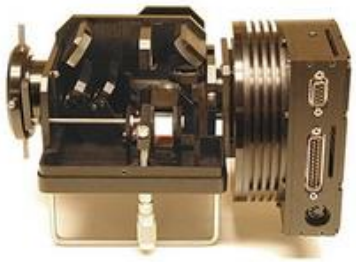

Figure 3.5.2 – (ATC, 2010) – ST-7E connected to the SBIG SGS at stage 6 in Figure 3.4.1.

KAF-0402E Specifications

Architecture	Full-Frame CCD: Enhanced Response
Total Number of Pixels	784 x 520
Number of Active Pixels	765 x 510
Pixel Size	9µm x 9µm
Average QE	~65%
Dark Current at 0ºC	1 e-
Read Noise	15 e-
Read-out	16 bit
Full Frame Download	1 second

Table 3.5 – (Kodak, 2003) – KAF-0402E specifications.

3.6 Optical fibre cable

The fibre cable used in BASIS is a COTS OM2 50/125/250 fibre used by the communications industry (Polymicro, 2008). There was a long discussion as to what fibre should be used to achieve the best performance possible, but it was decided that the OM2 fibre was as good as any science grade fibre when working with lengths of <5m. The length is the main factor in performance statistics. This is because of two main properties of the fibres known as "attenuation" and "Focal Ratio Degradation (FRD)". Attenuation is the name given to the amount of light lost in the fibre over the length specified. No fibre is perfect, and so when light propagates down the fibre some light is not reflected by the cladding and so escapes from the core (see Figure 3.6.1). There are times where the light is absorbed by the composite materials of the fibre itself, leading to a greater amount of light loss. FRD is the inherent property of fibres that roots itself in the fact that fibres are by no means perfect light guides. It is the property that describes the change in cone angle from the accepted light at the start of the fibre to the exited light at the end of the fibre (see Figure 3.6.1). There are a number of factors that contribute to this, mainly: how clean and polished the end-faces are, external stress on the fibre (i.e. glues, clamps, etc…) and the bend radius of the fibre (minimum radius to prevent this is ~10cm).

Optical fibres with a core size of 50+µm class as multi-mode fibre, meaning that they can accept multiple modes of light, rather than single-mode fibre (core size 8µm) that can only accept one mode of light. A crude way to think of this is that multi-mode fibres can accommodate multiple pathways that the light can travel on, whereas the single-mode fibre can only accommodate one pathway, a straight line down the optical axis of the fibre and therefore has no acceptance cone, but an acceptance column (a cone with an extremely small acceptance angle). The reason why 50µm core fibre was chosen was due to the science goals; creating a 50µm slit at the SBIG SGS to achieve a resolution of 7Å. As most instrumental parameters mean that if the result from deciding a parameter is good there will be one that is forced to be bad, the trade-off here is the fill-factor in the IFU. This is the ratio of total collecting area (summing up all fibre core areas) against the total spread area of the fibres. The implications of this will be discussed in §3.7.

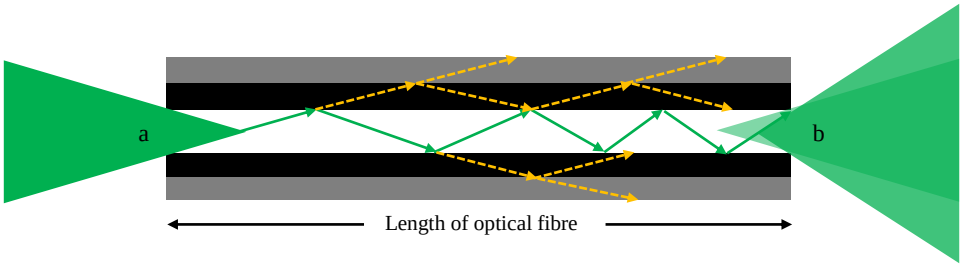

Figure 3.6.1 – Schematic of an optical fibre cable. The grey is the fibre buffer, 250µm diameter, the black is the fibre cladding, 125µm diameter, and the white channel is the fibre core, 50µm (Note: not to scale). The green cones a and b are the acceptance and exit cones respectively with the acceptance cone drawn over b to show FRD. The green arrows show the light path, note the greater angle of reflect through the length of the fibre due to FRD. The yellow arrows show the light escaping from the core, going into the cladding and eventually finding its way out of the fibre completely. This adds to the attenuation greatly.

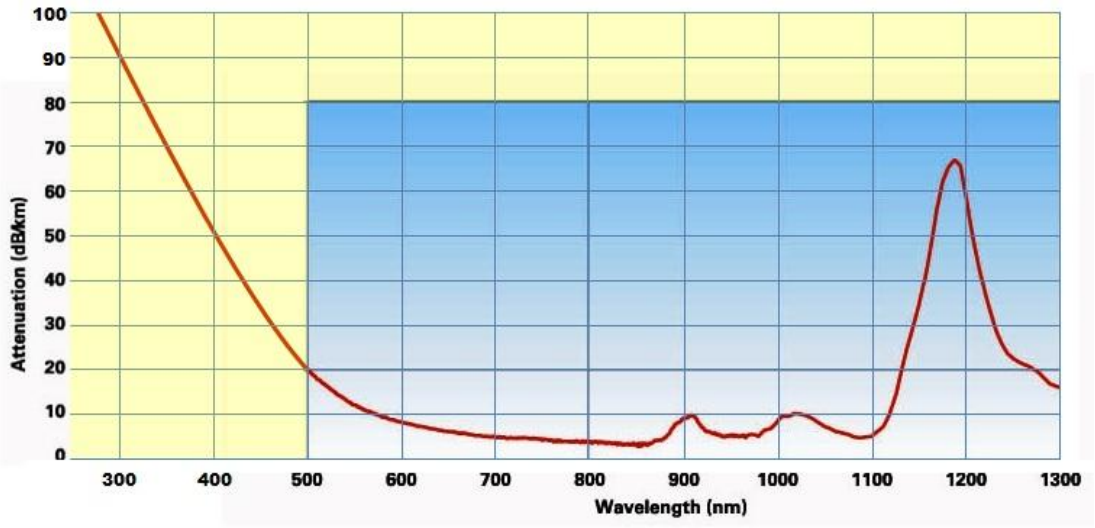

Figure 3.6.2 – Adapted from (Polymicro, 2008) – OM2 optical fibre attenuation. The blue area is the data from (Polymicro, 2008) and the yellow area is the estimated data. Data for sub-500nm is very rare as there is no need to go this far down in communications. Note the scale is in dB/km, so for a 5m length of fibre these values are greatly reduced.

$$dB = 10 \times \log_{10}\left(\frac{Power\ in}{Power\ out}\right)$$

[Eq.3.6]

The OM2 fibre that was purchased (see Appendix C) came as a loose bundle of 24 fibres protected in furcation tubing and then again in a rubber tube. This was ideal for use in BASIS as the total number of fibres used is 23 (19 in the bundle, 4 sky fibres), and so coming pre-protected saved time, effort and money. The redundant fibre was cut short to be out of the way, but there is no reason why it could not be used as a channel for something. It could have been an additional sky fibre, but the decision was made not to because it would break the symmetrical pattern of spectra on the CCD. The attenuation of the OM2 fibre used is shown in Figure 3.6.2. Note that the scale is in dB/km. The unit dB (decibel) is a logarithmic value defined in [Eq. 3.6]. Therefore, an attenuation of 5dB results in a power efficiency of $10^{-0.5}$ or 32%. When speaking of optical fibres, this value tells you how much light is being lost down the fibre. The convention of using units of dB/km for optical fibre is because the units are very small per metre. Looking at Figure 3.6.2, even in the short wavelengths where the attenuation is the greatest, ~50dB/km, for a 5m length of fibre the attenuation is only 0.25dB, which translates to 94% efficiency. Science grade fibre can produce a better efficiency, but only by a couple of percent at most when dealing with a 5m length. That couple of percent is negligible when dealing with the combined efficiencies of all the other components in BASIS, so saving a factor of 10 on cost as well as the ease of buying the fibre (you can buy communication grade fibre at a hardware store) warrants the use of the OM2 fibre.

3.7 Integral Field Unit (IFU)

Fibre fed integral field spectrographs give rise to a number of options when designing an IFU. The first choice is whether or not to use a micro-lens array. The advantage of using a micro-lens array is that you can greatly increase the fill factor and light coupling efficiency with the optical fibres, where the fibres are positioned at the back face of the array. The disadvantage is that having the micro-lenses in the optical path lowers the f/number. The f/number describes the acceptance cone angle where a high f/number, f/10, has a small acceptance angle and a long focal length, and a low f/number, f/2, has a large acceptance angle and a short focal length. At the Cassegrain focal plane (where the IFU is positioned), the LX200's light beam is f/10. If a standard micro-lens array were used, the beam would be reduced to f/2, which is at the limit of the OM2's acceptance. This takes us back to FRD, where the "degradation" is the reduction in f/number (the result is shown in Figure 3.6.1 and Figure 3.7.1).

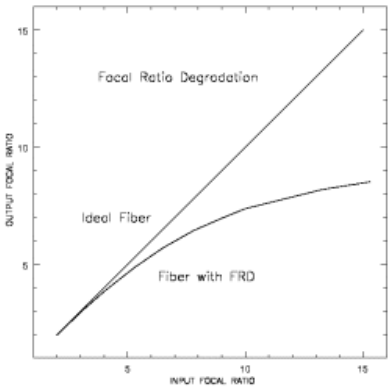

Figure 3.7.1 – (GSMT, 2002) – Focal Ratio Degradation in optical fibres. The larger the input f/number, the more FRD is present (more deviation from a perfect fibre).

If the micro-lens array were used then the f/2 beam would be more conserved through the fibre, but the problem comes when using the SBIG SGS as it is built to accept light beams with f/numbers between f/6.3 and f/10. The higher the f/number the more efficient the spectrograph will be, though too high and the focal length would be so long the spectrograph would be metres long. All of these factors come together when building a telescope instrument, and finding the correct proportions is a difficult task. As the LX200 and the SBIG SGS are "fixed" components then the IFU has to work to these parameters. The decision was made to omit the micro-lens array and have bare fibres at the focal plane. This means the fibres are coupled with the f/10 beam from the LX200, meaning that some FRD would take place. As mentioned in §3.6, the longer the fibre the more FRD, but for a 5m length of fibre the FRD is quite small. Without doing a full lab set up to measure the FRD in the OM2 fibre (which takes months to perform), it is safe to assume that the f/10 would be reduced to at most f/7 across the 5m length, where in fact is it likely to be less than this. The FRD to f/7 tells you the output cone angle of the OM2, which is within the acceptance of the SBIG SGS of f/6.3 to f/10. This validates the use of the OM2 and also omitting the micro-lens array.

The decision to omit the micro-lens array means the IFU would have bare fibres at the focal plane. The trade-off here is fill-factor and coupling efficiency. The 50μm core size of the OM2 fibre results in a poor fill-factor, where ideal cases would be >50%. If the fibres had their buffer removed, which is easily achieved with a sharp razor blade by scraping off the soft buffer, the closest the fibres could get to each other is a core-to-core separation (pitch) of 125μm. For a bundle of 19 fibres, taking five fibres width to be the diameter of the bundle, the fill-factor is given by [Eq.3.7.1]:

$$fill\ factor = \frac{sum\ of\ the\ aperture\ areas}{spread\ area\ of\ all\ apertures} = \frac{19\pi(50\mu m)^2}{\pi(5\times 125\mu m)^2} = 0.122 \approx 12\%\,.$$

[Eq.3.7.1]

Knowing that the IFU would be a 19-fibre bundle, the next challenge is exactly how one makes a fibre bundle, which in itself is a difficult and delicate task. The communications industry has dedicated machines to do this, which do it very accurately, but the cost of getting a small bundle made would run into thousands of pounds. Although outside the budget of this project, it would become a viable option if BASIS proves to be successful. The following list describes the various stages of the development of the IFU / fibre bundle. This process took most of the time in the project, effectively pushing the initial time-line so far that it was in effect scrapped, with last minute shuffling to be able to do the commissioning and get some on-sky data. In all, this process took ~4 months (including the time for the 1-D array).

Stage 1 There are various ways to make a fibre bundle; the best is the Hexabundle used in SAMI (Bland-Hawthorn et al., 2011) & (Croom et al., 2011). Unfortunately, there were no spare Hexabundles for use in this project, so the first attempt at making a bundle was using heat-shrink around a loose bundle of fibres. This was done at the University of Sydney in July 2011. It was somewhat successful, though could not give a circular bundle as the heat-shrink undergoes a non-uniform contraction. The result is given in Figure 3.7.2. Here there are 61 fibres and the bundle has had a light polish to remove most dust / imperfections. The fibres were cleaved with a pair of pliers, hence why some fibres have "snapped" end faces. This was the best one of about ten made; the others were a lot worse. Reproducing this method is not viable and the need to have more fibres than required to produce a working 19-fibre bundle somewhere in the array is wasteful. When done with only 19-fibres, the bundle was misshapen beyond use. Using heat-shrink is then not an option.

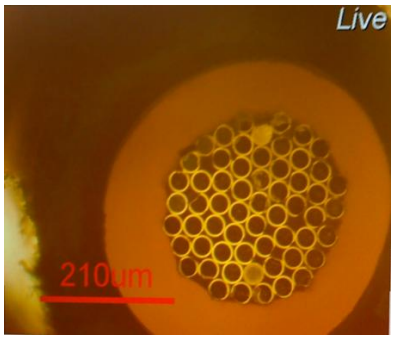

Figure 3.7.2 – Microscope image of heat-shrink fibre bundle after polishing.

Stage 2 After trying the heat-shrink method, an investigation into making a fibre positioning substrate was undertaken. It was this stage that took the longest (~2months). It was quickly discovered that making a fibre positioning substrate is not a trivial task, and one that pushes the limits of manufacturing in many areas. The first difficulty comes with trying to make 127µm holes in a substrate. No matter the material, this proved more problematic than originally thought. It is possible to buy 127µm drill bits, but they only have a thread that extends for ~1mm, which means the substrate has to be less than 1mm thick, not enough to hold a fibre in position. Threading fibres through two or even three substrates that had larger holes in them, and then interlocking the substrates to fix the position of the fibres was the next method. This would work in theory, but getting it to work practically was very tricky and so this method was dropped. Using a chrome mask to create the holes would work, but is very expensive (thousands of pounds), therefore, not deemed to be viable option either.

Sights were then focused on using an in-house 3D printer (Object3D®). This 3D printer uses the polymer material, FullCure™ – VeroBlack. 3D printers work by layering down a liquefied photosensitive polymer and immediately exposing it to UV light, hardening the substrate. This whole process is called, "Digital Light Processing (DLP)". There is a soft polymer support matrix that fills the gaps in the product design to give support during the printing process. The matrix is removed afterwards and the finished product is left. This all sounds very straight forward, but the unknown here is whether or not the 3D printer could print holes as small as 127µm and do so in substrates >1mm. A series of tests were then performed on the 3D printer to find its realised resolution. Figure 3.7.3 shows the array that were printed to perform this test, where as many parameters were varied as possible, including the hole size, hole shape, hole orientation, substrate thickness and manufacturing consistency.

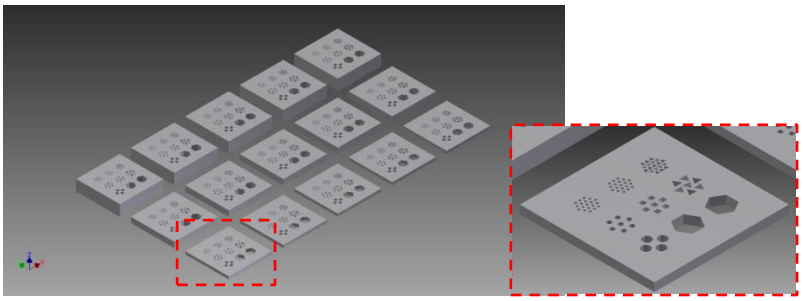

Figure 3.7.2 – Drawing of the 3D printer parameter test array. Each row is half the thickness of the previous starting with 2mm, 1mm then 0.5mm. A zoomed image of one substrate is given in the lower right. Here the holes in the first column are circular, the second are square, and the third are triangular. The first row has 130µm holes spaced 250µm apart. The second row has 260µm holes spaced 400µm apart. The third row has 400µm circular holes, a hexagon of edge-to-edge diameter of 1.275mm (five fibre diameters), and the same hexagon but rotated by 30º to get a vertex on the leading edge. The whole set was replicated five times giving the array in the main image. All substrates are 10mm (l) x 10mm (w).

The outcome of this parameter test revealed a consistent printing resolution of >200µm, which means printing holes of 130µm in size is not possible. The shape of the hole did not really make a difference, but when threading fibres through, the triangular holes were the easiest. The orientation of the hexagons produced no difference. The substrate thickness did have a big difference where the smaller holes on the 2mm thick substrate had closed up roughly half way down the hole. The 0.5mm substrate was too thin and therefore too flexible, so would not be able to hold the fibres properly.

The support matrix mentioned earlier had a large role in this test too as the matrix filled all of the holes. An optic fibre is not strong enough to push it out, and no metal wire that thin in diameter could refrain from bending. With multiple sets of the substrates, it was possible to do an investigation into using Caustic solution (Sodium Hydroxide, NaOH) to corrode away the matrix without harming the substrate. Solutions of 0.1M (0.1M = 0.1 Moles, where 1M of NaOH is 40g/Litre), 0.2M, 0.5M and 1M were made up, and each column of substrates from the array went into each solution respectively, with one column of substrates omitted for control. The results of this test took a couple of weeks, as it was repeated with a replicated substrate array. After 1hr in the solution, little had happened to any of the substrates, and with checks at 1hr, 2hrs, 4hrs, 6hrs, 8hrs, 24hrs and 36hrs only from the 24hr check did a real difference in the matrix become evident, which was only for the 1M solution too. After 36hrs, all of the substrates' matrixes were partially dissolved to allow the remainder to be pushed through with threading an optical fibre. To this end, all future parts printed had their matrix cleaned as much as possible by hand or the water jet cleaner, and then submersed in a 1M Caustic solution for ~24hrs, after which end stage cleaning is performed (i.e. wiping off the remnants of the matrix).

Stage 3

Due to the 3D printer not being able to print holes as small as 130µm, but being ok with holes of 260µm diameter and greater, it was decided to move away from using individual holes for individual fibres and instead use a larger hole to encompass all the fibres. The hexagonal holes printed in the *Stage 2* test turned out to be rather un-hexagonal, so trying to get the fibres to fit to a hexagonal hole will not work. The next step forward was to make a circular hole large enough to fit all the 19 fibres. This was relatively straight forward, but it became difficult trying to thread 19 fibres that have had their buffer removed, through a tight hole.

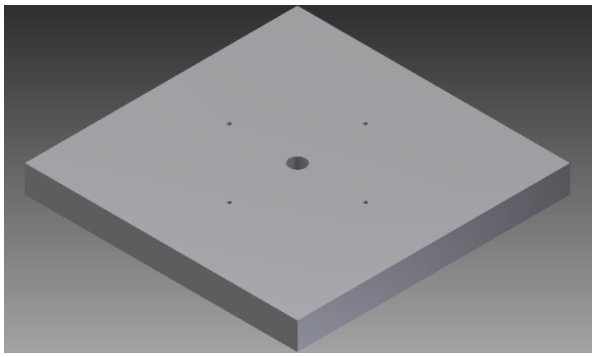

Figure 3.7.3 – Fibre positioning substrate with a 1.2mm hole in the middle and four 260µm holes displaced by 5mm from the centre of the middle hole. The substrate is 20mm (l) x 20mm (w) x 2mm (d).

When a fibre's buffer is removed, the unprotected glass is very fragile and needs little motivation to snap. Forcing fibres into a tight hole with lubrication puts too much stress on them and they snap, even for someone who is experienced with handling optical fibres. This resulted in the decision to leave the buffer on and have the bundle twice the size with the same number of fibres. The trade-off here is that the fill-factor goes down to ~4%. This is a very low fill-factor, but for a quick prototype, which BASIS currently is, it will suffice. Keeping the buffer on made the whole process much easier and the substrate that was printed is shown in Figure 3.7.3. The substrate was then cleaned, left in the 1M Caustic solution for ~24hrs and cleaned again. Fibres with their buffer on were threaded through the 260µm holes to clear out the residual matrix material. The central hole was expanded to 1.3mm using a drill bit (this size of drill bit has a thread of ~10mm long). The 19 fibres were then inserted into the hole.

Stage 4

After eventually arriving at a fibre positioning substrate that works, the next stage is glueing the fibres in place and polishing the entire unit down until a clean flat surface is achieved. Before glueing, the fibres were first threaded through the IFU Mount (see §3.9), which the fibre positioning substrate was connected to. All fibres in furcation tubes come with a lubricant, added during manufacture, so this had to be removed before glueing. A tissue was used at this stage to remove the silicone gel lubricant. The glue used was UHU Plus Endfest "300kg" Epoxy Adhesive (33g), a two-part room-temperature curing epoxy. This glue was chosen for its curing properties, cheapness and ease of purchase; though in hindsight registered optical glue may have been the better choice. As the fibres still have their buffer on they are protected, so most glues should not present stress issues to the fibres. The glue was mixed and poured over the substrate into the well of the IFU Mount (see Figure 3.7.4) and left for 24hrs to allow the glue to fully cure.

After the 24hr curing period, the fibres were cut short to the base using a pair of pliers. The whole unit was then polished using sand paper on a rotary grinder, P1200 grade, extremely coarse for fibre optics, but this was only to even out the glue / IFU Mount. Once the coarse polish was finished, a series of different graded fibre polishing papers were used to get the desired finish, starting at 30µm paper, then 12µm, 9µm, 3µm and finally 1µm paper. The end finish is as best it can be when polishing by hand. The result is shown in Figure 3.7.5 and turned out much better than expected. The organisation of the fibres within the bundle follows near concentric rings, very close to the shape of a Hexabundle. Even though this was a great result, there were some complications with the central fibres sliding in and out of the array due to residual lubricant.

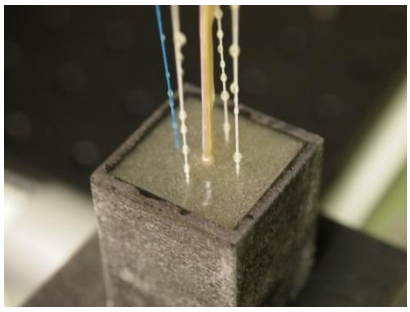

Figure 3.7.4 – Fibre positioning substrate connected to the IFU Mount and glued in place. The 19-fibre bundle is in the middle and the four sky fibres surround it. There are small droplets of glue on the fibres

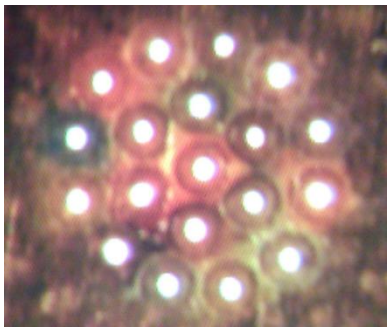

Figure 3.7.5 – Microscope image of the fibre bundle in the substrate after polishing. The bright "white" dots are due to the light that is coming out of the fibre cores. The colouring around the fibre cores comes from the fibre buffer. In the communications industry, the fibres are coloured to make channel recognition and matching easier.

Stage 5 The last problem to tackle in building the IFU was the residual lubricant on the fibres. A completely new unit was made, but this time Tetrahydrofuran (THF) was used to remove the silicone lubricant. It was rather persistent, hence the use of THF. If the fibres are left too long (tens of seconds) in the THF then the buffer is also stripped, so caution is needed not to exposure the fibres too long. Dipping them in and out of the solution a few times seemed to work the best, followed by a quick wash with distilled water and an air blow dry. The fibres were then "lubricated" with the UHU glue before threading in the central hole of the fibre positioning substrate. The same procedure of glueing, cutting and polishing from *Stage 4* was performed, and the result is shown in Figure 3.7.6. Again, the organisation of the fibres in the bundle is really good, though the polishing might be a bit better. The polishing was made difficult due to the proximity of the IFU Mount VeroBlack material, the glue not being the best type of glue for this application, and the fibre buffer appearing to be softer than that of science grade fibre previously worked on. This time the central fibres did not seem to slide in and out when moving the unit around, though this was later found not be the case, as discussion in §5.4.

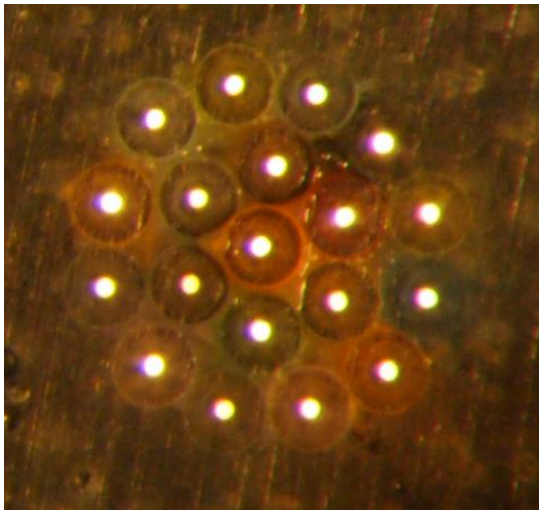

Figure 3.7.6 – Microscope image of the new fibre bundle in the substrate after polishing. Description is similar to that in Figure 3.7.5.

Even though the IFU took up the majority of time in this project, the process of getting to the result, shown in Figure 3.7.6, ruled out various alternate methods and discovered problems not originally thought of, all of which resulted in a decent and easily replicable IFU (instruction manual to follow report (Richards, 2012). This last version took only a few hours to build (not including the curing time), and shows the consistency in making the IFU using this method. Thinking about it some more, a fibre connector (possible an FC style connector) would work just as well over all, and possibly use four separate connectors for the sky fibres. This will be left for future work (discussed in §6) as time does not permit changes to be made within the deadline of this project.

3.8 1-D fibre array

With the IFU being on one end of the fibres, the other end is the 1-D fibre array (slit) connected to the SBIG SGS. To fit all the 23 fibres along the slit their buffers had to be removed, which meant handling the fibres very delicately. The conventional method of a 1-D fibre array is to use a V-Groove – a series of v-shaped channels in a substrate that allow the fibres to sit along them to ensure equal spacing and height. Equal spacing is desirable, as it will make the automated data reduction of the raw CCD spectra easier. Equal height is even more desirable, as any deviation in height will be reflected in the wavelength direction on the CCD. To account for any deviation in height a calibration emission source can be used (arc lamp), and the varying line positions on the CCD per spectrum will indicate any variations in the height of the fibres at the slit.

There were no facilities in-house to build a v-groove, and it was again out of this project's budget to get one made commercially (thousands of pounds). The decision made was to print a housing for the 1-D array using the 3D printer (see Figure 3.8.1 for the drawing), where instead of using v-groove channels to align the fibres, the fibres would be placed side-by-side along a flat surface with walls of width equal to the total number of fibres' width. A cap would then be placed on top and the fibres glued in place using the same UHU glue as before. Another desirable when building a 1-D array is to have the fibres organised in a patter relating to their position with the IFU. Figure 3.8.2 shows such a pattern, and is the one used here. This pattern is one that optimises the physical visualisation of the IFU when looking at raw CCD spectra. It also makes sure that the fibres that are receiving the least amount of light from a target (the outer right of the bundle and the sky fibres) are not next to the central core at the CCD. It removes the possibility of a false emission line from light leaking into adjacent spectra. To number the fibres in the IFU, individual fibres were illuminated whilst looking at the IFU through a microscope, making sure the other fibres were covered. One-by-one, the fibres were located in the IFU and a piece of tape with its position number was placed at the end of the fibre. This is a task that requires patience as locating a fibre position can sometimes be tricky.

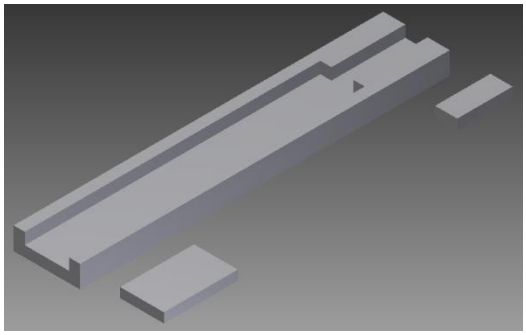

Figure 3.8.1 – Drawing of the 1-D array housing. It is 50mm long and an overall 3mm tall. The distance from the bottom of the housing to the inside surface is 1.438mm to take into account the radius of the fibres when aligning them to the centre of the housing. The caps are both 1mm in height and 10mm long, and fit into their adjacent sections. The width of the larger cap is 5.908mm and the small cap is 3mm to account for 23 fibres width with and without their buffer on respectively.

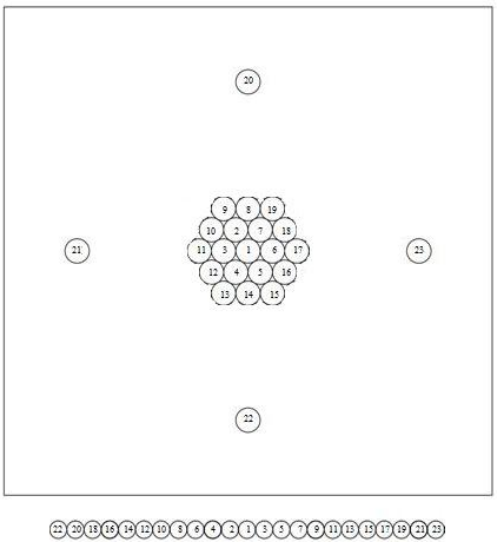

Figure 3.8.2 – Schematic of fibre number mapping from the IFU (top) to the 1-D array (bottom).

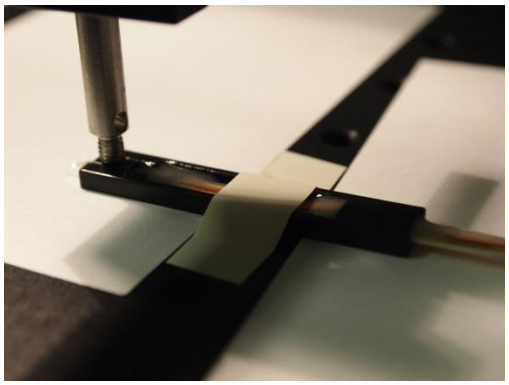

Figure 3.8.3 – Image of the 1-D array during the curing process, after the fibres had been aligned and the caps placed on. The end face is to the left and there is a clamp holding down the smaller cap to ensure there was no movement during curing.

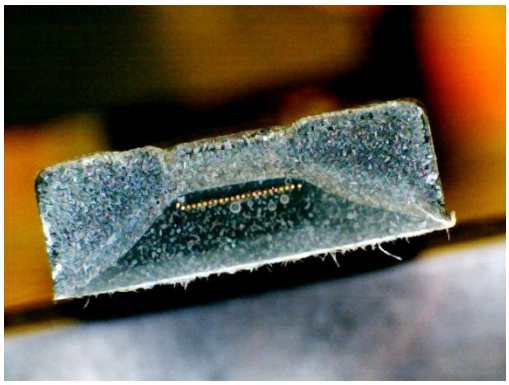

Figure 3.8.4 – Microscope image of the end face of the 1-D array after polishing. The yellow dots are the illuminated cores of the fibres. Note: fibre number 22 (left of array on image) is higher than the others, and the remnant bubbles left in the glue after curing.

To position the fibres in the 1-D array, the first task was to strip the buffer off, back to ~3cm, and then insert the fibres one-by-one into the housing starting with fibre number 22 and working the way through to fibre number 23 (as shown in Figure 3.8.2). This was difficult and required a lot of patience and calming of nerves. When fibres have had their buffer removed, they are brittle, and so it is a demanding task to thread 23 such fibres by eye, each of 125µm diameters, into a space ~3mm wide and 130µm tall, without breaking them. After the fibres had all been aligned in the 1-D array, the caps were placed on top and the fibres were glued in place (see Figure 3.8.3). The glue was left to cure and then the 1-D array was polished under the same conditions as *Stage 4* from §3.7. The result, shown in Figure 3.8.4, was again one that was better than expected, though could still be improved by allowing extra room in the width of the 1-D array, compromising on equal spacing. Fibre number 22 (fibre on the far left of Figure 3.8.4) is sitting slightly higher than the other fibres meaning that its spectra will be slightly blue-shifted at the CCD. Residual bubbles from the mixing of the UHU epoxy are also clearly visible, adding to the conclusion that glue better suited to this purpose should be use (possibly a one-part UV curing glue). All the fibres are active, and the array seems to be in working order.

3.9 Manufacturing of integration parts & wavelength calibration check

There are a few other parts needed to be built before the IFU can be attached to the telescope and the 1-D array connected to the SBIG SGS (hereon SGS Mount). Starting at the telescope, the IFU needed a mount and also a focuser mount. Figure 3.9.1 and Figure 3.9.2 show the drawings of the IFU Mount and 3-inch Focus Mount. These were both printed on the 3D printer, as it was easier to do this than to build from metal. Both of them came out as intended and there was no difficulty in attaching the IFU to the IFU Mount for glueing / polishing (see Figure 3.7.4). This was also the case for the new IFU when attaching it to the 3-inch Focus Mount using M3 nuts and bolts (M3 refers to the size and is classed as Metric 3mm – diameter of thread). The focuser that was available for use at the time of commissioning had a 2-inch mount, so one that would fit to the IFU using the M3 holes was milled from aluminium adapted from a scrap piece found in a "left-overs" draw at the University of Hertfordshire (see Figure 3.9.4). This was used for the first batch of commissioning, but after problems with acquisition (see §3.10) a 1¼-inch mount was needed, so one was printed using the 3D printer (see Figure 3.9.5). The SGS Mount was a bit more involved, but it printed as required (see Figure 3.9.3). The 1-D array housing slides inside the SGS Mount, which attaches to the SGS via M3 nuts and bolts. The reason for the oddly shaped M3 holes on the SGS Mount is to allow for rotation when connected. It was discovered when removing the slit mask from the SBIG SGS at the start that the slit had a slight tilt to it (~2º), to allow better coupling with the diffraction grating. Unsure on how much the 1-D array would need to be tilted, if any, the option was to allow for rotation. The ability to slide the 1-D array in and out of the SGS Mount allowed for focussing the array with respect to the spectrograph. The exact focal plane was unknown, so again having the option to allow for adjustment was needed.

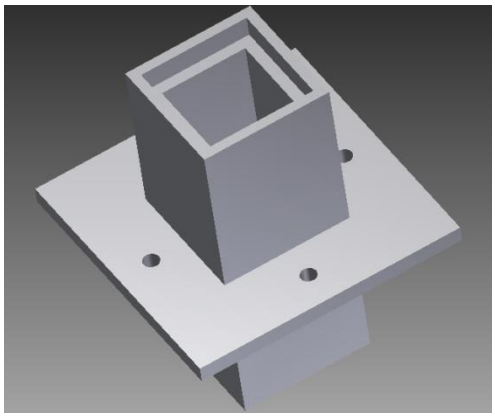

Figure 3.9.1 – Drawing of the IFU Mount. Relating to Figure 3.7.4 the fibre positioning substrate fits into the inset well at the top (20mm x 20mm). The overall length from end to end is 60mm with the attachment plate exactly half way. The holes are M3 holes and are used in the attachment of the IFU Mount to the Focus Mount.

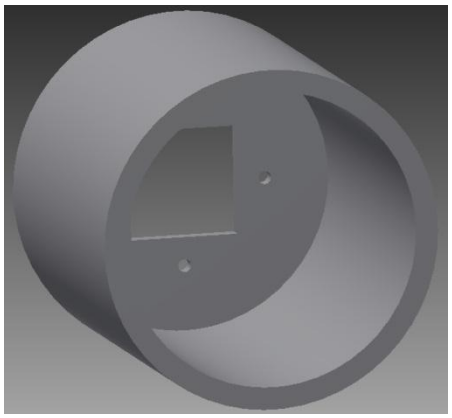

Figure 3.9.2 – Drawing of the 3-inch Focus Mount. The outer diameter of the Focus Mount is 3-inch to fit onto the telescope's 3-inch focuser, and the overall length of the Focus Mount is 76mm to back set the IFU for purposes of focusing and protection. The IFU Mount attaches to the back side of the Focus Mount using M3 nuts and bolts in the provided holes.

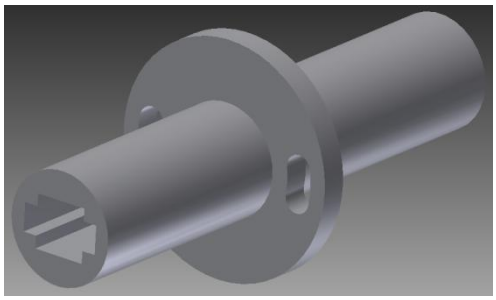

Figure 3.9.3 – Drawing of the SGS Mount. The overall length is 62mm with a diameter of 12.5mm to fit the entrance aperture hole in the SBIG SGS. The circular attachment plate has M3 sized holes that allow for rotation adjustment. The extra height at the entrance of the SGS Mount's slide is in case the rubber protection over the fibres needs to go inside as well.

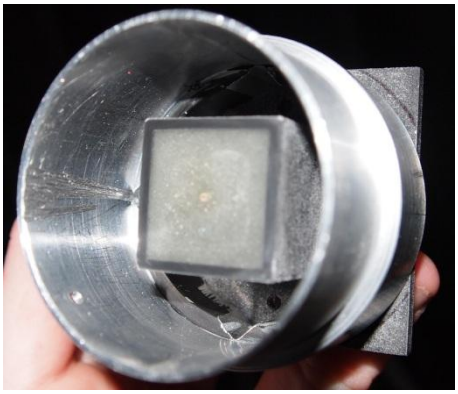

Figure 3.9.4.1 – Front image of the milled 2-inch Focus Mount. The IFU Mount is connected to the back via new M3 holes drilled in the diagonals of the IFU Mount plate.

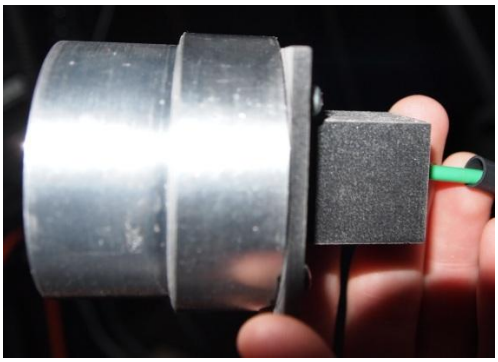

Figure 3.9.4.2 – Side image of the milled 2-inch Focus Mount. The M3 holes in the 2-inch Focus Mount were pre-existing so new M3 holes in the IFU Mount were drilled to match these.

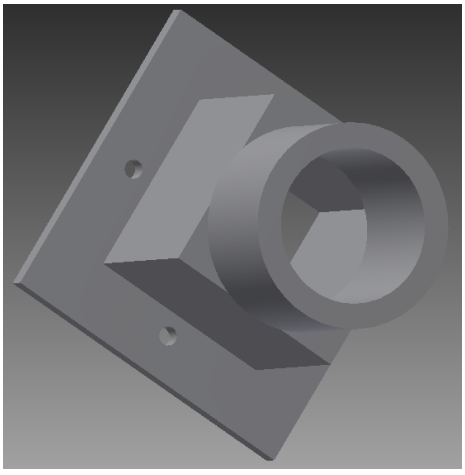

Figure 3.9.5 – Drawing of the 1¼-inch Focus Mount. The IFU insert into the back using the M3 holes for attachment. The square shaft accounts for the length of the respective IFU shaft, and the circular shaft is the 1¼-inch mount extending for 20mm.

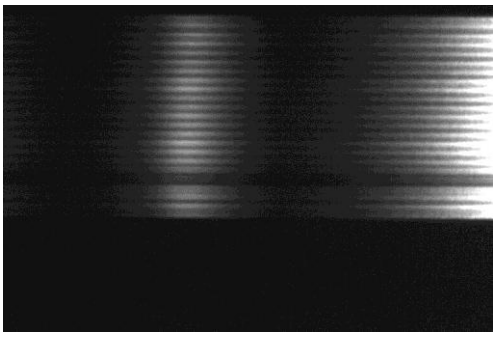

Figure 3.9.6 – First spectra through the entire instrument illuminated with a near white LED source. This is a 1s exposure and the bright blue part of the LED's spectrum is falling off just to the right of the CCD. Slight rotation is seen in the non-level spectra with respect to the CD. The haziness and overlapping of spectra indicates that it is out of focus.

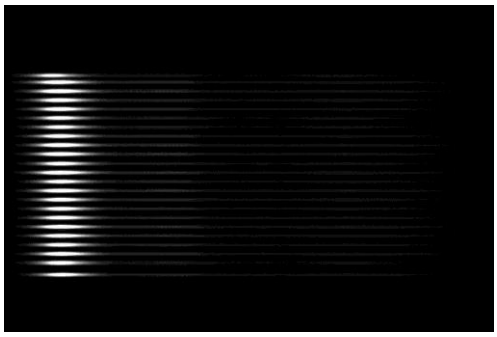

Figure 3.9.7 – 1s exposure after fixing the focus, rotation, and grating angle to adjust the wavelength. Spectra are clearly resolved. Note how the top fibre is slightly blue-shifted, corresponding to fibre number 22.

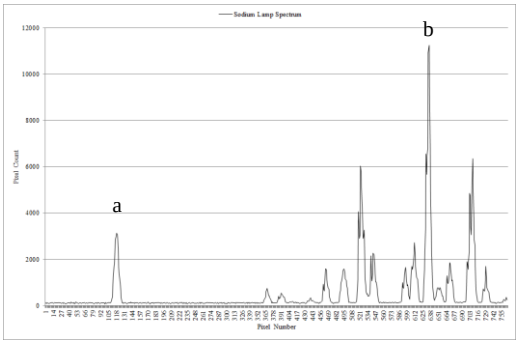

Figure 3.9.8 – Sodium Lamp spectrum from fibre number 1 when exposed for 60s.

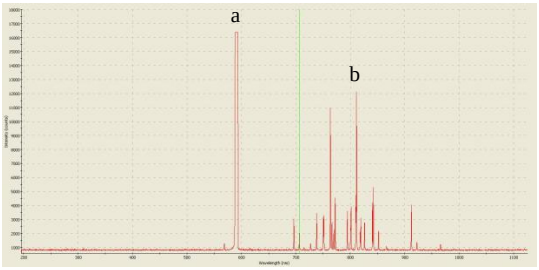

Figure 3.9.9 – Sodium Lamp spectrum using the Andor® lab single-fibre spectrograph. The x-axis here is in wavelength going from 200nm to 1100nm. Line markers a and b correspond to those in Figure 3.9.7 and have a reading of ~585nm and 815nm respectively.

After inserting the 1-D array into the SGS Mount and illuminating the fibres with a near white LED source, a 1s exposure using the ST-7E was taken to see if anything could be detected, the result of which is shown in Figure 3.9.6. Again this was better than expected, with the fibres near focus, only a slight rotation correction needed, and a small shift in wavelength using the micrometer to get the bright blue part of the LED over to the left hand side (note that the wavelength ascends from left to right on all spectrograph CCD exposures). Making the required adjustments, the result is shown in Figure 3.9.7, another 1s exposure.

This time the spectra are clearly resolved and the peak of the LED's spectrum is in roughly the correct location. This exposure proves that the whole instrument is working, and rather well at that. Note how the top fibre is slightly blue-shifted, corresponding to fibre number 22 mentioned at the end of §3.8. The bottom fibre is slightly displaced in the spatial axis here, which means that the corresponding fibre number 23 is not touching the adjacent fibre number 21 at the slit. It appears that in the process of moving the other fibres down to allow room for the last fibre has caused the end fibre number 22 to jump up in the 1-D array. There is little that can be done for it now, but even though this is the case, all of the spectra are still resolvable and able to be wavelength calibrated, so all should be ok.

To check the wavelength calibration the IFU was illuminated using a Sodium lamp and compared to the same spectrum on an Andor® single-fibre lab spectrograph with a resolution of ~1nm. The results are shown in Figure 3.9.8 and Figure 3.9.9. This exposure was taken after adjusting the micrometer, to capture these specific lines. Most of these lines are outside of the wavelength range of that specified in Figure 3.4.3, but this was just a test to have a comparison. The emission line markers a and b identify the corresponding lines in either exposure. From the Andor spectrograph they have readings of 585nm and 815nm respectively, which means that the spectral bandwidth of BASIS is larger than originally theorised in Figure 3.4.3, with a bandwidth of ~330nm instead of 212nm respectively (Note: the reason for the low "a" line in Figure 3.9.8 could be because the lamp was still warming up). This is a large increase in bandwidth, and so when observing, the extra bandwidth will be given to the blue end of the spectrum to see if it is possible to observe down to the OIIλ3727 emission line. If what is being seen here is correct then this opens up more science goals that BASIS could achieve, if it is somehow wrong, then nothing will have changed.

3.10 Control units and software (acquisition and guiding)

When reading through the commissioning reports given in Appendix D it becomes evident that there were real difficulties with the acquisition and guiding, the process of locating a target with the telescope such that it consistently lands in the centre of the IFU and the process of keeping said target in the middle of the IFU over any length of exposure respectively. 2m+ telescopes have systems for this that cost millions of dollars to build due to their importance. If the acquisition is not consistent then no reliable science can be achieved, and the same goes for not keeping the target in the same position throughout the exposure. Because the IFU is located at the Cassegrain focus of the telescope, it is not possible to use a camera at the same location. Therefore, a TeleVue® 102 refractor (102mm diameter, 540mm focal length, f/5.4) was side-mounted to the LX200 with an SBIG STL-6303 camera (9µm square pixels with an array of 3072 x 2048 pixels) (hereon TV will be used to describe the TeleVue and STL-6303). Using an eyepiece on the LX200, the TV was centre aligned as much as possible (within ~10 pixels) and then the cross-hair finder scope was also centred as best as possible. Because the LX200 had no tracking or auto-guiding on, this process had to be done quickly as the self-tracking in the telescope's mount cannot be relied upon over a few tens of seconds. To get within the ~10-pixel alignment tolerance, the process took ~30mins within re-centring the target in the eyepiece every ~30 seconds. It was rather tedious, but was necessary for accurate acquisition.

The IFU is by no means perfect and therefore it cannot be assumed that the fibre number 1 in the bundle is on the optical axis of the telescope. Due to this, the offset between the TV centre and the centre of the IFU needed to be known. Jupiter was used in this situation because it has an angular diameter of ~25" meaning that if centred in the IFU only fibre numbers 1 to 7 would be illuminated (see §5). Using a star to find the offset would be incredibly difficult due to the fill-factor of the IFU. After centre aligning the TV, it was discovered that due to the weight of the STL-6303 (~2kg) there was considerable flexure in the TV (~2') when pointing at different on-sky locations. This inconsistency is detrimental to the instrument, and needed to be corrected for before any automated or deep-sky observations with BASIS can be done. The decision was then made to use an off-axis guider (OAG), but in this case having the IFU in the off-axis side mount position where the guide camera normally goes. The primary mount in this case holds the STL-6303, removing the flexure problems in the TV set up. A new 1¼-inch mount (shown in Figure 3.9.5) was needed to attach the IFU as no OAG with a 2-inch side mount was available. With this in place, the acquisition and the guiding, using the tracking chip within the STL-6303 should be consistent and accurate, within five arc seconds.

The five arc second (5") tolerance on the acquisition and guiding is a tight one, but with the fibre aperture being 2.6" on-sky, the average seeing at Bayfordbury being ~3" and with the fibre pitch being 12.9" on-sky, 5" is within the overlap tolerance between fibres. The LX200 alone cannot achieve this level of accuracy, so the telescope control software "ACP" (Denny, 2012) was installed alongside the image processing software "MaxImDL V5" (Diffraction Limited, 2012). This combination has the ability to perform plate solving, the process of using stars within the field-of-view to locate where on the sky it is pointing and correct for any error in the pointing accordingly.

ACP can be used to train the telescope to a pointing accuracy of <5" when tens of pointings are performed across the observable sky. ACP was designed to be a full Observatory Control software, meaning that it can remotely run the telescope in a fully automated robotic mode, running from a scheduler; once the hardware to allow this has been installed. One telescope and dome unit at Bayfordbury Observatory (the CKT, another 16-inch Meade LX200) has already been upgraded to permit this. Following the lessons learnt with upgrading the CKT will mean that BASIS could become fully automated and be run from a scheduler. This would be required if a full survey is accepted.

3.11 BASIS instrument summary

As an overall instrument, BASIS has turned out to be a neat little instrument that has the potential to obtain the science goals as proposed in §2.2.2. After going through the instrument part-by-part (§3.2 to §3.10), Table 3.11 summarises all of the different parameters and goals of BASIS, some of which are currently not known, and so are shown in italics. Figure 3.11.1 and Figure 3.11.2 show a simulated velocity field and BPT diagrams respectively, and take into account the specifications of BASIS when equating the error bars.

BASIS Specifications

Telescope

Model	Meade LX200 (Schmidt Cassegrain)
Primary Mirror	16 inches (406.4mm)
Focal Length	4064mm
Focal Ratio	f/10
Focal Plate Scale	51.6 arc seconds per millimetre

Integral Field Unit

Model	Optical fibre bundle with displaced sky fibres
Optical Fibre	OM2 Communication Fibre - 50µm core, 125µm cladding, 250µm buffer
Fibre Aperture	50µm = 2.6 arc seconds on sky
Fibre Bundle	19 fibres bundled in a layered circular pattern
Bundle Aperture	54.2 arc seconds (leading edge of first fibre core to trailing edge of last core)
Fill-Factor	~4%
Sky Fibres	4 sky fibres symmetrically displaced by 5mm (4.3 arc minutes) from the bundle
Efficiency	0.68 (0.98 from attenuation for 5m fibre length, 0.7 from IFU construction)

Spectrograph

Model	Santa Barbara Instrument Group Self Guiding Spectrograph (SBIG SGS)
Slit	1-D array of 23 fibres with 50µm cores
Slit length	~2.9mm (23 fibres long without the buffer)
Grating	150 lines per millimetre
Camera Make	SBIG ST-7E
Camera CCD	Kodak KAF-0402E
CCD Pixel Size	9µm x 9µm
CCD Array Size	765 x 510 pixels
CCD Average QE	~65%
Spectral Resolution	~7Å
Spectral Bandwidth	~2120Å
Spectral Limits Chosen	4710Å to 6830Å
Central Wavelength	Adjustable

Overall Instrument

Integral Field Unit	19 fibre bundle and 4 displaced sky fibres
IFU On-sky Aperture	54 arc seconds (~1 arc minute)
Resolution	~7Å (*max of ~75kms^{-1}*)
Bandwidth	~2120Å (adjustable central wavelength)
Efficiency	*Expected: ~22%, Realistic: ~5%*
Signal-to-Noise	*~10 for a 20min exposure of a 13mag/arcsec^2 source (~ ±0.15 error on BPT diagram)*

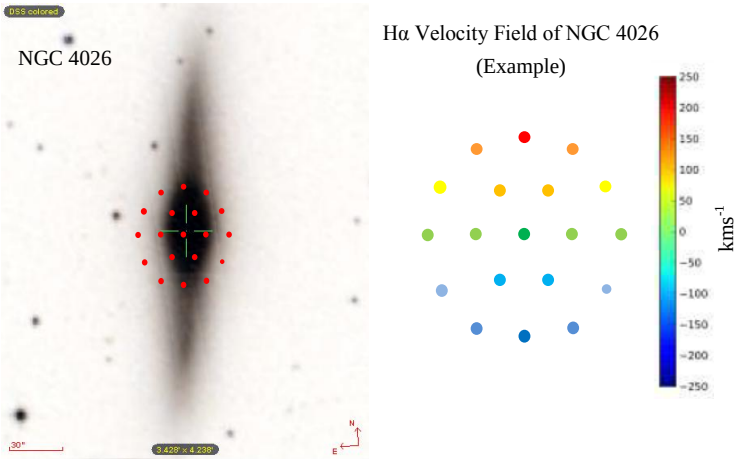

Figure 3.11.1 – Example Hα velocity field of NGC 4026, a suitable target for BASIS with the fibre bundle IFU overlaid to scale. The scale of the velocity field is in units of kms^{-1} and ~$75kms^{-1}$ is representative of BASIS's maximum resolution.

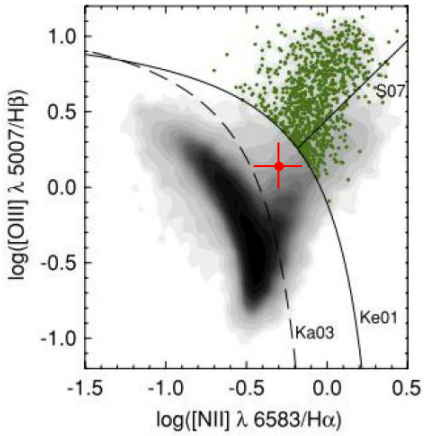

Figure 3.11.2 – Example of NGC 4026 placed on a BPT diagram (red) with error bars relating to that expected from BASIS (signal-to-noise ratio of ~10).

The signal-to-noise ratio (SNR) of ~10 for a 20min exposure of a $13mag/arcsec^2$ source was equated using the BASIS SNR calculator displayed in Appendix A. Here, an overall instrument efficiency of 5% was used instead of the expected 22% (a convolution of all individual expected efficiencies). The reason why 5% is used for this calculation is that instruments tend to always be under budget when it comes to efficiency, but even when accounting for this, a SNR of ~ 10 is ideal for the purposes of BASIS. Stacking exposures together can increase the SNR, and the brightest sources will be observed first to minimise the errors on the initial data. Target selection and observations are discussed in §6.

With this level of performance, BASIS could be used to carry out a full survey of hundreds, possibly thousands of galaxies, and gather useful data to aid our understanding of galaxy composition and evolution. Just what type of galaxies will be discussed in §7, but in summary they are nearby $z\sim10^{-3}$ such that their angular diameter matches well with the angular diameter of the IFU (~1') and have a surface brightness across this diameter of ~$13mag/arcsec^2$ to get the SNR needed for emission line analysis.

Because BASIS is designed for a small aperture telescope and uses existing equipment that many institutions around the world already have, its function can extend into the teaching of integral field spectroscopy for undergraduates, even postgraduates. With large integral field spectroscopy surveys on the horizon, including HETDEX (Hill et al., 2008), MaNGA (Law et al., 2012) and SAMI (Croom et al., 2011), it would seem fitting to start teaching integral field spectroscopy on an instrument that can produce the fundamentals of galaxy science and not take up time on what would be over-subscribed large aperture telescopes. The exact form of this teaching would be left to the discretion of the institution, but practicals could be written for students to follow. A good idea would be to have the student produce a velocity field of a galaxy, something that would work well in addition to the standard undergraduate practical of using a small radio dish to get the rotation curve of the Milky Way by observing the HI 21cm line features of the spiral arms.

Before any of this is possible, the biggest hurdle to overcome is the acquisition and guiding, which should be solved with the recent change to an off-axis IFU. The sky fibres might be compromised in this shift, though if sky subtraction is desired, then offset sky exposures could be taken additional to the galaxy observations, though this would increase the time overheads. As the sky brightness at Bayfordbury Observatory does not often exceed 17mag/arcsec^2, its contribution to observed spectra would be negligible and therefore the sky fibres are rendered mute. However, if long exposures (more than an hour) are desired, then they would need to be used to make sure there is no contribution due to the sky background. Proposed changes to the instrument for future use will be discussed in §6. Figure 3.11.3, Figure 3.11.4 and Figure 3.11.5 show BASIS installed on the telescope when in the design phase of using the 2-inch Focus Mount.

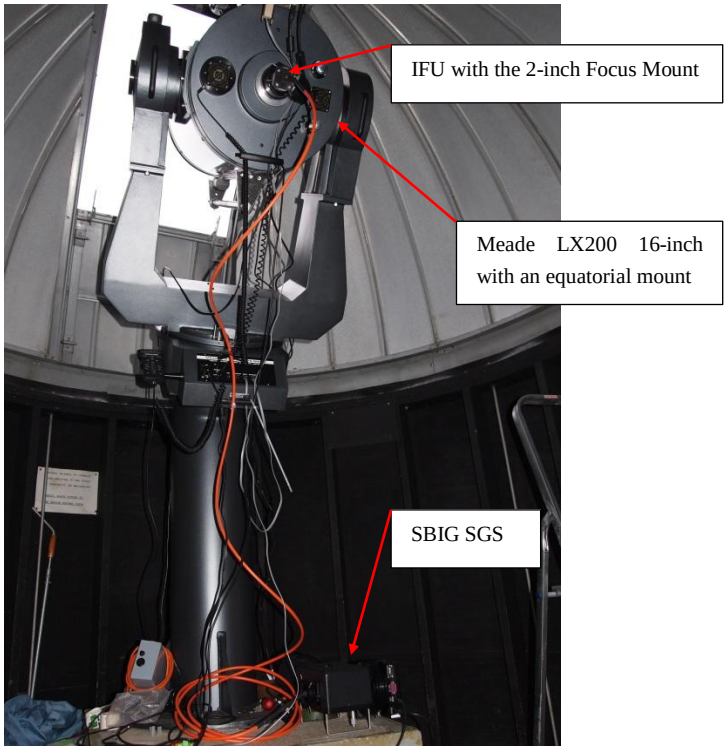

Figure 3.11.3 – Picture of BASIS on the LX200 from inside the telescope dome. The orange cable is the fibre optic cable, and the labels show the position of the IFU and the SBIG SGS.

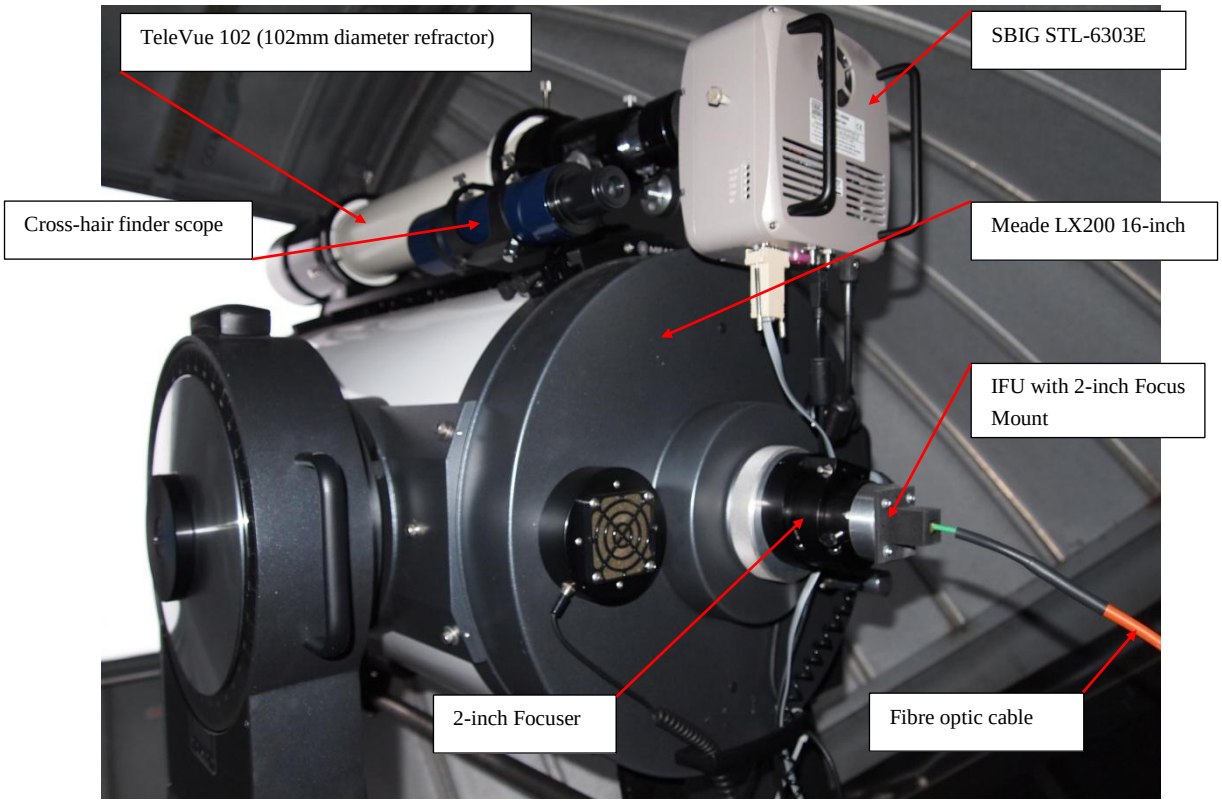

Figure 3.11.4 – Zoom-in of BASIS attached to the LX200. Note the labels for positions and descriptions.

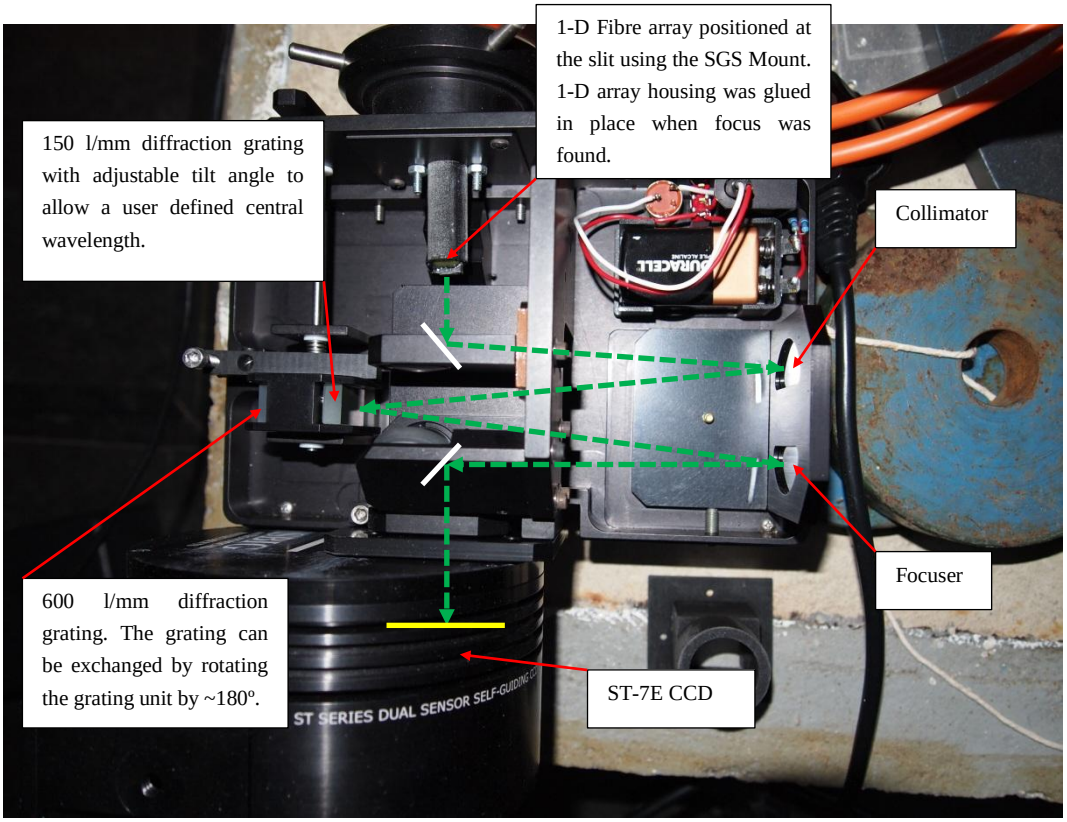
1-D Fibre array positioned at the slit using the SGS Mount. 1-D array housing was glued in place when focus was found.
150 l/mm diffraction grating with adjustable tilt angle to allow a user defined central wavelength.
Collimator
Focuser
600 l/mm diffraction grating. The grating can be exchanged by rotating the grating unit by ~180º.
ST-7E CCD
ST SERIES DUAL SENSOR SELF-GUIDING

Figure 3.11.5 Image of the SBIG SGS, as viewed from above, with the 1-D fibre array connected. See labels for descriptions. The dotted green line shows the optical path up to the yellow line which is the CCD, and the white lines represent the mirrors obscured by other components in this image.

4 DATA REDUCTION

Before any observations were taken, some thought had to be spent on finding a way to reduce the data that would be collect, as there is little point in having data you cannot be utilised. The following section discusses the various stages of data reduction.

4.1 First order data reduction

The obvious first step is to manually look at the data to find any interesting features. Because the spectra have been aligned on the CCD, it is possible to take a cut in the horizontal direction getting pixel values for each wavelength to extract a fibre's spectrum. Very simply, this can be done in two ways:

1. MaxImDL has a very useful graph tool (see Figure 5.5.5), which allows the user to place a horizontal line on an image and the graph window will display the pixel values along that line. This graph is essentially the spectrum from that fibre, and it can be exported as a .csv file for further analysis.

2. The .fit file of the exposure can be converted into a .ascii file, which can then be loaded into Microsoft Excel (or something similar). Graphs of the spectra can then be made using the inbuilt graphing tool.

In either case, wavelength calibration and sky subtraction can be performed, though spectral fitting will need to be done by a more advanced software package. Line ratios can be crudely taken from the un-fitted spectra, though the error bars would be larger (by how much would depend on the quality of the spectra, i.e. SNR).

4.2 Data reduction software

There are a few open source data reduction software packages for the purposes of fibre-fed integral field units, which can be easily obtained, the main ones being; IRAF (Tody, 1986), R3D (Sánchez, 2006) and the more recent p3d (Sandin et al., 2010). All of these can perform full data reduction to the point of creating a data-cube of the galaxy, which can then be used for full analysis. The main steps of data reduction, which are automated within software packages, are:

1. Subtraction of the dark frame (includes bias).

2. Removal of cosmic rays, which can be done using an integrated software routine (for example, MIDAS (Crane & Banse, 1982) using the filter/median script). If multiple exposures of the same target are available (≥3), it is possible to take their median and compare it (pixel-by-pixel) to each individual exposure. If the difference is greater than a specified sigma value then that pixel is replaced by the corresponding pixel in the median image. There are problems with this method when using data from world leading instruments, but for the purposes of BASIS, it should work well.

3. Performing aperture tracing, the process of taking a cut perpendicular to the dispersion and fitting a Gaussian profile to the light peaks. This provides knowledge of where on the CCD the spectra are, which will be used in the following steps.

4. Wavelength calibration using an arc frame (an exposure of an arc lamp that accurately provides known emission lines, preferably as narrow as possible). The pixel locations are then calibrated with the wavelengths so that in any of the observations the wavelength positions are well defined in each spectrum.

5. Correcting for throughput variations by taking a flat field (traditionally a twilight flat). Any variation in pixel counts between spectra is directly proportional to the variation in performance of their respective fibres. This can then be corrected similarly to a standard flat field used in photometric imaging.

6. Subtraction of sky background contribution. This is the primary purpose of having sky fibres outside the fibre bundle in the IFU. At this point, the sky fibres' spectra have gone through the above steps and then a median sky spectrum is created. If any contribution is observed, it is then directly subtracted from each of the fibre bundle's spectra.

7. Flux calibration using a standard star. This is done in near enough the same way as in photometric imaging where in this case a standard star is observed using one, or multiple fibres in the IFU, depending on the size of the IFU. The standard star's spectrum is then integrated and compared to a calibrated measurement to get flux units for the pixel values. When convolved with the throughput variations, the response factor for each fibre can be found.

8. The data cube can now be created, and is usually visualised with an overlay of the IFU's fibre positions, such that selecting a fibre will reveal its spectrum (as shown in Figure 4.2.2). The resulting data cube can then be used in the analysis of the spectra for purposes such as velocity fields and line ratios for BPT diagram placement.

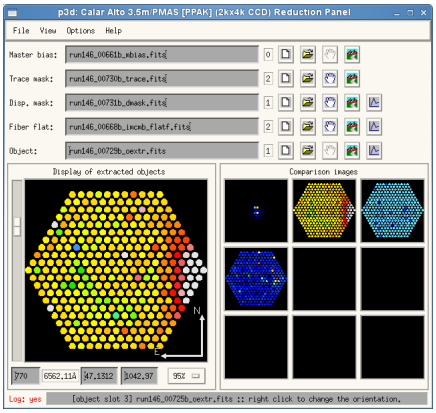

Figure 4.2.1 – A copy of Figure 1.1.3 for ease of reference – (p3d, 2011) – A screenshot of the p3d software using the Potsdam Multi-Aperture Spectrophotometer (PMAS) instrument as an example. Here is displayed the data cube.

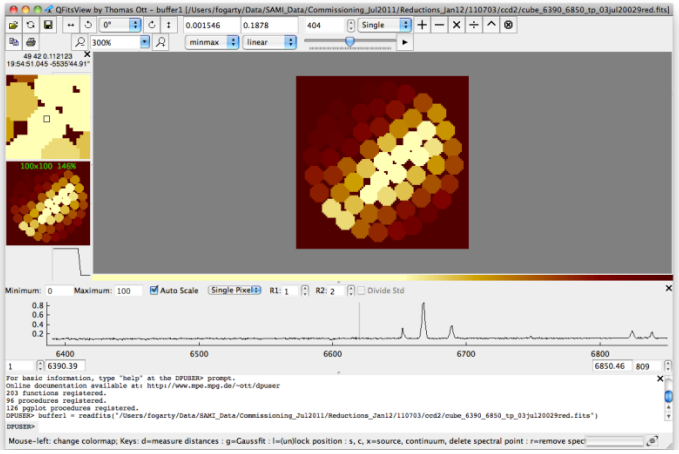

Figure 4.2.2 – (Fogarty, 2012) – A screen shot of SAMI_tools. When the cursor is placed over one of the spaxels (fibres) then the spectrum for that fibre is displayed underneath.

Out of the three data reduction software packages mentioned above, the one that would be the most suitable for BASIS is the p3d package (see Figure 4.2.1), as mentioned in the initial plan (§1.1). This is because with little effort (maybe quite involved for an undergraduate) it can be modified to accommodate any form of fibre-fed IFU, having a user interface that appears logical and friendly. Due to time constraints, the modification of the p3d has not been achieved, and so it would have to be part of the future work. Realistically, to diligently modify the p3d code into full working order as the BASIS data reduction software is an entire project on its own. There is another software package not yet mentioned that would also work well and that is SAMI_tools (Fogarty, 2012). This is the package written for the SAMI instrument that as previously mentioned uses fibre bundles (Hexabundles) for their IFUs, and so will closely match the data produced by BASIS. An example of a SAMI data cube is given in Figure 4.2.2, where the display is that explained in the final stage of the data reduction procedure above. Previous involvement on the SAMI instrument might make this a more favourable route to take.

4.3 Pipeline

The end goal would be to create a pipeline that takes in raw CCD spectra, performs the necessary calibration and line fittings, and outputs a data cube along with tabulated values for the galaxy's parameters. Again, it might be best to work alongside the SAMI team in using / modifying their pipeline.

5 COMMISSIONING

The commissioning of BASIS started in early February 2012 and the full reports can be found in Appendix D. This was rather later than initially hoped, but due to complications with the construction of BASIS explained in §3, the first working version of BASIS was that with the 2-inch Focus Mount. The following explain the steps taken for each commissioning task, and where relevant the complications that arose respectively. The very first step was to install / mount all the different pieces of equipment; SBIG STL-6303E onto the TeleVue 102, securing a safe position for the SBIG SGS at the base of the telescope mount, attaching the IFU onto the 2-inch focuser with the 2-inch Focus Mount.

5.1 Focus

By manually pointing the telescope at a star (HIP 31681) the TV was the first piece of equipment to be focussed. The TV has a manual focuser, so using short exposure time, the focus was found very quickly. Attempting to focus the LX200 was more involved. It was assumed that the focus of a 2-inch eyepiece would be at the back plate of the eyepiece, but after taking an observation of Mars with the IFU it was found that this was an incorrect assumption. A piece of fibre polishing paper (semi-transparent) was attached to the back of the focuser with no eyepiece (see Figure 5.1) and focus was found using the coarse focus on the LX200 by moving the primary mirror (unlocking the mirror for focus and locking it back up after focus had been found). The focuser was set all the way in, and after equating the in-set of the IFU to the 2-inch Focus Mount to be ~9.8mm, the 2-inch focuser was moved back to this distance. This seemed to work perfectly as further observations of Jupiter revealed that the size of Jupiter on the IFU was as expected (~25 arc seconds, only illuminating the central seven fibres in the bundle). This method of focussing the LX200 works well and will be used in all future cases were the focus is needed. The focus for the SBIG SGS was found in the lab as described in §3.9 and was glued in place so that it could not change.

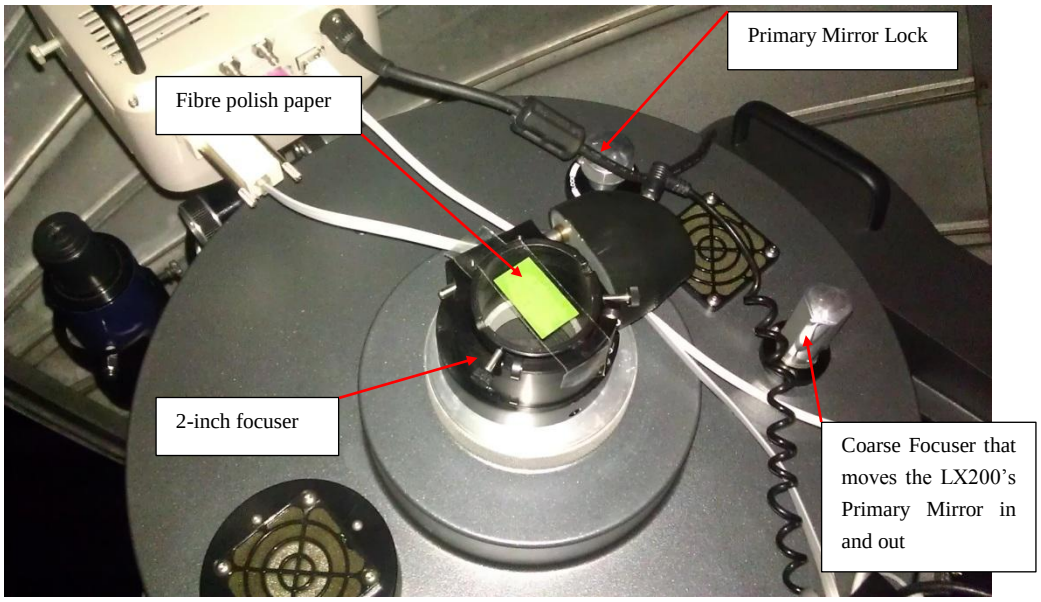

Figure 5.1 – Picture of the back of the LX200 where the fibre polish paper has been stuck to the back of the empty 2-inch focuser. Jupiter was used to find the focus using the coarse focus by moving the primary mirror in and out. See labels for descriptions.

5.2 Wavelength solution

A 650nm laser diode was used for the wavelength calibration in setting the central wavelength. It was calculated by using the galaxy template given in Figure 3.4.3 to be such that the 650nm laser would need to land on pixel number 646 (in the 765pix axis). Figure 5.2 shows one of the calibration images where the laser line has been set its required pixel value. Using the laser diode to set the wavelength is a good method and will be used for future calibration. The wavelength calibration for use in data reduction will be done by taking an exposure of an arc lamp similar to that done for Figure 3.9.8, though this time with the instrument on the telescope. No such exposure had been taken yet due to limited time and the priority to get some observational data.

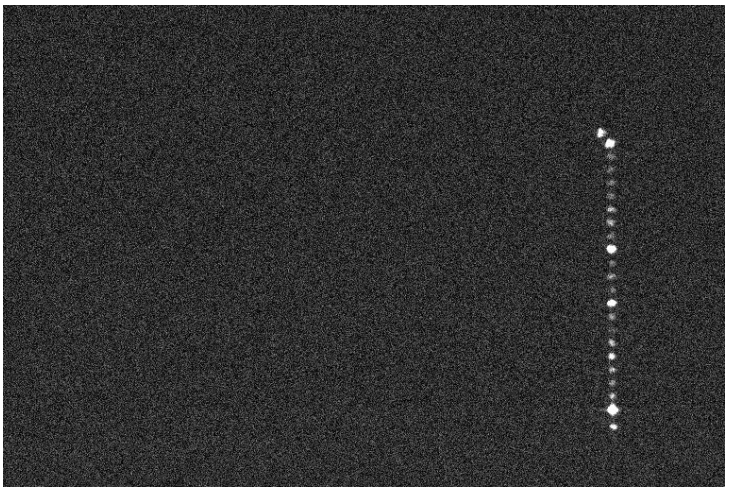

Figure 5.2 – A 1s exposure of the 650nm laser diode showing that it is set at the 646pixel location as desired. The variations in line strengths are primarily due to non-uniformity in illumination.

5.3 Alignment (position/rotation)

Because the IFU is at the Cassegrain focus of the telescope, there is no room for a camera to do the acquisition and guiding. As previously explained in §3.10 the SBIG STL-6303E camera was then mounted to a TeleVue 102 refractor that itself was side-mounted onto the LX200. The centre of the TV was aligned with the centre of the LX200 as best as possible by eye (roughly within 2arcmins), which had to be done quickly because the telescope drive cannot track that well by itself. It was then found, that this centring was inconsistent due to flexure in the TV, which can be read about in the Commission Reports given in Appendix D. The SBIG STL-6303E is too heavy to be used as the alignment camera. There are no other options in camera for use on the TV so a solution needs to be found that can permit accurate and consistent acquisition. The proposed idea is to use an off-axis guider mount with the SBIG STL-6303E in the primary mount position and the IFU in the off-axis mount position. This will correct the problem of flexure and will remove the need to align two different telescopes. The rotation of the IFU is set as best as possible by a spirit level, but when the acquisition is sorted, the exact rotation can be found by running on-sky North-South-East-West offsets with the IFU.

5.4 Throughput

Performing a flat field will give the fibre-to-fibre variations, and when coupled with a standard star observation the overall throughput of the instrument will be found. This has not been done yet as no standard star can be observed currently due to acquisition problems, and it was also found recently that the central fibres are again moving in and out of the bundle. At the end of *Stage 5* in §3.7 it was mention that the central fibres had indeed worked loose. Either this is due to the lubricant still being present despite using THF, or the glue not being applied properly. The latter would be the dominant cause, but in any case, it means a new IFU needs to be made. This is why no flat field has been taken, as the results would be in error beyond analysis. Care will be taken when making the next version that the glue is applied sufficiently.

5.5 Initial observations

Regardless of all the problems, it was possible to get some initial observations, the best being the 60s exposure of Jupiter (Figure 5.5.1) and the 60s exposure of the Moon (Figure 5.5.3) on the Fifth Commission Night. Both of these observations were taken with "brute force", i.e. pointing the telescope manually and not applying any cooling to the CCD or taking any dark frames. It was very close to the end of the night and the decision was made just to get some data, no matter how poor it might be. Surprisingly it came out rather well, and Figure 5.5.2 and Figure 5.5.4 show the spectra obtained from the central fibre in each observation, extracted by converting each exposure into a .ascii file and plotting with Microsoft Excel. As the light from these targets is essentially reflected sunlight they appear the same, though it is interesting that in both cases it is possible to see an absorption feature at pixel number 695, which corresponds to the O_2 atmospheric absorption line also seen in Figure 5.5.6. Figure 5.5.5 shows a vertical cut displaying clear separation of each fibre's spectrum and crudely indicates that their respective throughputs are somewhat variable. It is not possible to quantify the throughput from these exposures due to the conditions of observation (variable cloud cover, uneven illumination due to gibbous moon, etc…).

The most important claim to take from these observations is that the spectrum of Jupiter proves that integral field spectroscopy on small aperture telescopes is possible, and that spatially resolving an object can be done. The telluric absorption feature and the overall spectral profile of both Jupiter and the Moon correspond well with what is expected of these objects (see Figure 5.5.6). At the end of the day, if accurate and consistent acquisition can be achieved, something that is proving difficult to do on small aperture telescopes, it would be possible to get data cubes on galaxies. The exact throughput and efficiency of BASIS is yet to be determined, but light can get down the instrument, and enough light to get spectra. If it turns out that the efficiency is closer to the 5% used in the calculations for SNR then there should not be a problem when it comes to observing a galaxy. It would have been great to get galaxy observations within the time period of this project, but knowing that the concept does work, it is just a matter of time before the first velocity field is created.

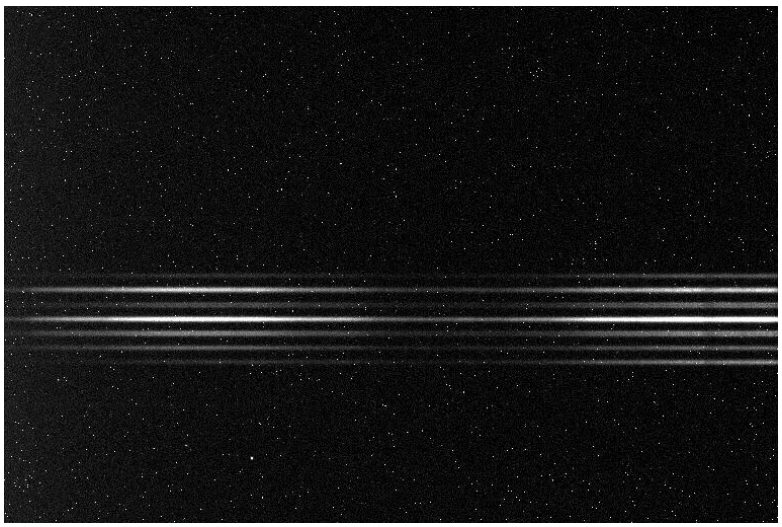

Figure 5.5.1 – A 60s exposure of Jupiter. Here fibre numbers 1 to 7 have been illuminated, where fibre number 1 is the central spectrum shown here. Wavelength is in the x-axis short to long wavelengths from left to right respectively (~4700Å to ~6800Å).

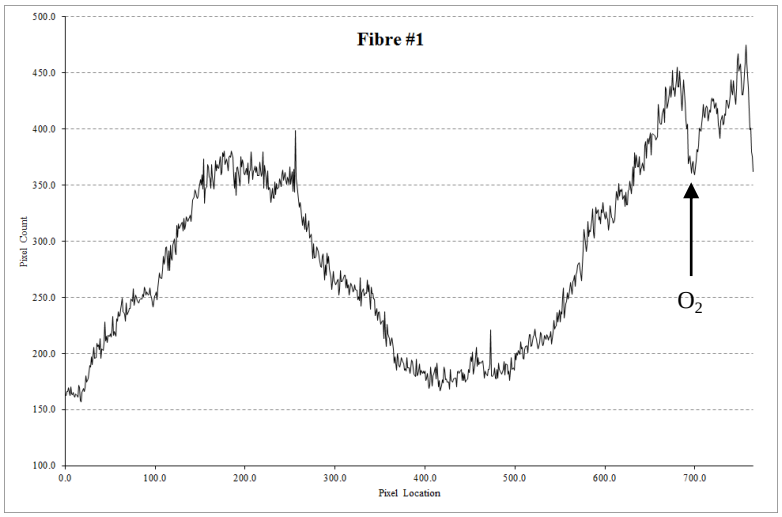

Figure 5.5.2 – Spectrum of fibre number 1 from the 60s exposure of Jupiter. Pixel location and counts have been assigned to the x and y axis accordingly, thought the x-axis is the wavelength axis from the CCD ranging from ~4700Å to ~6800Å. Note the O_2 telluric absorption feature at pixel number 695.

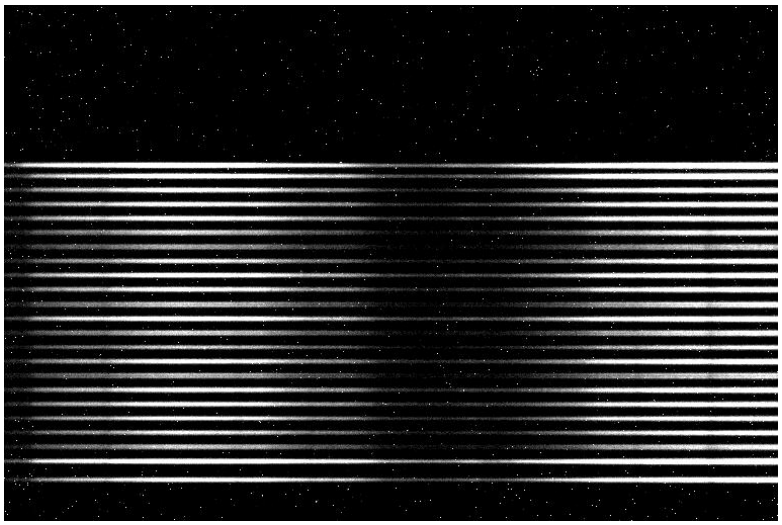

Figure 5.5.3 – A 60s exposure of the Moon. Here all fibres have been illuminated including the sky fibres, where fibre number 1 is the central spectrum shown here. Wavelength is in the x-axis short to long wavelengths from left to right respectively (~4700Å to ~6800Å).

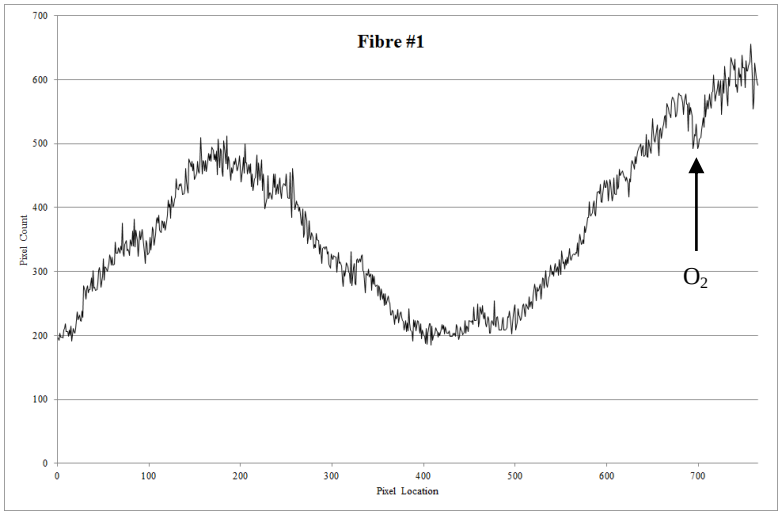

Figure 5.5.4 – Spectrum of fibre number 1 from the 60s exposure of the moon. Same description as Figure 5.5.2 (~4700Å to ~6800Å). Again, note the O_2 telluric absorption feature at pixel number 695.

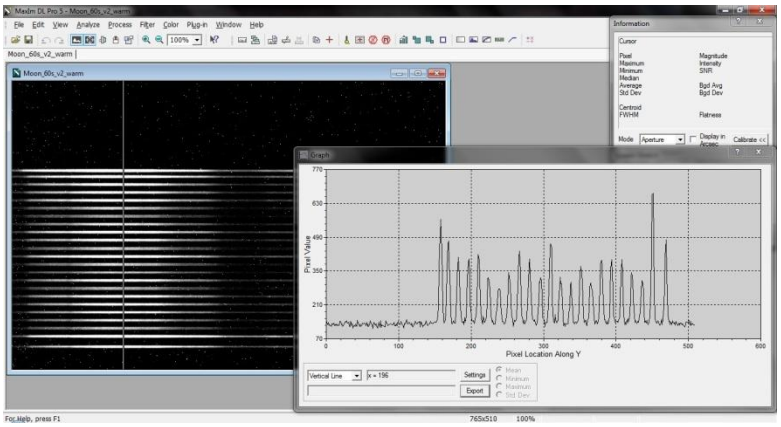

Figure 5.5.5 – A vertical cut through the 60s Moon exposure as shown by the MaxImDL Graph tool. The Graph window displays the intensity profile of the cut showing each fibre's spectrum.

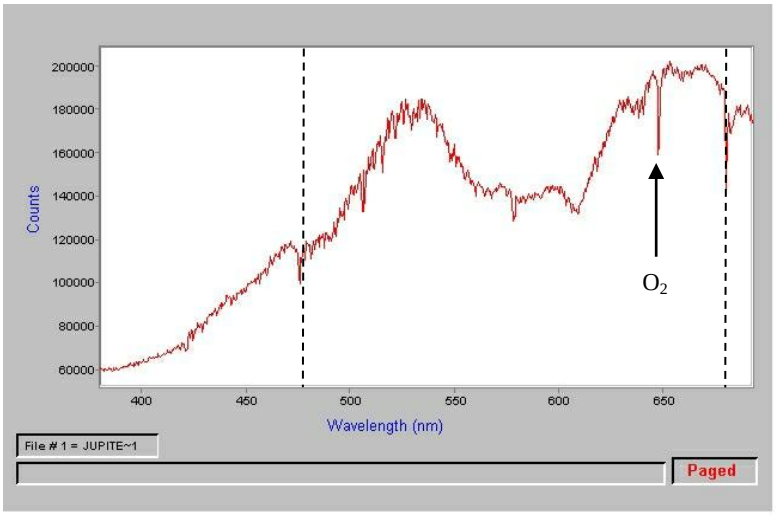

Figure 5.5.6 – (Dearden, 1999) – A 10s (100 x 1s) exposure of Jupiter using an MS-125 spectrograph with an InstaSpec MkIV CCD. Dotted black lines show the respective bandwidth of BASIS and the same O_2 absorption feature is also labelled.

6 PROPOSED INSTRUMENT UPGRADES

As a new IFU needs to be built and other instrument changes are needed, it is a good time to think about any improvements that can be made to the instrumentation to not only better the data but also the calibration and handling of the instrument. The proposed upgrades are:

IFU

1. Instead of using the fibre positioning substrate method for making the fibre bundle, FC connectors are to be used. FC connectors are standard commercial fibre optic connectors that have a plastic ferrule with a 127μm hole to thread the fibre down. The diameter of the ferrule is ~2.5mm and its length is ~15mm. It is then possible to use a 1.3mm drill bit to enlarge the hole such that the 19-fibre bundle can be threaded down. FC connectors also have a key lock that fixes rotation, which means that the rotation would be consistent if the IFU is taken off the telescope (for observatory open nights / maintenance) and then put back on for observations. It would also mean that the exact position of the fibres projected onto the sky could be known consistently. Sky fibres would possibly have their own connector, so there would be a total of five connectors. The FC connectors would also make the whole IFU unit much more robust meaning that it would last a lot longer when being handled.
2. Use a one-part epoxy for the glueing to remove the effect of bubble caused by the mixing process in two-part epoxy. The exact glue is unknown, but UV curing glue would work well.
3. When glueing the fibres in the bundle, be more diligent with the application of the glue to make sure that when the glue cures that no fibres can slide in and out of the bundle.

IFU Mount

1. To change to mount to a 1¼-inch mount such that the IFU could be placed in the off-axis position of an off-axis guider mount. This would allow the acquisition and guiding camera (at the moment the SBIG STL-6303E) to be placed at the primary position of the off-axis guider mount, meaning that the flexure problems with the camera mounted on the TeleVue would no longer be present. Thought would have to be taken on how to make sure sky fibres can be used in the off-axis position, but considering that a standard off axis guider has a CCD of 5mm x 5mm in size then it should not be too difficult to incorporate. The use of FC connectors with this proximity is a problem due to the overall diameter of an FC connector being 9mm. Separate sky exposure could be taken, but that increases the time overheads dramatically and would never be exact. There may be a way to include the sky fibres in the same FC connector as the fibre bundle, but it would be the separation of the sky fibres to the bundle would be at most 1 arc minute.

1-D Array

1. Extra room is needed in the 1-D array to ensure no fibres are pushed upwards as they are packed in to allow room for consecutive fibres. A V-groove would be ideal, but the cost just does not seem worth it in this case.

SBIG SGS No changes needed. It appears to be working as expected.

7 OBSERVATIONS

As it was not possible to get observations of standard stars and galaxies in the time of this project, the following section details the work in creating a target list of standard stars and galaxies for future observations.

7.1 Standard stars

To be able to get proper flux calibration out of BASIS it would need to observe bright standard stars. A full list of "Bright Northern BVRI Standard Stars" can be found at (TASS, 1997) (~120 stars), and this catalogue will be used for flux calibrating BASIS. Which standard star to observe will depend on the time of year and the conditions that night, i.e. if the moon is up then find one that is near zenith but furthest from the moon. The V-mag (M_V) of these stars range from 5.2 to 10.5, with ~60 of M_V <7, matching well with the performance of BASIS. Even though it is no longer used as a standard star for flux calibration, observing Vega would give a good idea of the performance of BASIS, as it is a well-studied star and has a $M_V = 0$.

7.2 Target galaxies

It has been mentioned a few times now that the performance of BASIS would mean that to get a SNR of 10, needed for spectral analysis, it would require a 20min exposure of a ~13mag/arcsec^2 galaxy with an angular diameter of ~1arcmin. To find galaxies that would fit this bill, the Third Reference of Bright Galaxies (RC3) (de Vaucouleurs et al., 1991) was reduced using the online catalogue tool VizieR (CDS, 2012). The RC3 includes most parameters of the galaxy, which meant that parameter constraints could be applied. After downloading the entire catalogue, the order of constraints was:

1. Declination greater than 0 degrees (Dec>0), V magnitude less than 15 (M_V<15), Isophotal diameter (up to a magnitude of 25) of greater than 1.25arcmin and less than 2.00arcmin (1.25<D25<2.00).
   2026 galaxies
2. B magnitude of less than 13 (M_B<13)
   686 galaxies
3. Visually selected from SuperCosmos (Read, 2008) 2arcmin square POSSIIR thumbnail images such that the galaxies would fit well into the 1arcmin angular diameter of the IFU.
   641 galaxies (list used for CKT images, see §7.3)
4. RA between 9 hours and 12 hours (9<RA<12) for the time of year of the commissioning nights (February to April 2012) and a Declination of greater than 45 degrees (Dec>45) to observe galaxies near zenith.
   94 galaxies
5. Declination between 60 and 70 degrees (60<Dec<70). Best visually selected from CKT images to get a reference on how well these galaxies are observed from Bayfordbury Observatory and on a Meade LX200 16-inch.
   17 galaxies
6. Best galaxies for each type: (see Figure 7.2.1) where the galaxies might be slightly oversized, but the first observations would be better with more light, so the IFU is centred more around the core of the galaxy. The BASIS IFU (of 1arcmin diameter) is overlaid for reference.

Any of the galaxies from the 641 galaxy list would be suitable for BASIS, which ones exactly would be due to the RA constraint on the time of year and the users discretion depending on what science is desired. The current constraint is to just get any galaxy observations, and so bright oversized galaxies would be the best to start with. More catalogues could be reduced via a similar selection criteria, e.g. NGC (Dreyer & Sinnott, 1988), HyperLEDA (Paturel et al., 2003) and NED (Schmitz et al., 2011) though at the moment the RC3 catalogue works very well.

Spiral (Edge-on) – NGC 4026	Spiral (Face-on) – NGC 4100	Elliptical – NGC 4125
J2000RA(h:m:s) = 11:59:25.6	J2000RA(h:m:s) = 11:59:25.6	J2000RA(h:m:s) = 11:59:25.6
J2000Dec (d:m:s) = +50:57:43	J2000Dec (d:m:s) = +50:57:43	J2000Dec (d:m:s) = +50:57:43
M_B = 11.61	M_B = 11.64	M_B = 10.80

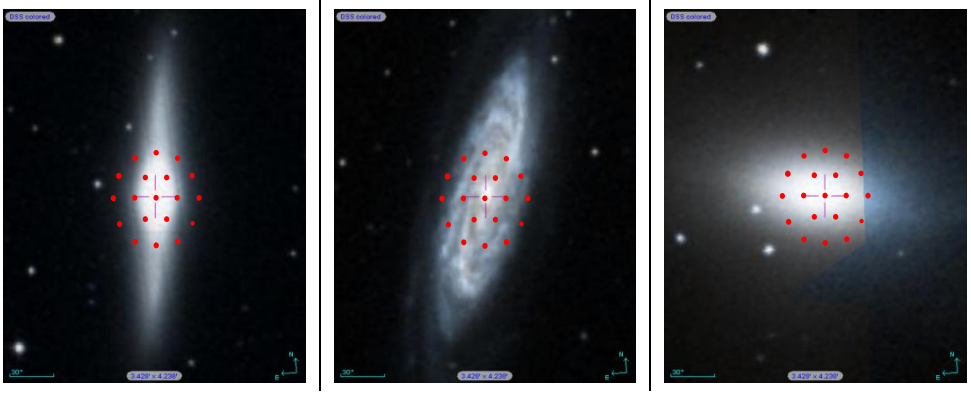

Figure 7.2.1 – Best first targets of BASIS of different galaxy types; Spiral (Edge-on), Spiral (Face-on) and Elliptical. The BASIS IFU of 1arcmin diameter is overlaid for reference. The images are taken from the DSS archive (DSS, 2010) via the Aladin reference tool (Bonnarel et al., 2000), where NGC 4125 happened to land at the border of two tiled exposures leaving the borderline shown. The RA and Dec is in J2000 and the M_B is from the RC3 catalogue.

7.3 Target galaxy imaging

To get a reference on the observing conditions BASIS would have to work to, the list of 641 galaxies as described in Step 3 of the selection criteria in §7.2 was submitted to the CKT for observations. The CKT is also a Meade LX200 16-inch telescope and uses an SBIG STL-6303E camera for photometric observations. It also is a fully automated and robotic telescope running the ACP Observatory Control software, meaning that it would work through the 641 galaxies when it could, as they were submitted at a low priority. The exposures are done with a clear filter and for 300 seconds. After checking the images, it was decided to run follow up 600s exposures using the Hα filter to see the distribution across the galaxy. After a couple of months, ~250 galaxies have been observed with 25% having Hα follow-ups. Figure 7.3 shows some examples of observed galaxies with their Hα counterparts.

The observations of all the galaxies came out rather well and show that this level of deep-sky observation is possible from Bayfordbury Observatory using a Meade LX200 16-inch telescope. Figure 7.3 clearly shows the Hα contribution for each galaxy, where the colour map has been set to “Rainbow” (black/dark blue is low flux and bright red is high flux) to bring out the features. NGC 3344 and NGC 3846’s Hα counterparts reveal star forming regions within the spiral arms of their respective galaxies, and NGC 2768 seems to exhibit weak extended Hα emission. The scale of the Rainbow colour map is normalised to each exposure so the range can be seen by how “dark” the background is, where the darker means the overall intensity is greater.

As time goes on, the CKT will work through the rest of the galaxies on the list of 641 galaxies and will also perform Hα follow-ups. This catalogue of galaxy images is a great reference tool for Bayfordbury, and having the Hα follow-ups can lead to some interesting investigations that will be left for another project (or many projects), albeit, seeing the extent of the Hα emission in a galaxy is a useful reference for BASIS and will be used when BASIS observes said galaxies.

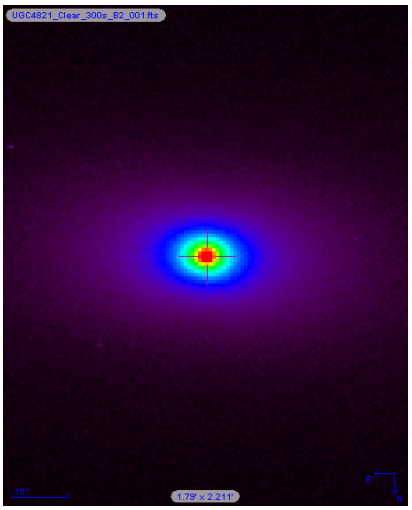

NGC 2768 Clear Filter 300s

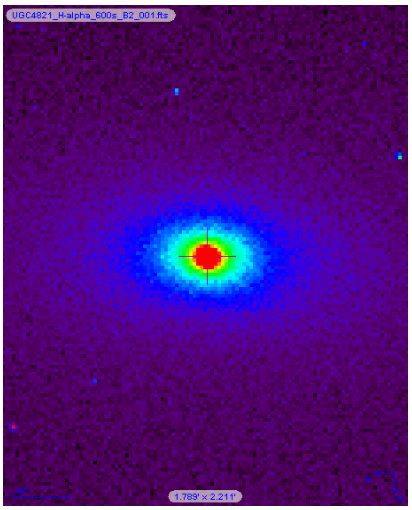

NGC 2768 Hα Filter 600s

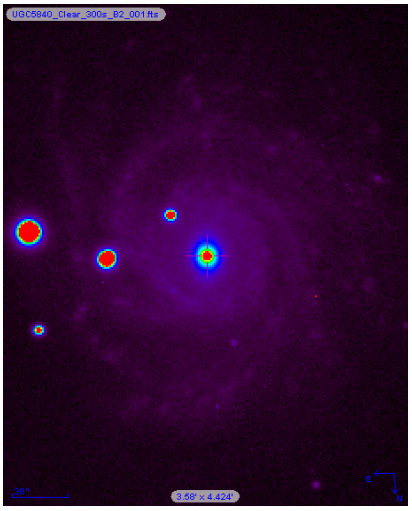

NGC 3344 Clear Filter 300s

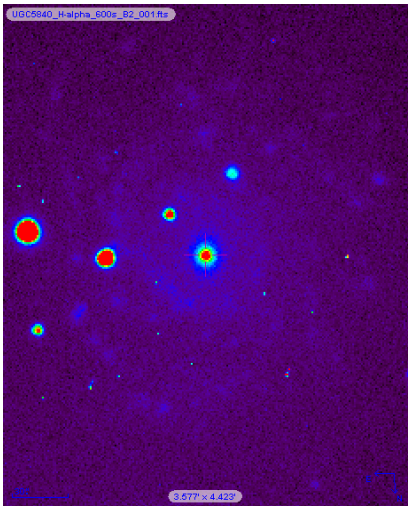

NGC 3344 Hα Filter 600s

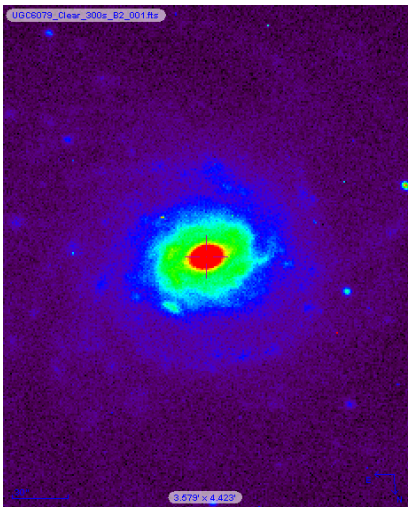

NGC 3486 Clear Filter 300s

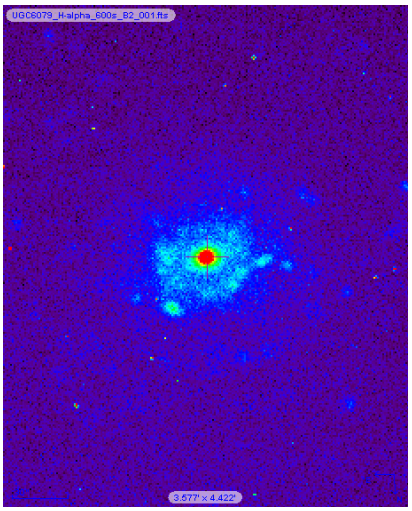

NGC 3486 Hα Filter 600s

Figure 7.3 – 300s Clear Filter and 600s Hα Filter exposures of various galaxies. A "Rainbow" colour map has been applied to bring out the features, where dark blue is low flux and bright red is high flux. The colour map is normalised to each exposure respectively. The dimensions at the bottom of the exposure are the size of the image here in arc minutes.

7.4 (super)nova watch

Due to the CKT taking exposures of nearby galaxies, there is a chance that the Hα follow up will reveal a (super)nova. Even though the chances are extremely small, it was thought that the Hα follow up of NGC 3344 did indeed show a (super)nova feature. Figure 7.4.1 shows the location of the feature, which is also visible in Figure 7.3. It's prominence in the Hα follow up and no respective feature in the Clear exposure leads one to believe that this must be a (super)nova. These exposures were only examined by eye on the 23/02/2012 and seeing that they were taken six days apart strengthened the possibility that it could be a (super)nova. The 24/02/2012 was cloudy and so no follow up could be done at Bayfordbury, so time was requested on the 2.5m Nordic Optical Telescope (NOT), located in La Palma and with thanks to Prof. Jesper Sollerman of Stockholm University (an expert in supernovae and gamma-ray bursts). The resulting exposure from the NOT is given in Figure 7.4.2, which shows no such (super)nova feature as seen in Figure 7.4.1. This means one of two things: 1. The (super)nova had already finished and had become too dim to see with the NOT, or 2. The (super)nova feature is in fact an instrument ghost. The former does not seem likely due to brightness of the feature in the CKT's Hα follow image and the NOT is a much more sensitive instrument. This means it is most likely that the feature is caused by an instrument ghost, a remnant from a previous exposure or an effect caused by the optics of the instrument set up.

An investigation was then carried out into what could have caused the ghost, given by the following steps:

1. Check other Hα follow up exposures for similar ghosts. Ghosts detected but not near any of the galaxies. Seem to be related to bright stars.
2. Check multiple exposure of the clear filter to see if it is a filter effect. Archival images from the CKT show similar ghosts still related to bright stars.
3. Check previous and following exposure to NGC 3344 Hα follow-up to see if ghost persists. No ghost found.
4. Check the CKT's observing log for the 03/02/2012. Found that the CKT observed another target between performing the Hα follow-ups. Target was NGC 3239 and the ghost lines up well with the bright foreground star BD+17 2217 (see Figure 7.4.3).

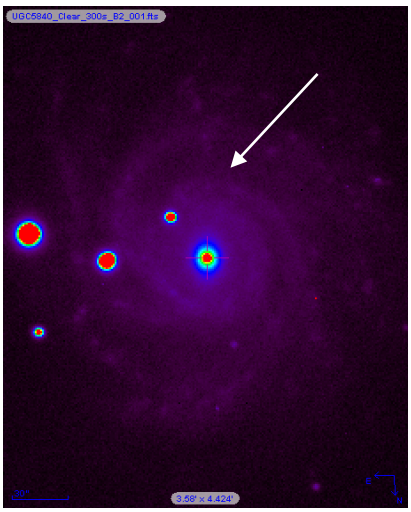

NGC 3344 Clear Filter 300s
Date: 27/01/2012
Time: 17:09

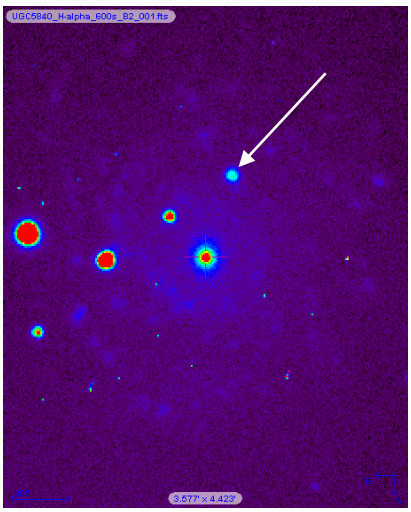

NGC 3344 Hα Filter 600s
Date: 03/02/2012
Time: 22:37

Figure 7.4.1 – 300s Clear Filter and 600s Hα Filter exposures of NGC 3344 showing the (super)nova feature, located by the white arrows. A "Rainbow" colour map has been applied to bring out the features, where dark blue is low flux and bright red is high flux. The colour map is normalised to each exposure respectively. The dimensions at the bottom of the exposure are the size of the image here in arc minutes.

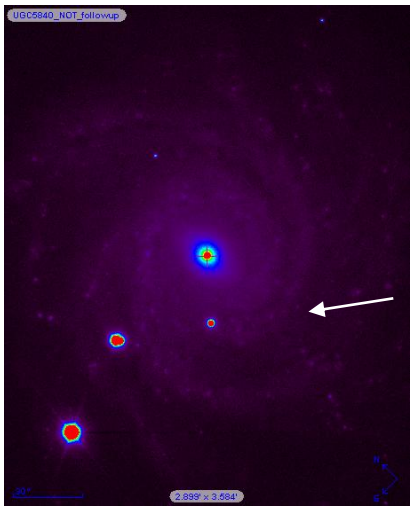

Figure 7.4.2 – 2.5s Open Filter exposure of NGC 3344 taken by the 2.5m NOT showing no (super)nova feature (expected position located by the white arrow). A "Rainbow" colour map has been applied to bring out the features, where dark blue is low flux and bright red is high flux. The dimensions at the bottom of the exposure are the size of the image here in arc minutes. Note the rotational difference from Figure 7.4.1 given by the compass bearing in the lower right.

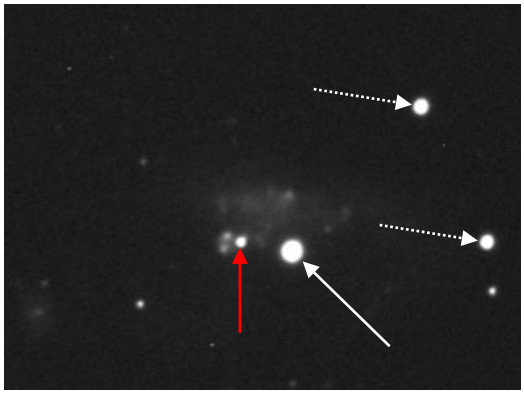

NGC 3239 Clear Filter 300s
Date: 27/01/2012
Time: 17:09

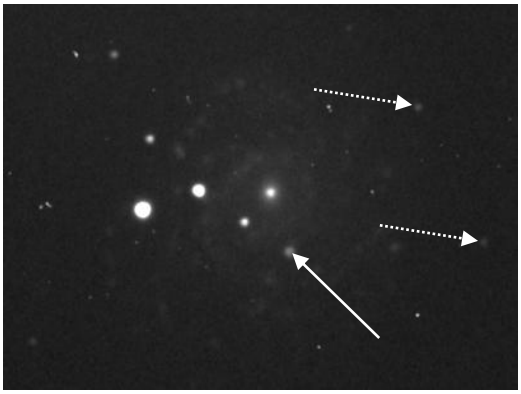

NGC 3344 Hα Filter 600s
Date: 03/02/2012
Time: 22:37

Figure 7.4.3 – 600s Clear Filter exposure of NGC 3239 and 600s Hα Filter exposure of NGC 3344 taken by the CKT showing the ghost (located by the solid white arrow). The images have been cropped from their original size, but there is no difference in pixel location. The dotted white arrows show additional residual ghost features from bright foreground stars. The red arrow shows the location of SN 2012a.

The ghost is due to an effect called "Residual Bulk Image (RBI)", which is the residual charge on the CCD substrate, due to saturated pixels, falling back into the pixels after read-out. The RBI seems to be inherent on all KAF CCD chips, and poses a real problem for photometry, and of course creating (super)nova false positives. To deplete the RBI it takes ~25mins to let all / most of the charge fall into the pixels from the substrate. You can get around this by performing an infrared flash on the CCD, which equalises the RBI across the entire CCD and can then be corrected with the bias frame. This is something that might prove difficult with the CKT, but a solution must be found before accurate photometry can be performed. There is no risk of the RBI being a problem with the SBIG ST-7E because the photon count will be too low from observations and therefore never saturate the CCD. It is an amusing coincidence that the exposure that caused the RBI to create the ghost in the exposure of NGC 3344 was of NGC 3239, which was only being observed because it does have a supernova (SN2012a, see Figure 7.4.3, red arrow) so the CKT was getting another measurement for its light curve.

8 FUTURE WORK

As this project is something that could actually gather new scientific data and one that could be replicated by others, the decision was made to submit it to the SPIE Astronomical Telescopes and Instrumentation 2012 conference in July 2012 titled, "BASIS: Bayfordbury single-object integral field spectrograph". The relevant deadlines were marked in the Project Line shown in §1.2, which were met and the project was accepted for the conference in form of a poster. SPIE requests that a manuscript be published in the conference proceedings, which is to be of equivalent standard to a research paper being published in a journal. For the purposes of this paper and also for continued help throughout the project, a small BASIS Team was created that includes the individual people noted in the start of the acknowledgements.

Additional to the SPIE conference, a poster presentation has also been accepted to the UK-Germany National Astronomy Meeting 2012 (NAM 2012) conference in Manchester, UK (March 2012), and also to the Scientific Committee on Antarctic Research – Astronomy & Astrophysics from Antarctica 2012 (SCAR AAA 2012) conference in Portland, Oregon, USA (July 2012). The poster for the NAM and SCAR AAA conferences will be a more generic topic of "Integral field spectroscopy on small aperture telescopes". In addition to conferences, there will be a push for a press release once a galaxy has been observed and its data cube analysed. Talks/seminars at research institutions will be sought after, with the first one being for the Science and Technology Research Institute (STRI) at the University of Hertfordshire on the 23/03/2012. Public outreach of BASIS and the science of integral field spectroscopy has already started with involvement at the Public Open Nights at the Bayfordbury Observatory.

The project will inevitably be continued beyond the deadline of this report, and the instrument developed further to incorporate the changes as proposed in §6. The target for the SPIE paper is to have at least 50 galaxies observed, which does not leave much time to resolve all of the current complications, though the success here will come from time and effort, which have been applied since the start of this project. Sights will be set to utilise the SAMI_tools package in the data reduction of such galaxy observations. Bridging the divide between amateur astronomy and scientific research is something I have a passion for. For that reason, I would like to see this instrument and its science used by as many people as possible. A document providing full instructions on how to build such an instrument and to carry out the science will be provided in due course when an instrument in full working order has been completed (Richards, 2012). Once in full completion, an article will be submitted to astronomy magazine, such as "Astronomy Now", so a wider audience, including amateur astronomers, can read about BASIS.

9 CONCLUSIONS

Integral field spectroscopy on small aperture telescopes is a difficult task, but is one that with the advent of BASIS has been proven to be possible. The use of fibre optics coupled with the existing equipment of the Meade LX200 16-inch telescope and the SBIG SGS enables a relatively simple design, which can be replicated for use at most observatories around the world that would be otherwise classed as a teaching observatory. As this class of observatories accommodate undergraduate and/or postgraduate teaching then the institution also has the option to offer the practical teaching of integral field spectroscopy, something that has been very restricted before. However, given the expected performance of BASIS, it is not limited to just being used as a teaching instrument, but truly bridges the divide between amateur astronomy and scientific research. The goal to obtain observations and analysis of at least 50 galaxies will act as the proof-of-concept for a full-scale survey of 10^3 nearby galaxies over ~100 clear nights (translating to a period of a couple of years at Bayfordbury Observatory).

As an instrument, the hoped-for costing of <$500 was achieved when utilising the existing telescope (~$20,000) and spectrograph (~$5,000). Even with this low cost, the prototype version (the one reported here) still managed to do everything it was asked to do after a bit of gentle persuasion and upgrading. The resulting instrument is one that is pleasing, and paves the way to a full working instrument after a few necessary upgrades are carried out, including changing the design of the IFU to fit within an FC connector and be able to be mounted on the off-axis position of an off-axis guider mount. Once this is done the instrument will be ready to observe the proposed target galaxies in §7.2 taking advantage of the ACP Observatory Control Software.

This project also acts as the pre-cursor of many other related projects including the pipeline needed to reduce and analyse the integral field spectra gathered by BASIS and the mapping of HII regions using the galaxy images taken by the CKT. It becomes evident then that upon the success of this instrument, larger involvement in the form of a BASIS Team to help with such data reduction is needed. It is exciting to think about the role of BASIS in the years to come.

10 REFERENCES

Allington-Smith, J., 2006. Basic principles of integral field spectroscopy. *New Astronomy Reviews*, 50(4-5), pp.244-51.

ATC, 2010. CCD kamery SBIG. *http://www.atc-astro.eu/Sbig/*.

Bacon, R. et al., 2001. The SAURON project - I. The panoramic integral-field spectrograph. *MNRAS*, 326(1), pp.23-35.

Baldwin, J.A., Phillips, M.M. & Terlevich, R., 1981. Classification parameters for the emission-line spectra of extragalactic objects. *Publications of The Astronomical Society of the Pacific*, 93, pp.5-19.

Bayfordbury, 2012. All Sky Camera. *http://star.herts.ac.uk/allsky/*.

Bland-Hawthorn, J. et al., 2011. Hexabundles: imaging fiber arrays for low-light astronomical applications. *Optics Express*, 19(3).

Bonnarel, F. et al., 2000. The ALADIN interactive sky atlas. A reference tool for identification of astronomical sources. *Astronomy and Astrophysics Supplement* , 143((http://aladin.u-strasbg.fr/)), pp.33-40.

Buttenshaw, N., 2011. Telling LIERs from LINERs. *Final Year Projects, PAM, University of Hertfordshire, Hatfield, Hertfordshire, AL10 9AB*.

Cappellari, M. et al., 2011. The ATLAS3D project - I. A volume-limited sample of 260 nearby early-type galaxies: science goals and selection criteria. *Monthly Notices of the Royal Astronomical Society*, 413(2), pp.813-36.

CDS, 2012. Centre de Données astronomiques de Strasbourg - VizieR catalogue service. *http://vizier.u-strasbg.fr/cgi-bin/VizieR*.

Crane, P. & Banse, K., 1982. The Munich Image Data Analysis System. *Memorie della Societa Astronomica Italiana*, 53(1), pp.19-29.

Croom, S.M. et al., 2011. The Sydney-AAO Multi-object Integral field spectrograph (SAMI). *Monthly Notices of the Royal Astronomical Society*, arXiv:1112.3367, p.accepted Dec.2011.

Dahari, O. & De Robertis, M.M., 1988. A statistical study of properties of Seyfert and starburst galaxies. *Astrophysical Journal Supplement Series*, 67, pp.249-77.

de Vaucouleurs, G. et al., 1991. Third Reference Catalogue of Bright Galaxies. *Springer-Verlag Berlin Heidelberg New York*, 1-3(XII), p.2069.

Dearden, S.J., 1999. A Comparative Review of some. *http://users.erols.com/njastro/faas/pages/paper001.htm*.

Denny, R.B., 2012. ACP Observatory Control Software [DC-3 Dreams]. *http://acp.dc3.com/index2.html*.

Diffraction Limited, 2012. MaxIm DL Version 5. *http://www.cyanogen.com/maxim_main.php*.

Dreyer, J.L.E. & Sinnott, R.W., 1988. The Complete New General Catalogue and Index Catalogue of Nebulae and Star Clusters | Source Catalog Reference: NGC 2000.0. *Sky Publishing Corporation and Cambridge University Press*.

DSS, 2010. Digitized Sky Survey - STScI/NASA, Healpixed by CDS. *http://alasky.u-strasbg.fr/DssColor*.

Dunlop, J.S., 2011. The Cosmic History of Star Formation. *Science*, 333(no.6039), pp.178-81.

Fogarty, L., 2012. Private Correspondence.

Galactica, 2012. LX200 ACF 16" F/10 UHTC C/ PÉ EQUATORIAL. *http://www.galactica.pt/ver/3051/1/3/19/meade-lx200-acf-16-f10-uhtc-c-pe-equatorial.php*.

GSMT, 2002. Section 4.7.1: Wide-Field Multi-Object Multi-Fiber Optical Spectrograph (MOMFOS). *http://www.gsmt.noao.edu/book/ch4/4_7_1.html*.

Hill, G.J. et al., 2008. The Hobby-Eberly Telescope Dark Energy Experiment (HETDEX): Description and Early Pilot Survey Results. *Panoramic Views of Galaxy Formation and Evolution ASP Conference Series*, 399, p.115.

Ho, L.C., Filippenko, A.V. & Sargent, W.L.W., 1993. A Reevaluation of the Excitation Mechanism of LINERs. *The Astrophysical Journal*, 417, p.63.

Holmes, A., 2011. Private Correspondence.

Holmes, A., 2012. Private Correspondence.

Holmes, A. & SBIG, 2001. Operating instructions for the SBIG SGS and spectra analysis software. *http://www.sbig.com/images/documents/products/222*.

Hook, I.M. et al., 2004. The Gemini-North Multi-Object Spectrograph: Performance in Imaging, Long-Slit, and Multi-Object Spectroscopic Modes. *PSAP*, 116(819), pp.425-40.

Kauffmann, G. et al., 2003. The host galaxies of active galactic nuclei. *Monthly Notices of the Royal Astronomical Society*, 346(4), pp.1055-77.

Kewley, L.J. et al., 2001. Theoretical Modeling of Starburst Galaxies. *The Astrophysical Journal*, 556(1), pp.121-40.

Kewley, L.J., Groves, B., Kauffmann, G. & Heckman, T., 2006. The host galaxies and classification of active galactic nuclei. *Monthly Notices of the Royal Astronomical Society*, 372(3), pp.961-76.

Kinney, A.L. et al., 1996. Template ultraviolet to near-infrared spectra of star-forming galaxies and their application to K-corrections. *The Astrophysical Journal*, 467, pp.38-60.

Kodak, 2003. KAF-0402E/ME Device Performance Specification Document. *http://www.eso.org/sci/facilities/paranal/instruments/mascot/doc/KAF-0402ELongSpec.pdf*, (1), p.17.

Lahav, O. & Suto, Y., 2004. Measuring our Universe from Galaxy Redshift Surveys. *Living Rev. Relativity 7*, http://www.livingreviews.org/lrr-2004-8.

Law, D., Weijmans, A.-M. & Wright, S., 2012. The Mapping Nearby Galaxies at APO (MaNGA). *http://dunlap.utoronto.ca/research/surveys/*.

Osterbrock, D.E., 1991. Active galactic nuclei. *Reports on Progress in Physics*, 54(4), p.579.

p3d, 2011. Screenshots. *http://p3d.sourceforge.net/index.php?page=screens*.

Pasquini, L. et al., 2002. Installation and commissioning of FLAMES, the VLT Multifibre Facility. *The Messenger*, (No. 110), pp.1-9.

Paturel, G. et al., 2003. HYPERLEDA. I. Identification and designation of galaxies. *Astronomy and Astrophysics*, 412, pp.45-55.

Polymicro, 2008. Low OH and High OH Optical Fiber. *http://www.polymicro.com/catalog/2_15.htm*.

Read, M., 2008. SuperCOSMOS Sky Surveys (SSS) -- Batch form - pixel data. *http://www-wfau.roe.ac.uk/sss/batchfile.html*, p.(extracted 2012).

Rees, M.J., 1984. Black Hole Models for Active Galactic Nuclei. *Annual Review of Astronomy and Astrophysics*, 22, pp.471-506.

Richards, 2012. Contact to request BASIS Instruction Manual: samuelnathanrichards@gmail.com.

Sánchez, S.F., 2006. Techniques for reducing fiber-fed and integral-field spectroscopy data: An implementation on R3D. *Astronomische Nachrichten*, 327(9), p.850.

Sanchez, S.F., Cardiel, N., Verheijen, M. & Benitez, N., 2007. Integral Field Spectroscopy of the core of Abell 2218. *ESO Astrophysics Symposia*, pp.193-98.

Sandin, C. et al., 2010. p3d : a general data-reduction tool for fiber-fed integral-field spectrographs. *A&A*, 515(id.A35).

Schawinski, K. et al., 2007. Observational evidence for AGN feedback in early-type galaxies. *Monthly Notices of the Royal Astronomical Society*, 382(4), pp.1415-31.

Schawinski, K. et al., 2010. Galaxy Zoo: The Fundamentally Different Co-Evolution of Supermassive Black Holes and Their Early- and Late-Type Host Galaxies. *The Astrophysical Journal*, 711(1), pp.284-302.

Schmidt, M. & Green, R.F., 1983. Quasar evolution derived from the Palomar bright quasar survey and other complete quasar surveys. *The Astrophysical Journal*, 269(Part 1), pp.352-74.

Schmitz, M. et al., 2011. The NASA/IPAC Extragalactic Database (NED): Enhanced Content and New Functionality. *American Astronomical Society, AAS Meeting #217, #344.08; Bulletin of the American Astronomical Society*, 43.

Sharp, R. & SPIRAL Team, 2006. The SPIRAL IFU: integral field spectroscopy at the AAT. *AAO Newsletter*, (No. 110), p.24.

SUSS, 2011. Image courtesy of SUSS - Hexagonal grid micro-lens array. *http://www.suss-microoptics.com/shop/microlens-arrays/fused-silica/circular-lenses-hexagonal-grid/microlens-array-nr-13-9910-101-000.html*.

TASS, 1997. Bright Northern BVRI Standards. *http://stupendous.rit.edu/tass/refs/skiff_photom.html*.

Tody, D., 1986. The IRAF Data Reduction and Analysis System. *Society of PhotoOptical Instrumentation Engineers SPIE Conference Series*, p.733.

Westmoquette, M.S. et al., 2009. The integral field spectroscopy (IFS) wiki. *arXiv:0905.3054*, This article accompanies the opening of the IFS wiki site http://ifs.wikidot.com.

11 APPENDIX A – BASIS SNR CALCULATOR

BASIS SNR Calculator

ST-7E CCD

Stellar Magnitude	445nm SNR (Dark)	551nm SNR (Dark)	658nm SNR (Dark)	806nm SNR (Dark)	445nm SNR (Bright)	551nm SNR (Bright)	658nm SNR (Bright)	806nm SNR (Bright)
10.0	52.94	56.98	53.12	34.78	51.92	55.85	52.10	34.24
10.5	39.07	42.29	39.22	24.81	38.05	41.14	38.19	24.32
11.0	28.14	30.65	28.25	17.24	27.19	29.57	27.30	16.83
11.5	19.74	21.65	19.82	11.69	18.93	20.70	19.01	11.37
12.0	13.50	14.90	13.56	7.77	12.86	14.13	12.91	7.53
12.5	9.03	10.02	9.07	5.08	8.55	9.44	8.59	4.91
13.0	5.94	6.61	5.96	3.28	5.60	6.20	5.62	3.17
13.5	3.85	4.30	3.87	2.10	3.62	4.01	3.63	2.03
14.0	2.47	2.77	2.49	1.34	2.32	2.58	2.33	1.29
14.5	1.58	1.77	1.59	0.85	1.48	1.65	1.49	0.82
15.0	1.00	1.13	1.01	0.54	0.94	1.05	0.94	0.52
15.5	0.64	0.71	0.64	0.34	0.60	0.66	0.60	0.33
16.0	0.40	0.45	0.41	0.22	0.38	0.42	0.38	0.21
16.5	0.25	0.29	0.26	0.14	0.24	0.27	0.24	0.13
17.0	0.16	0.18	0.16	0.09	0.15	0.17	0.15	0.08
17.5	0.10	0.11	0.10	0.05	0.09	0.11	0.10	0.05
18.0	0.06	0.07	0.06	0.03	0.06	0.07	0.06	0.03

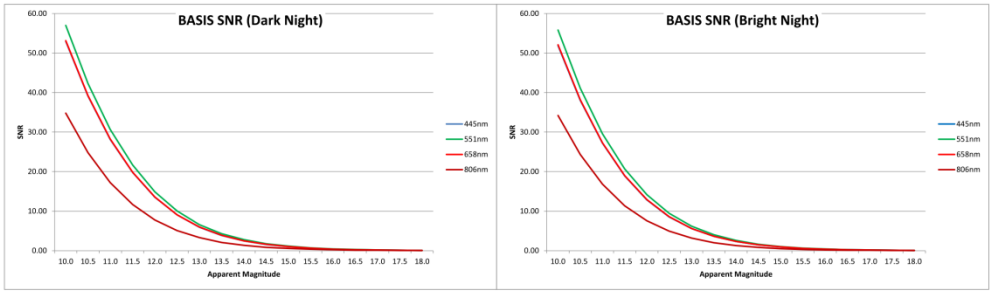

ST-7E Specs — Dual CCD: Kodak KAF-0402ME+TI TC-237

Pixels	Pixel Size (microns)	CCD Size (mm)	Total Pixels	Exposure (s)	Cooling (K)	A/D Converter	A/D Gain	Back Focus (cm)
764 x 510	9 x 9	6.9 x 4.6	390,000	0.12 to 3600	228 +/-0.1	16 Bits	2.3e-/ADU	2.3

Detector Specs

Chip	ReadNoise	Dark	QE 445nm	QE 551nm	QE 658nm	QE 806nm	DT	RN^2
KAF-0402ME	15	1	0.54	0.71	0.74	0.48	1200	225

Sky Brightness	mag arcsec^-2	mag arcsec^-2	mag arcsec^-2	mag arcsec^-2	N_{pht} s^-1	N_{pht} s^-1	N_{pht} s^-1	N_{pht} s^-1
Night	445nm	551nm	658nm	806nm	445nm	551nm	658nm	806nm
Dark	20	20	20	20	1.46E-05	1.00E-05	7.38E-06	4.89E-06
Bright	15	15	15	15	1.46E-03	1.00E-03	7.38E-04	4.89E-04

BASIS Specs	
LX200 Effective Area (m^2)	0.114
Total Throughput	0.05
Exposure Time (s)	1200
Resolution (lambda/∂l)	750
Pixels/Res. Element	1.5
Spatial pixels	5.5

Constants	
h (ergsec)	6.63E-27
c (Åsec^-1)	3.00E+18
Z_445nm (Wm^-2μ^-1)	7.18
Z_551nm (Wm^-2μ^-1)	7.442
Z_658nm (Wm^-2μ^-1)	7.64
Z_806nm (Wm^-2μ^-1)	7.91

Fluxes	F_{lambda}	F_{lambda}	F_{lambda}	F_{lambda}				
Stellar Magnitude	445nm	551nm	658nm	806nm	N_{pht} s^-1 445nm	N_{pht} s^-1 551nm	N_{pht} s^-1 658nm	N_{pht} s^-1 806nm
10.0	6.61E-13	3.61E-13	2.29E-13	1.23E-13	1.46E-01	1.00E-01	7.38E-02	4.89E-02
10.5	4.17E-13	2.28E-13	1.45E-13	7.76E-14	9.23E-02	6.31E-02	4.66E-02	3.09E-02
11.0	2.63E-13	1.44E-13	9.12E-14	4.90E-14	5.83E-02	3.98E-02	2.94E-02	1.95E-02
11.5	1.66E-13	9.08E-14	5.75E-14	3.09E-14	3.68E-02	2.51E-02	1.85E-02	1.23E-02
12.0	1.05E-13	5.73E-14	3.63E-14	1.95E-14	2.32E-02	1.59E-02	1.17E-02	7.75E-03
12.5	6.61E-14	3.61E-14	2.29E-14	1.23E-14	1.46E-02	1.00E-02	7.38E-03	4.89E-03
13.0	4.17E-14	2.28E-14	1.45E-14	7.76E-15	9.23E-03	6.31E-03	4.66E-03	3.09E-03
13.5	2.63E-14	1.44E-14	9.12E-15	4.90E-15	5.83E-03	3.98E-03	2.94E-03	1.95E-03
14.0	1.66E-14	9.08E-15	5.75E-15	3.09E-15	3.68E-03	2.51E-03	1.85E-03	1.23E-03
14.5	1.05E-14	5.73E-15	3.63E-15	1.95E-15	2.32E-03	1.59E-03	1.17E-03	7.75E-04
15.0	6.61E-15	3.61E-15	2.29E-15	1.23E-15	1.46E-03	1.00E-03	7.38E-04	4.89E-04
15.5	4.17E-15	2.28E-15	1.45E-15	7.76E-16	9.23E-04	6.31E-04	4.66E-04	3.09E-04
16.0	2.63E-15	1.44E-15	9.12E-16	4.90E-16	5.83E-04	3.98E-04	2.94E-04	1.95E-04
16.5	1.66E-15	9.08E-16	5.75E-16	3.09E-16	3.68E-04	2.51E-04	1.85E-04	1.23E-04
17.0	1.05E-15	5.73E-16	3.63E-16	1.95E-16	2.32E-04	1.59E-04	1.17E-04	7.75E-05
17.5	6.61E-16	3.61E-16	2.29E-16	1.23E-16	1.46E-04	1.00E-04	7.38E-05	4.89E-05
18.0	4.17E-16	2.28E-16	1.45E-16	7.76E-17	9.23E-05	6.31E-05	4.66E-05	3.09E-05

Stellar Magnitude	445nm Src Y'/pix	551nm Src Y'/pix	658nm Src Y'/pix	806nm Src Y'/pix
10.0	7118.1	6083.9	5221.8	4272.8
10.5	4491.2	3838.7	3294.7	2696.0
11.0	2833.8	2422.1	2078.8	1701.0
11.5	1788.0	1528.2	1311.6	1073.3
12.0	1128.1	964.2	827.6	677.2
12.5	711.8	608.4	522.2	427.3
13.0	449.1	383.9	329.5	269.6
13.5	283.4	242.2	207.9	170.1
14.0	178.8	152.8	131.2	107.3
14.5	112.8	96.4	82.8	67.7
15.0	71.2	60.8	52.2	42.7
15.5	44.9	38.4	32.9	27.0
16.0	28.3	24.2	20.8	17.0
16.5	17.9	15.3	13.1	10.7
17.0	11.3	9.6	8.3	6.8
17.5	7.1	6.1	5.2	4.3
18.0	4.5	3.8	3.3	2.7

445nm Dark Sky Y'/pix	551nm Dark Sky Y'/pix	658nm Dark Sky Y'/pix	806nm Dark Sky Y'/pix
3.9	3.3	2.9	2.4
445nm Bright Sky Y'/pix	551nm Bright Sky Y'/pix	658nm Bright Sky Y'/pix	806nm Bright Sky Y'/pix
391.5	334.6	287.2	235.0

12 APPENDIX B – BASIS TIME-LINE CHART

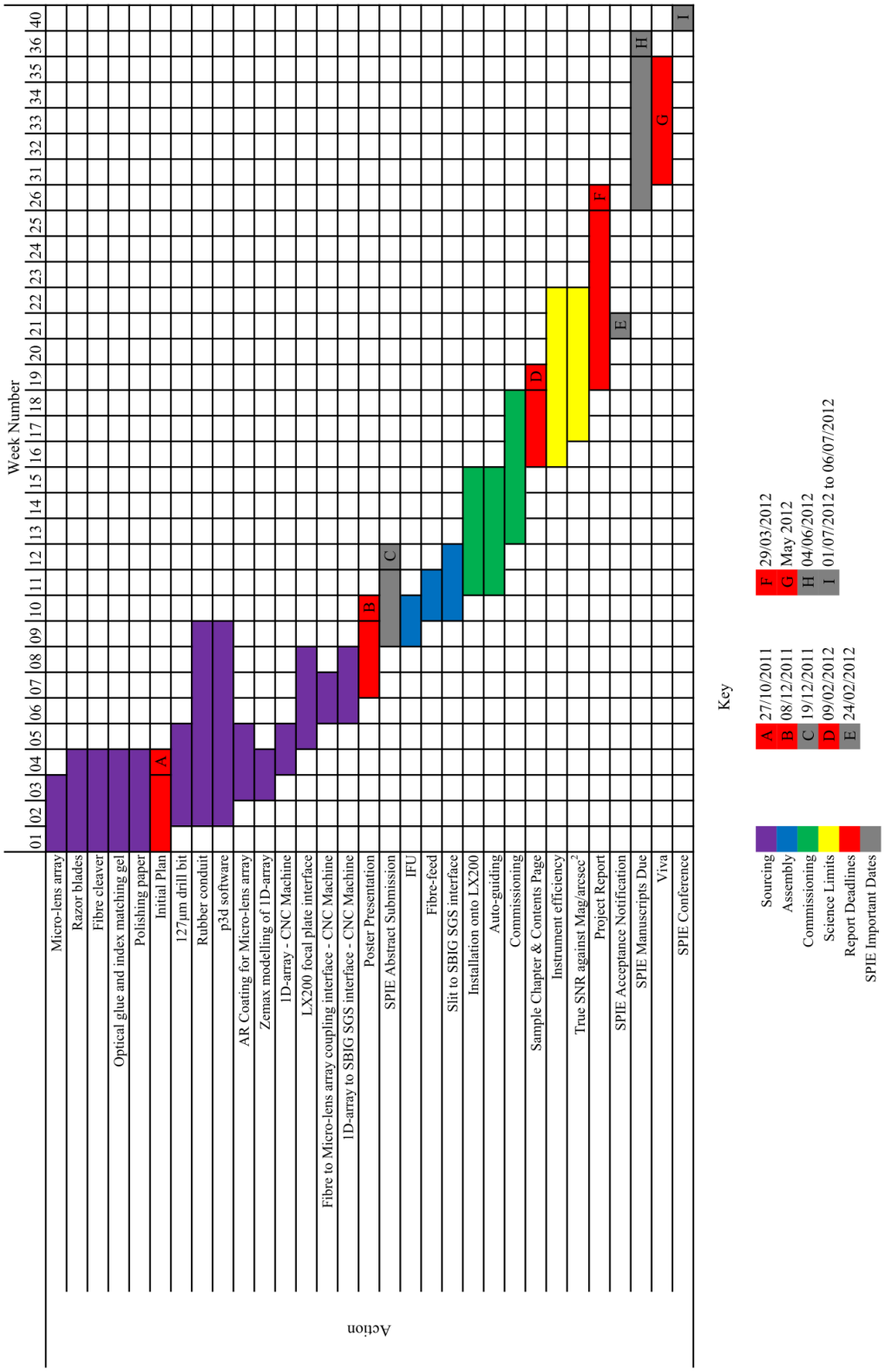

13 APPENDIX C – BASIS PURCHASED PRODUCTS LIST

Item	Product Number	Product Description	Source	Qty.	Price (each)	P&P	Total
Optical Fibre	002-005-006-xxx	Internal/External Loose Tube 50/125 (24 core)	http://www.cablemonkey.co.uk/acatalog/Loose_Tube_OM2_fibre_cable.html	20	£2.70	£6.00	£60.00
Polishing Paper	(30µm) 00A-001-002-18 (12µm) 00A-001-002-16 (09µm) 00A-001-002-15 (03µm) 00A-001-002-13 (01µm) 00A-001-002-12	Fibre Lapping Film (30µm/12µm/9µm / 3µm/1µm)	http://www.cablemonkey.co.uk/acatalog/Fibre_Lapping_Film.html	4 (30µm) 4 (12µm) 4 (9µm) 4 (3µm) 4 (1µm)	£2.16 £2.03 £1.68 £2.03 £1.88	£6.00	£45.12
Glue		UHU Plus Endfast "300kg" Epoxy Adhesive (33g)	http://www.sylmasta.com/acatalog/UHU_Adhesives.html	1	£8.78	£3.95	£12.73
Fibre Cleaver	DCS-MJ018A	Pen Cleaver	http://www.tools4it.com/fibre-optic-tools/pen-cleavers/pen-cleaver/prod_22.html	1	£15.54	£5.50	£21.04
3D Printing	Object3D®	FullCure™ VeroBlack	In-house (CAIR)	4 parts			Estimated Total £100.00

~Total	£238.89
@1.6 exchange	US$382.25
†Contingency Total	£400.00

† The contingency total allows for changes to the above list. Changes are likely as the project develops due to obstacles that need to be overcome. The interface components for the spectrograph and the telescope will be constructed using the Object3D® Printer in-house at the University of Hertfordshire.

14 APPENDIX D – COMMISSION REPORTS

14.1 First Night

Date: 03/02/2012	Start Time:19:00	End Time: 21:00
Site: Bayfordbury Observatory	Overall Weather: Cloudy	Moon: High gibbous moon
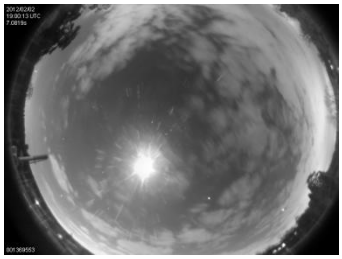 19:00 Sky Brightness: 17.99mag/arcsec^2	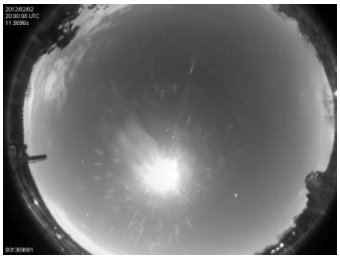 20:00 Sky Brightness: 18.06mag/arcsec^2	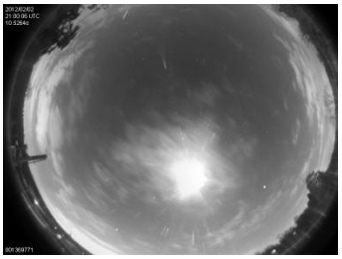 21:00 Sky Brightness: 17.99mag/arcsec^2

Notes:

1. Installed BASIS onto the telescope.
2. Installed the SBIG-6303E camera onto the TeleVue 102 (TV hereon).
3. Ensured telescope/mount fixings were tight.
4. Focussed TV.
5. Centre aligned HIP 31681 on the TV to check accuracy of centre alignment (within a couple of pixels)

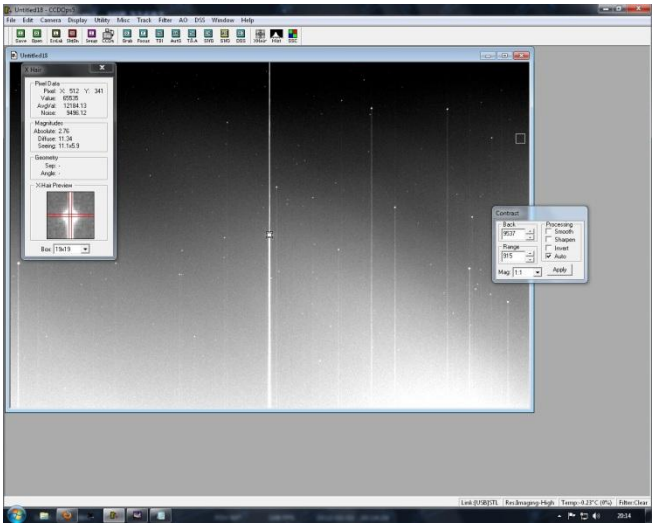

6. Cloud cover too much to continue. More cloud coming in.
7. End of night.

Report:

All parts of BASIS fit on the telescope and are in apparent working order. Centre alignment on the TV CCD can be achieved, though offset to the IFU still needs to be found. Cloud cover stopped observations.

To do on next commissioning night:

1. Calibrate the wavelength on the SBIG SGS with 650nm laser.
2. Find offset to IFU.
3. Observe standard star HIP 31681.
4. Observe

14.2 Second Night

Date: 03/02/2012	Start Time:19:00	End Time: 02:00
Site: Bayfordbury Observatory	Overall Weather: Clear	Moon: High gibbous moon
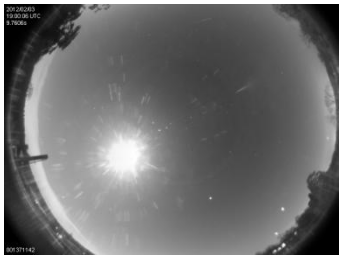	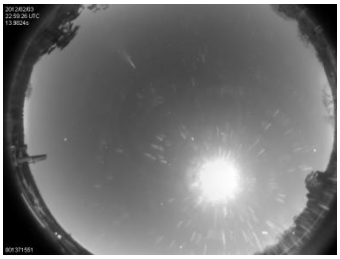	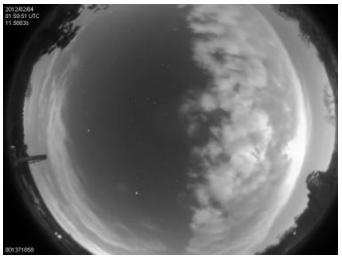
19:00 Sky Brightness: 18.11mag/arcsec^2	23:00 Sky Brightness: 18.09mag/arcsec^2	02:00 Sky Brightness: 18.74mag/arcsec^2

Notes:

total of 765pix = 212nm
683-650 = 33
33/212 = 0.1557
0.1557*765 = 119.0802
765-119.0802 = 646pix (align 650nm laser) = 2.4775microns on micrometer
---
gamma gem = Hip 31681
---
test1 - not long enough exposure, 60s
test2 - long enough exposure, not centred (NC), 120s
moved TV 4pix left
test3 - NC, 4pix not enough
moved TV 8pix left
test4 - NC, no spectra (NS) as was not doing the auto guiding control correctly. (this one was 12pix left on TV)
moved TV correctly back to 4pix left
test5 - NC, NS
go back to centre on AG to get reference point once more
test6 - NC, NS, not sure why NS. maybe previous was scattered light from moon as is close by.
went 5pix right on TV (offset = +5,0)
test7 - NC, NS
offset 0,+5
test8 - NC, NS
offset -5,0
test9 - NC, NS
offset 0,-5
test10 - NC, NS, not sure what to do except go to an object about 30" diameter and bright.

Quick observation of Orion's nebula by centring the bright centre to the centre of the TV.
m42 centred on guide camera to bright region
m42_test1 - NS, 120s
take longer exposure of m42
Scrap that... going to Mars as is brighter and saves time. now 22:50

Quickly take 25s exposure of Moon

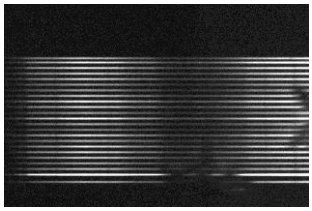

Light down all fibres! Good result. Strange features on the CCD. Absorption features visible!

Mars centred on TV and nearby star is being used for auto guiding (near bottom just to right)

mars_test1 - NC, NS, checked eyepiece and it was not centred on eyepiece.

Moved telescope until Mars was centred on eyepiece (best by eye), TV with nearby star just underneath and to the right of Mars.

mars_test2 - NC, S!, will perform crosshair offsets of 5pix again until centre found.

offset 0,+5

mars_test3 - NC, S, carry on with offsets

offset -5,0

mars_test4 - NC, S, carry on with offsets

offset 0,-5

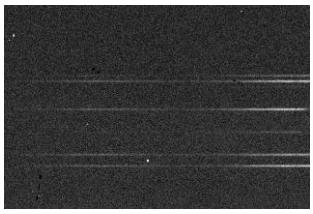

mars_test5 - NC, S, first time illuminating 1st ring. finish crosshair offset before testing either side of this position.

offset +5,0

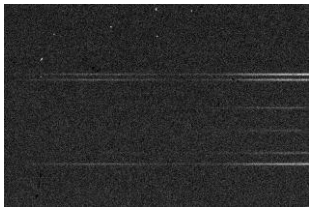

mars_test6 - NC, S, 1st ring visible still so assume in between these two offsets. will go for the corner of the offset square.

offset +5,-5

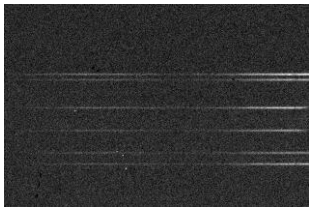

mars_test7 - NC, S, getting closer as lines are brighter, will halve the offset in both directions.

offset +2.5,-2.5 (if AG allows half pixels?)

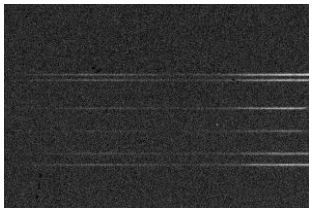

mars_test8 - NC, S, didn't illuminate central core so will try further away

offset +7.5,-7.5

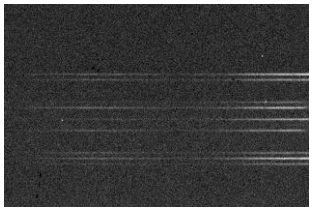

mars_test9 - C!, S!, best it's going to get at the moment. Will now apply same offsets to a galaxy field.

Pointing was rubbish, and can't manually point due to no visual reference stars. Finish for the night.

END

Report:

It went well, and stayed clear, but unfortunately no galaxy spectra. I had to do some more calibration checks on the acquisition and guiding, and that lead to more problems arising. After temporarily sorting them out, I tried to centre a star on the central core, but could not find the IFU let alone a core. I then observed the Moon and got light down the instrument (it works), and then Mars, ran some offsets and found the IFU and located the offset of the IFU. This took the best part of 5hrs to do.

I also wavelength calibrated the spectrograph in situ, ready for observations using a 650nm laser diode.

No galaxy spectra because the pointing on the telescope was all over the place (half the night sky out!) so I need to sort that out before attempted to point at galaxies. I could find bright objects by eye, and slew the telescope accurately enough, but the galaxies I have on the list are "in the middle of nowhere" and so do not have any naked eye reference stars.

Note should be taken that Mars is only 4” on sky and so to have light from Mars falling down all areas of the IFU means that the telescope is out of focus. The eyepiece and IFU don’t have the same Focal Plane. This needs to be fixed.

To do on next commissioning night:

1. Align the telescope properly.
2. Focus the telescope to the IFU.
3. Find offset again.
4. Observe standard star.
5. Observe galaxy.

14.3 Third Night

Date: 10/02/2012	Start Time:19:00	End Time: 23:00
Site: Bayfordbury Observatory	Overall Weather: Clear	Moon: Below Horizon
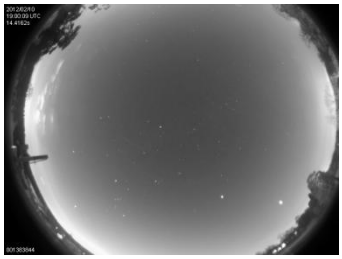 19:00 Sky Brightness: 19.18mag/arcsec^2	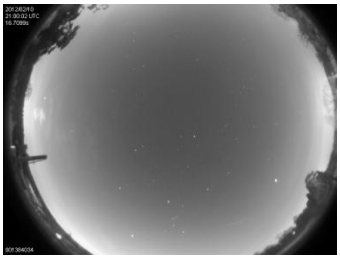 21:00 Sky Brightness: 19.18mag/arcsec^2	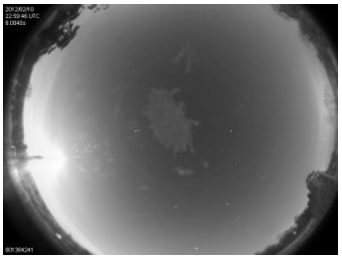 23:00 Sky Brightness: 18.78mag/arcsec^2

Notes:

Some galaxies to observe if able:
NGC 2748 z=0.005
NGC 3079 z=0.0038
NGC 3877 z=0.00016
NGC 4026 z=0.00019
NGC 4125 z=0.0045

Stars to do the 2-star alignment with:
Dubhe
Alpheratz

Balanced telescope with weights on adjustable bar mount. in park position.
performed two star alignment on Capellar and Betelgeuse
alignment failed (maybe too close in RA) - will perform two star alignment on Dubhe and Alpheratz

---

alignment worked
alignment check on Betelgeuse showed some offset
auto guiding on star near Betelgeuse

Moved to point at Jupiter (manually centred in TV)
focus on fibre polish paper with focuser all the way in.

– Green paper was used to focus on.

Moved mirror. Jupiter now not in centre of telescope so will have to centre it and re-align guide scope then re-align system. Focuser will be offset by IFU inset to counter adjust focal plane.
pointed Jupiter in centre of telescope using paper as guide and callipers as measurement (half of focuser outer diameter all the way around)
re-aligned guide scope with sticker on screen showing crosshair CCD centre

these are the hand control hold mode coordinates:
RA 02:08:36
DEC 11:54:34
Jupiter is on sky via Stellarium:
RA 02:07:29
DEC 11:47:37
Will point back to Betelgeuse to see alignment if any pointing offset.

Betelgeuse is out of centre
handset says:
05:55:53
07:24:41
moved to centre:
Betelgeuse is off TV centre but re telescope centre with callipers. change TV centre
after centring
handset says:
05:56:09
07:24:42
need to re-align telescope via two star align
---
align v3
Dubhe
Almaak
Dubhe centred
Almaak centred
telescope two star align successful
go to Betelgeuse for align check

Betelgeuse (BG) is off centre by a lot.
handset says BG is:
05:55:51
07:24:25
after moving BG to centre of TV handset says:
05:58:51
07:03:29
offset equals:
+00:03:00
-00:20:56
go to Regulus to check offset

Regulus not in centre
handset says:
10:09:02
11:54:01
apply previous offset =
10:12:02
11:33:05
go to these coordinates via handset
Regulus is way off after applying offset v1
when centred Regulus the handset says:

10:11:48
11:45:50
Regulus centre aligned offset v2

Arbitrary error in pointing each time. not going to be able to run offsets with telescope.

End night 23:14 after discussion with David Campbell about running automated system on LX200. Need MaxImDL licence and manually moved dome.

Report:

It got to -10degC tonight. After having all the pointing issues last time, I started the night by re-balancing the telescope (completed) and then proceeded to align the telescope via a "Two Star Align" standard procedure.

1. 1st alignment failed as I used stars with not enough RA separation.
2. 2nd alignment completed using stars Dubhe and Alpheratz.
3. Slewed to Jupiter, not in centre of telescope so alignment did not really work.
4. Whilst at Jupiter I fixed the focus problems (that last seem to be responsible for the ~1000 times less efficiency from last time). I did this by focussing on a piece of paper (similar to what was done for SAMI in the rotation calibration). Amusingly you could see Jupiter's cloud bands on the paper projection.
5. Re-centred and re-aligned everything all over including the calibration of centring the guide scope.
6. Re-ran the Two Star Align procedure. Went to another star to check alignment, and yet again still off (by ~20arcmin).
7. Calculated telescope offset and went to another star (it again was off centre). Applied the calculated offset, and after was still ~10arcmin off centre.
8. Pointing accuracy seems to change depending on the location of sky, so simple offsets cannot be done.
9. Ended the night, as I need to seriously come up with some fix for this issue before I can observe anything. I think David Campbell and I came up with the solution, so should be better by next time.

To do on next commissioning night:

1. Obtain MaxImDL Licence.
2. Install ACP software.
3. Re-calibrate whole set-up.

14.4 Fourth Night

Date: 01/03/2012	Start Time:19:00	End Time: 22:00
Site: Bayfordbury Observatory	Overall Weather: Cloudy	Moon: High gibbous moon
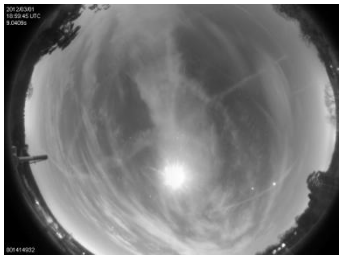	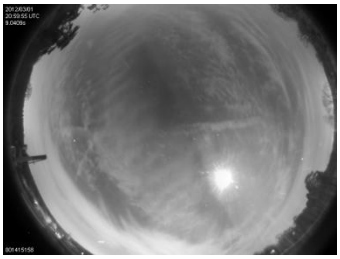	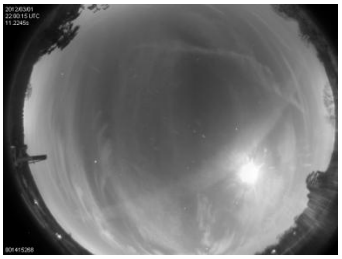
19:00 Sky Brightness: 17.74mag/arcsec^2	21:00 Sky Brightness: 18.02mag/arcsec^2	22:00 Sky Brightness: 18.78mag/arcsec^2

Notes:

IFU was dismounted for Open Night.
Complete recalibration needed.
BASIS still works though spectra are off centre (vertical).
Wavelength set to 2.4775micron on SGS micrometer (see Second Commission Night Notes).
Mounted SBIG STL-6303E to TV.
Got TV in rough focus.
Too cloudy to do anything.

Wrote instructions for ACP calibration:
Run setup scripts:
LimitingMagnitude.vbs
CalibrateGuider.vbs
Train Corrector.vbs
ACP Preferences:
- PinPoint: Exp.interval= ~20s (set by LimitingMagnitude.vbs)
Max pointing err=0.08arcmin (~5arcsec=seeing Note: may fail)
Skip targets if pointing update fails (tick)
- Weather: WeatherWatcher.Weather
ACP-Weather.vbs (parks when weather says anything but clear)
(set up, but needs activating each time via "connect")
- Observatory: Draw limiting angle ~40deg from zero horizon (maybe more)
MaximDL:
CameraControl\Exposure\Autosave
Collect 20 10min darks
Collect 50 biases
Collect ~20 twilight flats (can average a later date)
via ACP - run AutoFlat.vbs for sky flats
write script for targets (top ~10 then top ~50)
check user manual for script guide and #tags
apply offset via force RA and Dec

Report:

Re-mounted all equipment as it had been taken off due to an Open Night and maintenance. Too cloudy to do any observations.

To do on next commissioning night:

1. Everything!

14.5 Fifth Night

Date: 03/03/2012	Start Time:19:00	End Time: 00:00
Site: Bayfordbury Observatory	Overall Weather: Clear	Moon: High gibbous moon
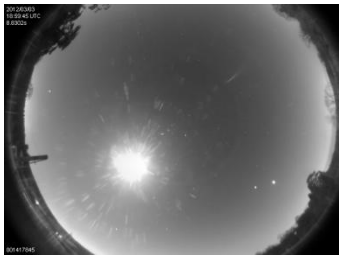 19:00 Sky Brightness: 18.09mag/arcsec^2	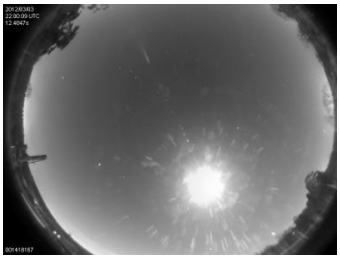 22:00 Sky Brightness: 18.35mag/arcsec^2	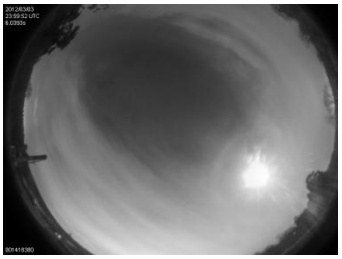 00:00 Sky Brightness: 17.89mag/arcsec^2

Notes:

Aligned crosshair scope
1536x1024
768x512 = centre on MaximDL (2bin)
1024x682
512x341 = centre on CCDOPS (full-low)
TV aligned

Reset telescope and run 2-star align using Dubhe and Alpheratz
Align successful.
check with Alhena (pointing still way off)
hoping ACP will correct this

Will initialise ACP
---
telescope connection failed so will need David Campbell onsite to fix
find offset with Jupiter using manual alignment

IFU inset of 1.29cm
IFU length of 2.27cm
focus offset is 0.98 – this will be used for the 2-inch focus mount from now on.
focus offset applied
---
hopefully get spectra from Jupiter (via MaximDL)
Manually centred Jupiter using the spectra as a spatial guide. Took 60s exposure.

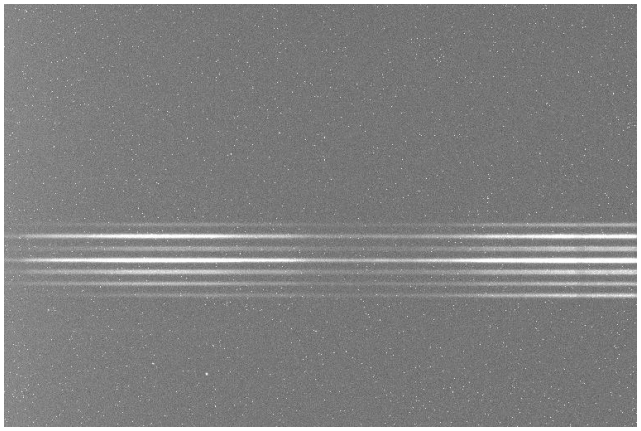

Really good result, and knowing that Jupiter is ~25" in diameter then only illuminating the inner cores means the focus is good.

Jupiter is too low and it is too cloudy to do any more observations.

Go to the Moon to get spectra down all fibres

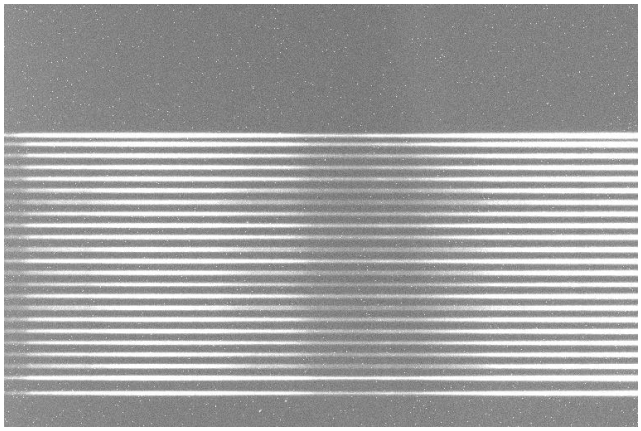

Again great result! All fibres illuminated and looks relatively consistent across fibres

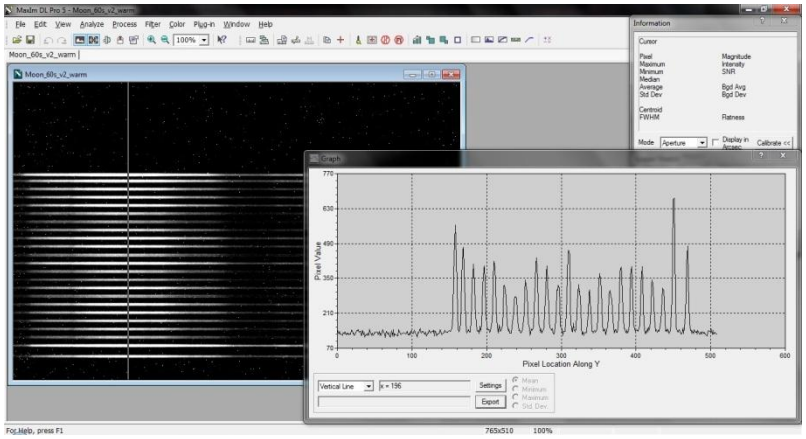

Vertical cut shows different in fibres, but can't be certain on throughput variations etc… at this point.

End due to cloud = 23:50

Report:

ACP could not connect to the telescope so I did manual pointings. Went to Jupiter and found the IFU (this time in ~focus). Took a 60s exposure, please find attached. This is completely raw, i.e. no dark subtraction, no cooling. Literally just took an exposure to see what would happen. At this point Jupiter was near the horizon so I did not have time to set everything up for an ideal exposure. The attached exposure shows Jupiter falling on the inner 7 cores (f.o.v ~25"). It took some time to centre it (by no means perfect), where the only reference was how bright each core spectra was. Jupiter then set, so I went to the Moon as clouds came in. Took a 60s spectrum of the Moon to get all cores illuminated (note, clouds made the Moon ~faint, hence 60s exposure). All in all, I'm glad to get some spectra from BASIS.

To do on next commissioning night:

1. Properly calibrate ACP.
2. Find a solution to the inconsistent pointings and inconsistent offset to the IFU due to flexure in the TV. Cannot do any deep sky observations until this is sorted.

End of Commissioning Reports.

15 APPENDIX E – ORIGINAL INITIAL PLAN

1 INITIAL PLAN

1.1 A brief overview of the project

The Bayfordbury Observatory, University of Hertfordshire, UK, is acclaimed to be the best teaching observatory in the UK with six optical telescopes, four 16-inch and two 14-inch, a 4.5m radio dish, and a 115m-baseline radio interferometer. Due to the number of telescopes available, it has been possible for the optical telescopes to each host a different instrument. Current instruments available are high spec CCDs, a fast frame rate camera for planetary or lunar imaging, a slit spectrograph (SBIG SGS), an Hα filter for solar observations, and more. Recent developments have now enabled a robotic drive for one of the 16-inch telescopes, once again pushing Bayfordbury Observatory further into the lead as the UK's best teaching observatory. To keep in line with Bayfordbury Observatory's status, I will build and commission an Integral Field Unit (IFU) instrument for one of the 16-inch telescopes. It appears that not only will this be the UK's first teaching IFU, but also the first IFU hosted by such a class of telescope.

The benefit of using an IFU is that it enables the observer to obtain spatially resolved spectra of a certain target in a single observation. In the field of Astronomy, IFUs are primarily used to observe galaxies, nebulae and Hα features, and can come in a variety of array sizes depending on the specifications of the host telescope and science goals. Current world-leading IFUs include FLAMES (Pasquini et al., 2002) based at VLT, GMOS (Hook et al., 2004) at Gemini North-South, SAURON (Bacon et al., 2001) at WHT, and SPIRAL (Sharp & SPIRAL Team, 2006) at AAT. All of these are monolithic lenslet arrays that chase similar science goals – galactic kinematics, stellar mass and population, host halo mass, and merger history. As BASIS uses an IFU, it would pursue similar science goals, though sights will first be set on finding the instrument's limits to see which science goals are possible.

BASIS's IFU is a 37-element hexagonal grid micro-lens array (see Figure 1), out of which coupled optical fibres feed an SBIG SGS. Originally, the IFU was to be a 1x19 Hexabundle (Bland-Hawthorn et al., 2011), but it was not possible to source one in time. The other reason for changing to a micro-lens array over the Hexabundle is that a single aperture of the micro-lens array is a factor of 2.5 greater than that of a single aperture of the Hexabundle, meaning that more light is collected per aperture if the micro-lens array were to be used. Considering the Meade LX200 (LX200 from here on) that will host BASIS has a 16-inch primary mirror, the larger single-aperture is the better choice.

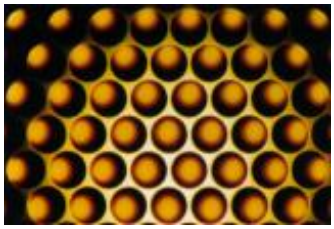

Figure 1 – (SUSS, 2011) – A hexagonal grid micro-lens array.

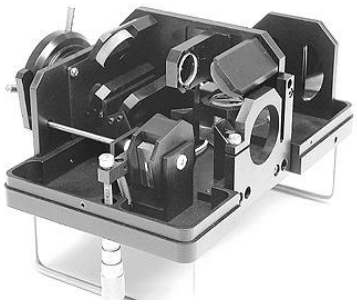

Figure 2 – (Holmes & SBIG, 2001) – SBIG SGS

The SBIG SGS (Figure 2) has a slit length of ~6mm, which is long for such a compact spectrograph. This length is what constricts how many fibres can be used in this system as the fibres are positioned along the slit in a 1D-array, and therefore constricts how many elements can be used in the IFU. The fibre to be used is Corning50/125CPS (50µm core and 125µm cladding), which gives rise to a 5.125mm long 1D-array comprising of the 37-element IFU and 4 sky fibres coupled to what would-be redundant micro-lenses in the array structure (see Figure 3). The fibre feed will be ~2m long and protected in a flexible and lightweight rubber conduit for protection. Mounts for both the IFU onto the telescope and the 1D-array onto the SBIG SGS will be made using a Computer Numerical Control (CNC) machine. The plate scale of the LX200 is 51.6"/mm meaning that each IFU element (of 250µm diameter) has an aperture of 12.9". Therefore, the 37-element hexagonal grid micro-lens array will have a major-axis aperture of 1.5'.

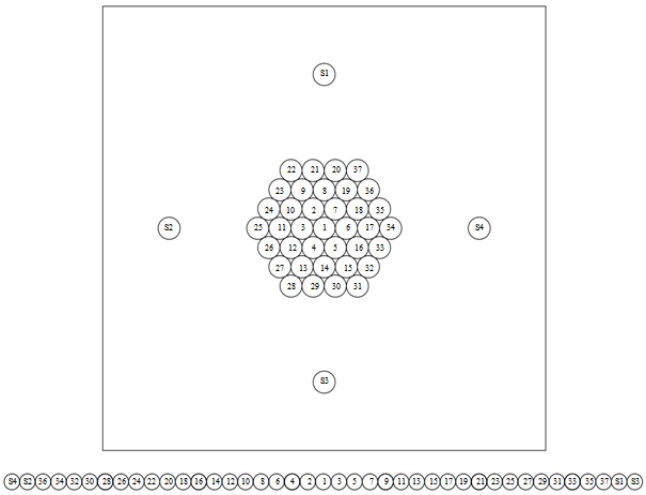

Figure 3 – (Top) Schematic of the micro-lens array configuration with sky fibres (S1-S4), noting that the empty space within the perimeter contains redundant micro-lenses the same size as those shown, with the perimeter being the edge of the ~5mm x ~5mm array. (Bottom) Configuration of 1D-array with mapped fibres.

The SBIG SGS's camera is an ST-7E, which uses a Kodak KAF-0402ME chip with 9µm pixels in a 764x510 array (Holmes & SBIG, 2001). Using the 600lines/mm grating, and with the 1D-fibre-array giving a 50µm slit, it is possible to obtain a resolution of R≈750 at 500nm. This means that with taking into account the specifications of the SBIG SGS, and applying an overall instrument efficiency/Total Throughput of 0.05, a 20min exposure of a ~12mag source gives a possible SNR of 10 (see Appendix A). If multiple exposures were stacked to produce a 2hr exposure it would be possible to get a Signal-to-Noise Ratio (SNR) of 12 for ~12mag and SNR of 10 for ~13mag source.

The overall instrument efficiency/Total Throughput of 5% is a harsh estimation. The reason for setting it at this level is that instruments always perform worse than originally predicted. The SBIG SGS has five optical surfaces between the slit and the CCD. Most of the components of the SBIG SGS have good coatings and come from Melles Griot (Holmes, 2011) giving a 0.90 efficiency per surface. The ST-7E uses a Kodak KAF-0402ME CCD chip that has an average optical quantum efficiency (QE) of ~0.65. Therefore, the efficiency of the SBIG SGS equates to 0.38, say 0.35 including misalignment of the spectrograph optical. For the rest of the instrument there are a number of efficiency factors to take into account; 0.90 due to the IFU interface, 0.90 due to the slit interface, 0.95 due to the Corning50/125CPS's attenuation at 500nm for 2m length, 0.70 due to focal-ratio-degradation (FRD) of Corning50/125CPS at 500nm for 2m length, ~0.92 due to Fresnel reflection losses at both ends of the fibre, and ~0.90 due to the Meade LX200 16-inch. Accounting for all of these factors, the expected instrument efficiency/Total Throughput would be ~17%.

There is an uncertainty in the efficiencies set for the IFU and slit interfaces, and have the possibility of swinging either way. The main constraint on these interfaces would be the selected tolerances. This will depend on a number of factors; CNC/Machining tolerances including cost factors, the alignment of the fibres to the micro-lens array, the alignment of the fibres at the slit with respect to the optical axis of the spectrograph optics, the thermal expansion and the variable expansions between different materials, the quality of end face polishing, and the induced stress on the fibres when housed/glued in the interfaces.

The components needed to build this instrument are listed in §1.2 under the header Sourcing and those to be purchased are listed in Appendix C. The micro-lens array is the most critical component and so is the one that will hold up progress if it is delayed. The Corning50/125CPS fibre has already been sourced.

A stand-alone camera will be mounted to the guide scope of the LX200, which will do the acquisition and guiding. This is necessary as the SBIG SGS self-guiding feature only works when using the slit at the focal plane of the LX200, not when using a pseudo slit comprising of fibre optics.

To reduce the data given by the ST-7E I intend to use pre-written software called "p3d" (Sandin et al., 2010) (see Figure 4). p3d, is a general data-reduction tool for fibre-fed Integral Field Spectrographs (IFSs). It has a user-friendly interface, and includes a vast range of options for case specific data-reduction.

There will be an inevitable uncertainty on the expected performance of this instrument, so decisions on exact science goals and the use of the instrument will be left for a future project. My aim will be to carry out various observations to discover the limits of the instrument so viable science goals can be drawn. To do this I will reduce various catalogues; NGC (Dreyer & Sinnott, 1988), HyperLEDA (Paturel et al., 2003) and NED (Schmitz et al., 2011) to find suitable targets (see Figure 5).

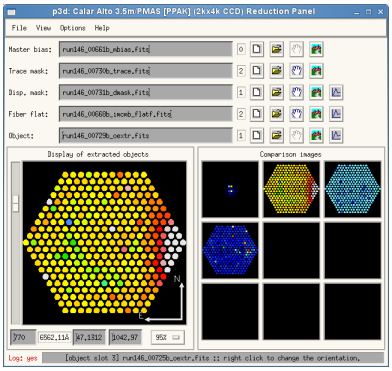

Figure 4 – (p3d, 2011) – A screenshot of the p3d software using the Potsdam Multi-Aperture Spectrophotometer (PMAS) instrument as an example.

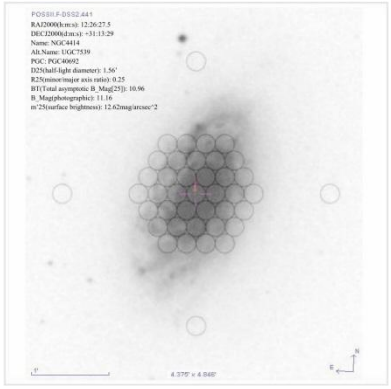

Figure 5 – Example of a suitable target selected from the NGC catalogue with the BASIS IFU overlaid to scale.

1.2 Project Time-Line

For this project, there will be four main stages: Sourcing, Assembly, Commissioning, and Science Limits. Due to the nature of instrument building, the dates assigned to the following tasks are deadlines, meaning that as long as they are completed before this date the project is on track, though I will endeavour to complete the tasks ahead of these dates to allow for inevitable delays. The dates shown are in Week Number (w#), where Week Number 1 (w1) is the week starting 03/10/2011. A visual spreadsheet representation is provided in Appendix B.

Sourcing:

w03	Micro-lens array
w04	Razor blades
w04	Fibre cleaver
w04	Optical glue and index matching gel
w04	Polishing paper
w04	Zemax modelling of 1D-array
w05	1D-array housing (CNC)
w05	127μm drill bit
w05	Micro-lens array AR Coating (Siltint)
w07	Fibre to Micro-lens array coupling interface (CNC)
w08	LX200 focal plate interface
w08	1D-array to SBIG SGS interface (CNC)
w09	Rubber conduit
w09	p3d software

Assembly:

w10	IFU
w11	Fibre-feed
w12	Slit to SBIG SGS interface

Commissioning:

w15	Installation onto LX200
w15	Auto-guiding
w18	Commissioning

Science Limits:

w22	Instrument efficiency
w22	True SNR against mag/arcsec2

Report Deadlines:

27/10/2011(w04)	Initial Plan
08/12/2011(w10)	Poster Presentation
09/02/2012(w19)	Sample Chapter & Contents Page
29/03/2012(w26)	Project Report & Viva (in May)

SPIE Important Dates:

19/13/2011(w12)	Abstract Submission
24/02/2012(w21)	Author Acceptance Notification
04/06/2012(w36)	Manuscripts Due
01-06/07/2012(w40)	Conference (Amsterdam, NLD)

2 REFERENCES (Note: Original Initial Plan references only)

Bacon, R. et al., 2001. The SAURON project - I. The panoramic integral-field spectrograph. MNRAS, 326(1), pp.23-35.

Bland-Hawthorn, J. et al., 2011. Hexabundles: imaging fiber arrays for low-light astronomical applications. Optics Express, 19(3).

Dreyer, J.L.E. & Sinnott, R.W., 1988. The Complete New General Catalogue and Index Catalogue of Nebulae and Star Clusters | Source Catalog Reference: NGC 2000.0. Sky Publishing Corporation and Cambridge University Press.

Holmes, A., 2011. Private Correspondence.

Holmes, A. & SBIG, 2001. Operating instructions for the SBIG SGS and spectra analysis software. http://www.sbig.com/images/documents/products/222.

Hook, I.M. et al., 2004. The Gemini-North Multi-Object Spectrograph: Performance in Imaging, Long-Slit, and Multi-Object Spectroscopic Modes. PSAP, 116(819), pp.425-40.

p3d, 2011. Screenshots. http://p3d.sourceforge.net/index.php?page=screens.

Pasquini, L. et al., 2002. Installation and commissioning of FLAMES, the VLT Multifibre Facility. The Messenger, (No. 110), pp.1-9.

Paturel, G. et al., 2003. HYPERLEDA. I. Identification and designation of galaxies. Astronomy and Astrophysics, 412, pp.45-55.

Sandin, C. et al., 2010. p3d : a general data-reduction tool for fiber-fed integral-field spectrographs. A&A, 515(id.A35).

Schmitz, M. et al., 2011. The NASA/IPAC Extragalactic Database (NED): Enhanced Content and New Functionality. American Astronomical Society, AAS Meeting #217, #344.08; Bulletin of the American Astronomical Society, 43.

Sharp, R. & SPIRAL Team, 2006. The SPIRAL IFU: integral field spectroscopy at the AAT. AAO Newsletter, (No. 110), p.24.

SUSS, 2011. Image courtesy of SUSS - Hexagonal grid micro-lens array. http://www.suss-microoptics.com/shop/microlens-arrays/fused-silica/circular-lenses-hexagonal-grid/microlens-array-nr-13-9910-101-000.html.

End of Original Initial Plan.

End